Dissertation

The Use of Magnesium-based Bioresorbable Screws in the Surgical Treatment of Fractures

submitted by

Dr. med. univ.

Viktor Labmayr

for the Academic Degree of

Doctor of Medical Science

Dr. scient. med.

at the

Medical University of Graz

Department of Orthopaedics and Trauma

under the Supervision of

Priv.-Doz. Dr. med. univ. Dr. scient. med. Patrick Holweg

October 2024

Declaration

I hereby declare that this thesis is my own original work and that I have fully acknowledged by name all of those individuals and organisations that have contributed to the research for this thesis. Due acknowledgement has been made in the text to all other material used. Throughout this thesis and in all related publications I followed the "Guidelines of the Medical University of Graz on Good Scientific Practice".

Viktor Labmayr

Graz, October 2024

Disclosures

Thesis communications

Parts of this thesis have been published in Clinical Orthopaedics and Related Research.

Labmayr V[1], Suljevic O[1], Sommer NG[1], Schwarze UY[1,2], Marek RL[1], Brcic I[3], Foessl I[4], Leithner A[1], Seibert FJ[1], Herber V[5], Holweg PL[1]. Mg-Zn-Ca Alloy (ZX00) Screws Are Resorbed at a Mean of 2.5 Years After Medial Malleolar Fracture Fixation: Follow-up of a First-in-humans Application and Insights From a Sheep Model. Clin Orthop Relat Res. 2023 Aug 21;482(1):184–97. DOI: 10.1097/CORR.0000000000002799

[1]Department of Orthopaedics and Trauma, Medical University Graz, Austria

[2]Department of Dentistry and Oral Health, Davison of Oral Surgery and Orthodontics, Medical University of Graz, Austria

[3]Diagnostic and Research Institute of Pathology, Medical University of Graz, Austria

[4]Department of Internal Medicine, Division of Endocrinology and Diabetology, Medical University Graz, Austria

[5]Department of Oral Surgery, University Center for Dental Medicine, University of Basel, Switzerland

All authors have agreed to the use of their data in this thesis.

Figures and Copyright

- Figure 1a, Figure 1c and Figure 2c: Published in Holweg et al. (Bone Joint Res., 2020). This is an open-access article distributed under the terms of the Creative Commons Attribution Non-Commercial No Derivatives (CC BY-NC-ND 4.0) license, which permits the copying and redistribution of the work only, and provided the original author and source are credited.

- Figure 1c, Figure 3c, Figure 8c, Figure 12c, Figure 13c, and Figure 14c: Published in Labmayr et al. (Clin Orthop Relat Res., 2024). This is an open access article distributed under the terms of the Creative Commons Attribution Non-Commercial No Derivatives (CC BY-NC-ND 4.0) license, where it is permissible to share the work provided it is properly cited. The work cannot be changed in any way or used commercially without permission from the journal.

- Figure 4c, Figure 6c, Figure 10a, Figure 10c and Figure 15c: Published in Herber et al. (Injury, 2022). This is an open access article under the CC BY license.

- Figure 6a and Figure 6c: Published in Holweg et al. (Trauma Case Rep., 2022). This is an open access article under the CC BY license.

Acknowledgements

This work was performed in the doctoral program Bones, Muscles, Joints at the Medical University of Graz.

I would like to take this opportunity to thank Patrick Holweg, the main supervisor of my dissertation, for his guidance and support in scientific and clinical matters. We have successfully completed several projects over the past years. I thank Paul Puchwein and Barbara Obermayer-Pietsch for supervising this study. I thank my colleagues and collaborators who dedicated significant time to both the project and my personal development: Nicole Sommer, who taught me important aspects of scientific work and has been supportive throughout the years; Ines Fößl, for her technical expertise and data collection around high-resolution imaging (XtremeCT); Franz-Josef Seibert, for his clinical guidance; Martin Ornig, my clinical mentor in foot and ankle surgery; Annelie Weinberg, who laid the foundation for our research on bioresorbable magnesium-based implants. Thanks are also due to Andreas Leithner, head of the Department of Orthopaedics and Trauma, who has provided helpful advice on career decisions and supported clinical research. Finally, I want to thank my family and friends for their support.

Table of Contents

Abbreviations and Definitions

AO/ASIF	Arbeitsgemeinschaft für Osteosynthesefragen / Association of the Study of Internal Fixation
AOFAS	American Orthopaedic Foot & Ankle Society
ASTM	American Society for Testing and Materials
AP	Antero-posterior (view)
Ca	Calcium
CRPS	Complex regional pain syndrome
CT	Computed tomography
FDA	Food and Drug Administration (FDA)
HR-CT	High-resolution computed tomography
K-wire	Kirschner wire
Mg	Magnesium
Mn	Manganese
MRI:	Magnetic resonance imaging
N	Newton
OCL	Osteochondral lesion
PGA	Polyglycolic acid
PDLLA	Poly(D,L-lactide)
PLLA	Poly(L-lactic acid)
PROMs	Patient-reported outcome measures
RE	Rare earth (metals)
ROM	Range of motion

VAS	Visual analogue scale
wt%	Weight percent
Y	Yttrium
Zn	Zinc
Zr	Zirconium

All magnesium-based alloys are identified by technical abbreviations, such as *ZX00*, *ZX10*, *ZX20*, *ZX50*, *W4*, *WZ21*, and *WE43*. Additionally, the *Mg-Y-RE-Zr* alloy is a specific formulation relevant to this context. A comprehensive overview of these alloys is provided in Section 1.4 on magnesium-based bone implants.

The terms *bioresorbable* or *resorbable* are consistently used in this work to describe implants designed for gradual decomposition within the body. It is worth noting that different sources may employ varied terminology, such as absorbable or bioabsorbable, among others.

Ankle fracture management involves a variety of surgical techniques, with screws classified by their specific functions. The lag screw principle establishes interfragmentary compression. In oblique distal fibula fractures, this is achieved with a cortical screw placed in a gliding hole (near cortex) and an engaging hole (far cortex). A plate is added to neutralize bending forces. In stable medial malleolar fractures, compression is generated via cannulated screws that engage with their partially threaded end in the trabecular bone. In contrast, positioning screws, such as those used in syndesmotic injuries, stabilize the tibiofibular joint by maintaining bone alignment until healing and are typically removed after 6–8 weeks via a minimally invasive incision.

List of Figures

List of Tables

Abstract (English)

Background: In a pilot study, the magnesium-based screw ZX00 demonstrated successful healing of medial malleolar fractures while gradually resorbing. The proof of concept and excellent 1-year outcomes generated interest beyond the first year. This study reports the clinical outcomes after 2½ years and investigates the changes in bone microarchitecture following the resorption of ZX00, as well as after the removal of conventional implants around the ankle joint.

Methods: All imaging data from the pilot study involving ZX00 screws for medial malleolar fractures were analyzed. The initial study included 20 adults who received either one or two ZX00 screws (most commonly two) for medial malleolar fracture fixation. Each 3.5 mm ZX00 screw had a volume of 243.3 mm^3. In cases of combined injuries, conventional fibulo-tibial positioning screws were used for syndesmotic instability (n=9), and conventional plates/screws were applied for additional fractures (n=14). Fibulo-tibial positioning screws were removed after 6–8 weeks, while plates/screws were removed based on patient preference or discomfort (n=8). Two cases were lost to follow-up or excluded. Clinical follow-up and radiographs for the remaining 18 patients extended to an average of 2½ years post-ZX00 implantation. Of these, 15 patients underwent CT scans at an average of 3½ years post-implantation, including six cases with high-resolution CTs (HR-CTs) conducted between 2 and 3 years. CT scans were analyzed for changes in bone microarchitecture following ZX00 resorption. HR-CTs specifically evaluated ZX00 traces and enabled volumetric measurements of trabecular voids at the former ZX00 implantation sites. Lastly, the cohort comprised eleven patients with CT scans after hardware removal, allowing the evaluation of implantation sites of conventional implants (n=12).

Results: At around 2½ years, there were no clinical complications, and patients remained pain-free. The radiographs revealed no visibility of ZX00 screws in 94% (17 of 18) of cases. Additionally, bone texture at the ZX00 implantation site was rated as homogeneous in 83% (15 of 18) of cases and slightly inhomogeneous in 17% (3 of 18). CT scans demonstrated sclerotic voids in the trabecular bone following ZX00 resorption in 100% (15 cases) after approximately 3½ years. Among the six HR-CTs conducted between 2 and 3

years, one case showed complete ZX00 screw resorption, while five cases exhibited tiny, irregularly shaped ZX00 traces. The trabecular void volumes measured in HR-CT were 596.2 ± 275.7 mm^3. The CTs after conventional hardware removal showed sclerotic screw holes in the trabecular bone, both following the removal of fibulo-tibial positioning screws (6-8 weeks implant residence) and plates/screws (approximately 1½ years).

Discussion: The clinical outcomes confirm the success of the intervention with ZX00 screws, demonstrating true bioresorbability with near-complete resorption 2 to 3 years post-implantation. Radiographs show an increasingly homogeneous bone texture at the ZX00 implantation sites over time, reflecting remodeling and strengthening of adjacent trabecular bone, a phenomenon also observed after conventional screw removal. However, CT and HR-CT scans reveal the full extent of structural changes following ZX00 screw resorption, including voids that differ in size from those associated with conventional screws. This underscores the need for advanced imaging techniques when assessing bioresorbable implants.

Abstract (German)

Hintergrund: In einer Pilotstudie ermöglichten magnesiumbasierte ZX00-Schrauben eine erfolgreiche Heilung von Innenknöchelfrakturen bei gleichzeitiger Resorption der Schrauben. Der Machbarkeitsnachweis und ausgezeichnete 1-Jahres-Ergebnisse weckten Interesse am weiteren Verlauf. Diese Studie berichtet über die klinischen Ergebnisse nach 2½ Jahren und untersucht die Mikroarchitektur des Knochens nach der Resorption von ZX00 sowie nach der Entfernung konventioneller Implantate rund um das Sprunggelenk.

Methoden: Es wurden alle verfügbaren Bildgebungsdaten der Pilotstudie zur ZX00-Verschraubung von Innenknöchelfrakturen analysiert. Die ursprüngliche Studie umfasste 20 Erwachsene, die entweder mit einer oder zwei ZX00-Schrauben (meistens zwei) versorgt wurden. Das Volumen einer 3,5 mm ZX00-Schraube betrug 243,3 mm³. Bei kombinierten Sprunggelenksverletzungen wurden konventionelle Stellschrauben zur Stabilisierung der Syndesmose (n=9) sowie Platten/Schrauben für zusätzliche Frakturen (n=14) verwendet. Die Stellschrauben wurden nach 6-8 Wochen entfernt, die Platten/Schrauben bei Beschwerden oder auf Patientenwunsch (n=8). Ein Fall ging bei der Nachuntersuchung verloren, ein weiterer wurde ausgeschlossen. Die klinische Nachuntersuchung und die Röntgenaufnahmen der verbleibenden 18 Patienten erfolgten durchschnittlich 2½ Jahre nach der ZX00-Implantation. Bei 15 dieser Patienten wurde nach durchschnittlich 3½ Jahren eine CT-Untersuchung durchgeführt, darunter sechs Fälle mit hochauflösenden CTs (HR-CTs), die im Zeitraum von 2 bis 3 Jahren gemacht wurden. Die CTs wurden auf Veränderungen der knöchernen Mikroarchitektur bewertet. Mittels HR-CTs wurden ZX00-Reste detektiert und die Volumina der Hohlräume an den Implantationsstellen vermessen. Unter allen CTs fanden sich elf Patienten mit Zustand nach Metallentfernung zur Beurteilung der Implantationsstellen konventioneller Implantate (n=12).

Ergebnisse: Bis zum 2½-Jahres Follow-up traten keine klinischen Komplikationen auf und die Patienten und Patientinnen waren schmerzfrei. Die Röntgenaufnahmen zeigten in 94 % der Fälle (17 von 18) keine Sichtbarkeit der ZX00-Schrauben. Die Knochenstruktur an der ZX00-Implantationsstelle wurde in 83 % der Röntgenbilder (15

von 18) als homogen und in 17 % (3 von 18) als leicht inhomogen bewertet. Die CT-Scans zeigten in allen Fällen (100 %, 15 von 15) nach etwa 3½ Jahren sklerotische Hohlräume im Trabekelknochen. Von den sechs HR-CTs lag in einem Fall eine vollständige Resorption der ZX00 Schrauben vor, während in fünf Fällen winzige, unregelmäßig geformte ZX00-Reste zwischen 2 und 3 Jahren sichtbar waren. Die Volumina der trabekulären Hohlräume in der HR-CT Messung betrugen 596,2 ± 275,7 mm³. Die CTs nach der Entfernung konventioneller Implantate zeigten durchgehend sklerotische Schraubenlöcher, sowohl nach der Entfernung der Stellschrauben (6–8 Wochen Liegedauer) als auch nach der Entfernung der Platten/Schrauben (ca. 1½ Jahre).

Diskussion: Die klinischen Ergebnisse bestätigen den Erfolg der Intervention mit ZX00-Schrauben, die 2 bis 3 Jahre nach der Implantation nahezu vollständig resorbiert sind. Die Röntgenaufnahmen weisen im Laufe der Zeit eine zunehmend homogene Knochenstruktur an den Implantationsstellen der ZX00-Schrauben auf, was auf eine Remodellierung und Stärkung des benachbarten trabekulären Knochens hinweist – ein Phänomen, das auch nach der Entfernung konventioneller Schrauben beobachtet wird. Die CT-Scans zeigen trabekuläre Hohlräume nach der Resorption der ZX00-Schrauben, die sich in ihrer Größe von den Löchern der konventionellen Schrauben unterscheiden. Dies unterstreicht die Notwendigkeit weiterführender Bildgebung bei der Beurteilung bioresorbierbarer Implantate.

1 INTRODUCTION

1.1 Bone Healing

A bone fracture is a break or crack in a bone resulting from forces or stresses that exceed its structural capacity. The body has two distinct methods for mending fractured bones, each aimed at restoring their function and both their macroscopic and microscopic composition. Consequently, the potential for complete bone healing, known as *restitutio ad integrum*, exists (1,2).

The healing process of a fractured bone is intricately tied to the concept of mechanical stability and the strain the fracture experiences. In this context, strain refers to the deformation of bone tissue in response to external forces or stress. The direction of this strain can be either tensile (stretching) or compressive (compression), depending on the forces applied (3). A strain below 2% allows the bone to heal directly (4). When the strain falls within the 2% to 10% range, cartilage forms, which initially stabilizes the fracture site, paving the way for subsequent bone formation (4). Strains exceeding 10% are beyond the strain tolerance of bone tissue, making physiological tissue healing impossible and leading to delayed union or non-union (5). At a cellular level these responses are mediated by mesenchymal stem cells that are equipped with mechanosensors. Depending on their mechanical environment, these mesenchymal stem cells can differentiate into osteoblasts, chondroblasts, or fibroblasts/adipocyte (6). There are two different pathways of bone healing: primary bone formation, which involves direct bone formation from primitive connective tissue or mesenchyme, and secondary bone formation, characterized by an indirect process through the formation of cartilaginous matrix (callus) as a precursor with subsequent transformation into bone tissue (1,7).

Examples of both pathways of bone healing can be traced back to our evolutionary history (8). First, cartilage appeared, giving rise to tooth-like structures and protective shields. The evolution from softer cartilage-like structures to robust bone marked a significant milestone in the evolution of skeletal structures (9). Then, another key transition in vertebrate evolution was the shift from exoskeletons to endoskeletons. This shift allowed for greater mobility and adaptation to new environments. Endoskeletons extended limb

length, facilitating faster movement and adaptability, expanding the potential for vertebrate life (10).

In the formation of specific skeletal structures, such as the skull, mandible, and clavicles, primary bone formation predominantly plays a role, while secondary bone formation, preceded by cartilage formation, contributes to the axial and paraxial skeleton (11). This process, known as 'biomineralization,' is particularly important for the growth of long bones. The center of active growth in these bones is referred to as the 'physis,' initially comprised of cartilage capable of growth and later undergoing ossification. The completion of growth is marked by the ossification of the physis (8).

1.1.1 Healing in Long Bone

'Endochondral ossification' specifically refers to a process of bone formation or bone healing, also known as secondary bone healing. It is most comprehensively understood within the context of long bone fractures and represents the more naturally occurring mode of fracture healing. The process initiates with an acute inflammatory response triggered by the fracture, resulting in the formation of a fracture hematoma containing essential molecules. These molecules play a crucial role in recruiting mesenchymal stem cells, which, in turn, work to stabilize the fracture gap by forming a cartilaginous callus. Over time, this callus undergoes calcification and gradually gives way to woven bone, ultimately maturing into lamellar bone through a process of remodeling (12,13). It occurs when some stability of a fracture is established, but some motion between fracture fragments is possible (14). The means by which this ‘relative stability’ is achieved is not critical; it can either occur naturally through rest and casting or be attained through surgical interventions such as external fixation, internal fixation with locking plates, bridging plates, or intramedullary nailing (15–17). In all these scenarios, a shared characteristic is the preservation of a certain degree of movement around the fractured bone, hence the term 'relative stability,' which facilitates the formation of callus and, ultimately, ossification (18). In short, long bone healing mimics fetal endochondral bone development, involving a cartilage-to-bone transformation that repairs and regenerates the damaged bone.

'Intramembranous ossification' refers to direct bone formation, also known as primary bone healing. This process is initiated when direct bone contact and rigid fixation is achieved, often with the use of surgical methods like lag screws with neutralization plating, compression plating, or tension band wiring (4,15,19). 'Gap healing' occurs when there is a small gap between the fracture parts, typically measuring less than 1 millimeter. In this case, osteoblasts deposit mineralized bone matrix to bridge the gap. Over time, this matrix undergoes continuous remodeling, gradually transitioning from woven to mature lamellar bone. The size of the gap is critical and should be below 800 to 1000 µm (=1 mm) (12). This healing process requires replacement of the primary bone structure with longitudinally oriented osteons (12). 'Contact healing' is possible when there is direct bone-to-bone contact between the fracture ends, along with the presence of ‘absolute stability’ and a substantial reduction in interfragmentary strain. Under these conditions, osteoclasts create pathways through cortical bone in the shape of cutting cones (13). They facilitate the ingrowth of blood vessels and undifferentiated mesenchymal stem cells, which differentiate into osteoprogenitor cells for osteoblasts (1,2). These osteoblasts subsequently fill these cavities with bone tissue, connecting and aligning it with the surrounding Haversian system of lamellar bone (19,20).

1.1.2 Healing in Trabecular Bone

While much attention is given to the healing of long bones, it is crucial to understand the vital role of trabecular bone, also known as cancellous or spongy bone. Trabecular bone constitutes a substantial part of overall bone structure and holds clinical relevance in fractures like those occurring in the distal radius, proximal hip, and distal tibia. These fractures often involve the metaphysis, situated at the end of long bones, which primarily consists of trabecular bone. Understanding trabecular bone is also key in conditions like vertebral fractures and bone marrow edema, which can be observed in tarsal bones rich in trabecular bone. The study of healing processes in trabecular bone has gained attention in recent years, which is distinct from the cortical healing of long bones (21,22). Trabecular bone in the endosteum is rich in mesenchymal stem cells, which respond well to healing signals. In contrast, the bone cavity and its central bone marrow contain fewer of these cells, and they are less active (23). The abundance of mesenchymal stem cells in trabecular bone allows for a rapid healing response to injuries. The healing mechanism involves the direct formation of woven bone, but this process has limitations—it can only

cover a few millimeters as it is spatially restricted (24,25). This mechanism appears to be specific for trabecular bone and could be named inter-trabecular bone formation (25). Consequently, endochondral healing thus not play a role in the healing of trabecular bone.

Early evidence of woven bone formation within the trabecular bone date back to the 1950s when the English orthopaedic surgeon J. Charnley published a knee arthrodesis biopsy demonstrating new woven bone formation at the bone ends four weeks after surgery (26). P. Aspenberg, a Swedish orthopaedic surgeon and researcher, has dedicated his work to understanding trabecular bone. In a clinical setting during surgery for distal radius fractures, his team took biopsies 1 to 4 weeks after the fracture. The histological results revealed mostly direct bone formation within the trabecular bone in the form of disorganized woven bone and absent or only minimal cartilage formation (27). Studies involving drill holes in the proximal tibial metaphysis of rats demonstrated that these holes filled rapidly with woven bone within one week. After two weeks, most of the bone within the holes had been replaced by a marrow cavity. Notably, the density of the surrounding bone initially increased during the first week but subsequently decreased. This suggests that forces may have been distributed across a network of trabecular or cortical bone (22). Aspenberg's research group shed light on how trabecular bone responds to various stimuli. Inserting a screw into a drill hole increased bone density around the hole and the screw. This density persisted, leading to the integration of the implanted screw, offering a model for implant study. In contrast, small-diameter drill holes (0.6 – 1.2 mm) healed with new bone within a week. However, large-diameter drill holes (>2.0 mm) faced challenges in healing, resulting in fibrous tissue in the central region and the hole's persistence. They concluded, that osteogenic cells within the trabecular bone have limitations in their ability to migrate and deposit new bone (28).

1.2 Ankle Fracture

1.2.1 Classification and Treatment

The two primary classification systems for ankle injuries are the Weber classification, also known as the Danis-Weber classification, and the Lauge-Hansen classification. The Weber classification categorizes ankle fractures into three types: Type A, Type B, and Type C, based on their specific location on the distal fibula and their involvement with the distal tibiofibular syndesmosis (29). As a rule of thumb, Weber Type A fractures can be treated conservatively and Weber Type B and C are generally treated with open reduction and internal fixation, although there is ongoing debate if surgery yields superiority especially in those over 60 years of age (30). When analyzing studies that report comprehensive analysis of surgical treatment ankle fractures, Weber B accounted for approximately 67.4 to 75% and Weber C for around 12 to 20% of cases (30–32). In contrast, the Lauge-Hansen classification system identifies four main types of ankle fractures based on the mechanism of injury: supination-adduction, supination-external rotation, pronation-abduction, and pronation-external rotation (33,34). Ankle fracture account for 8.5% to 10.3% of all fractures in adults (35–37). Among these, 25% to 40% require surgery, making it a common procedure in the field of orthopaedic surgery (38–40). Surgical intervention, with the primary goal of anatomical restoration and achieving stable fixation, encompasses several fracture fixation principles. The main techniques involve fibular plating, often combined with a lag screw, and cannulated screws at the medial malleolus (41). In cases where intraoperative instability of the ankle joint arises due to a rupture in the distal tibiofibular syndesmosis, a specific intervention is required. This involves the placement of a fibulo-tibial positioning screw, often referred to as a 'syndesmotic screw,' extending from the fibula to the tibia (42). However, it is crucial to note that this fibulo-tibial screw should be removed before allowing the patient to bear weight to prevent potential breakage of the screw (43). Removal is typically scheduled when healing is reached, typically around 6 to 8 weeks after surgery. The surgical success is undoubted for higher order ankle fractures (those with disruption of the tibio-fibular syndesmosis) and complications are reportedly low (44). A study using California's hospital discharge database examined over 57,000 patients who underwent open reduction and internal fixation for ankle fractures (uni-, bi-, and trimalleolar) over a decade. The findings revealed low short-term complication rates, including pulmonary embolism

(0.34%), mortality (1.07%), wound infection (1.44%), amputation (0.16%), and revision open reduction and internal fixation (0.82%). Additionally, intermediate-term reoperation rates were also low, with ankle fusion or replacement performed in only 0.96% of patients within a 5-year follow-up period (40).

1.2.2 Medial Malleolar Fracture

Medial malleolar fractures, according to the Weber and Lauge-Hansen classification, usually occur in conjunction with other fractures (e.g., lateral malleolus, posterior malleolus). However, these fractures can also occur in isolation, although they are less prevalent. The majority of fractures at the medial malleolus can be managed with two cannulated screws (34). More vertically oriented medial malleolar fractures can result from a supination-adduction injury mechanism. Since these fractures extend further into the tibia, they should be fixed with an antiglide plate to prevent vertical migration (45,46). The medial malleolus is easily accessible, making it an excellent model for research on bioresorbable implants. However, the use of bioresorbable materials for medial malleolar fracture fixation remains largely experimental, with most applications limited to case series and various implant types explored over the years. The following list provides an overview of the existing clinical literature to date.

- In 1989, Böstman et al (Finland) reported ankle fracture fixation (lateral and bimalleolar fractures) with synthetic polymers (lactide-glycolide copolymer and polyglycolide) in 102 patients with fracture union and high return to sports rates, however sinus formation with remnant of the degrading implants was seen in six patients after 2 to 4 months postoperatively (47).
- In 1992, Frøkjaer and Møller (Denmark) tried biodegradable fixation with polymer rods (Biofix, see (48)) for ankle fractures, including medial malleolus, but reported sinus formation, osteolysis, and non-union secondary to fracture displacement (49).
- In 1993, Dijkema et al. (The Netherlands) published their attempts to fix fractures of the ankle joint (lateral and bimalleolar fractures) with rods made from PGA (polyglycolic acid) in 43 patients, mostly young men. They reported no postoperative complications with a mean follow-up of around ½ year. Sterile sinus formation was not seen (50).

- In 1994, R.W. Bucholz (Texas) published a study comparing medial malleolar fracture fixation with 4.0-millimeter polylactide screws (83 patients) against fixation with 4.0-millimeter stainless-steel screws (72 patients). The study found that radiographic and functional results were equivalent at an average of around 3 years, with no late drainage of hydrolyzed polylactide noted (51).
- In 1998, Springer et al. from The Netherlands reported on the successful use of polymer rods and screws (Biofix) for ankle fractures, including medial malleolar fractures, in 22 patients. They observed three cases with sterile sinus tract formation (52).
- In 2013, Jin et al. (China) compared PDLLA screw with metal screws in 1230 patients with simple medial malleolus fracture and found excellent outcomes in both groups (53).
- In 2018, Kose et al. (Turkey) reported on the treatment of medial malleolar fractures in 11 patients using magnesium-based (Mg-Y-RE-Zr) screws. Their study demonstrated satisfactory fixation and fracture healing without complications within 1 to 2 years (54).
- In 2020, May et al. (Turkey) compared the fixation of medial malleolar fractures using conventional titanium screws to magnesium-based (Mg-Y-RE-Zr) screws. They found that both methods demonstrated similar therapeutic efficacy. However, within a mean follow-up period of two years, 20% required removal of the titanium screws, while none of the magnesium-based screws needed removal (55).
- In 2020, we, Holweg et al. (Austria), published early results on magnesium-based (ZX00) medial malleolar screw fixation, highlighting excellent early clinical outcomes with 100% fracture union and absence of complications (56).
- In 2021, Xie et al. (Shanghai) published a study on the use of 3.5-millimeter magnesium-based (Mg-Nd-Zn-Zr) alloy screws for the treatment of medial malleolar fractures in nine patients and followed them over 1 year (12 months ± 5 months). Their findings revealed an absence of infection, implant failure, or malunion occurrences. Radiographic analysis unveiled the presence of radiolucent zones surrounding the screws, which progressively diminished 3 months after implantation (57).

1.3 Hardware Removal

1.3.1 The Benefits and Risks

In current surgical practice with conventional implants, the removal of hardware in patients experiencing postoperative hardware irritation is a common strategy (58). The findings of a prospective clinical study conducted at a New York hospital shed light on the efficacy of this approach (59). Examining patients who underwent metallic hardware implantation for fractures across various anatomical sites, subsequent hardware removal yielded no observed adverse events or complications during the one-year follow-up. Notably, patients reported significant improvements in pain relief and functional recovery, underscoring the potential benefits of this surgical intervention (59).

However, complications associated with implant removal do occur. A study conducted by a Japanese group investigated 80 patients who underwent implant removal after ankle fracture and open reduction and internal fixation, revealing complications in 14% of cases, including arterial injury, blistering, nerve injury, skin necrosis, and infection (60). Moreover, re-fracture is an issue and its risk is highest in the first weeks after implant removal (61–63). During this period, fractures often occur around the drill or screw hole, which remains a stress riser (64,65). The mechanical effects of bone drilling are well studied (65,66). Drilling diminishes the load tolerance of bone; for instance, a single 3.5-mm drill hole in a fibula reduces the mean load to failure from approximately 360 to 215 N, resulting in the conclusion that a fibula with a single drilled hole fails when subjected to 60% of the applied load (67). In the early days of osteosynthesis and implantology, researchers studied the impact of drilling on bone strength (68). They observed that within the first month, the stress-concentrating effect of a drill hole was mitigated by 'adaptive changes' or 'a system for transmitting forces around the hole' (68). This phenomenon is now understood to be due to bone remodeling around the screw hole (69). Recent studies highlight that trabecular bone undergoes a different healing process compared to cortical bone, with spatial limitations in healing observed in trabecular bone (28). This could explain why screw holes in trabecular bone may remain visible even years after metal screw removal (70). The surrounding bone is able to transmit the forces around the hole, adaptively strengthening the remaining structures, without the need to refill the hole (71–73).

1.3.2 The Costs of Hardware Removal

A Finnish registry study spanning 20 years (1997-2016) involving 68,865 patients who underwent open reduction and internal fixation for ankle fractures revealed that hardware removal procedures were performed in 18,648 (27%) cases (74). In the 1990s, Finland's implant removal rate was as high as 90 per 100.000 person-years (75) The 20-year registry study reported an incidence 31 per 100.000 person-years in 2001 and 13 per 100.000 in 2016.(74) That year, the diagnostic related groups (DRGs) costs for one hardware removal surgery was EUR 797 (74). A ten year follow-up from a prospective US-American study on ankle fractures showed that 11% of patients underwent implant removal procedures (31). In Norway, a study group reported that 17% of patients underwent implant removal following ankle fracture treated with open reduction and internal fixation (76). An analysis conducted at a German level one trauma center revealed that removal of metal around the ankle joint was the most prevalent region for hardware removal procedures, accounting for 21% of cases (77). Similarly, the Finnish registry identified hardware removal after ankle fractures as among the most prominent of all fracture types (75). Regarding cost considerations, an Irish group of orthopaedic surgeons reported an average cost of hardware removal of EUR 1113. Among 1482 patients surgically treated for ankle fractures with open reduction and internal fixation over a ten-year period, 185 (12.5%) required hardware removal, with associated costs averaging EUR 1113 per procedure (32). Notably, half of these removal cases (6.1%) were planned for removal of the fibulo-tibial positioning screw after successful healing.

1.4 Magnesium-based Bone Implants

The pursuit of bioresorbable implants addresses the challenges of conventional orthopedic hardware, particularly hardware irritation and the need for secondary removal surgeries. Magnesium is a promising candidate for bioresorbable implants, with the main challenge being to achieve an optimal corrosion rate while maintaining sufficient stability for fracture or osteotomy fixation. Magnesium-based implants can either contain rare earth (RE) metals or be free of them.

In 2013, Syntellix AG (Hannover, Germany) introduced Magnezix®, a magnesium-based screw containing rare earth (RE) metals (Mg-Y-RE-Zr), which received CE marking and entered the European market in 2014 (78,79). Others have tried to develop an alloy consisting exclusively of metals naturally found in the human body, such as magnesium, zinc, and calcium. These efforts led to the FDA approval in 2023 of a RE-free magnesium-based screw, utilizing the ZX00 alloy (80).The bioresorbable ZX00 screw is marketed as RemeOs™ screw by Bioretec Ltd. (Tampere, Finland) since 2023. At the time of writing this thesis, the European market approval (CE label) had not yet been completed (81). In vitro assessments confirmed the non-toxic nature of tested Mg-Zn-Ca alloys (82). Preclinical research confirmed biocompatibility in various preclinical setups, including studies involving rats (83–86) and sheep (87,88). By changing the content of alloying partner (Zn, Ca), the mechanical properties and corrosion rate can be tailored. Higher zinc content enhances tensile strength and elongation (82). However, minor adjustments in the content of Zn effect the degradation rate, with even small increases of half of a percent by mass accelerating the degradation rate (89).

The following list of magnesium-based alloys is sorted according to their composition, ranging from high degrees of yttrium and other REs to RE-free alloys with stepwise decreasing Zn content, culminating in ZX00. This partially reflects the technological evolution of magnesium-based implants over the last 15 years.

1.4.1 Alloy Mg-Y-RE-Zr

The alloy consists of 90 wt% magnesium, along with yttrium, other RE metals, and zirconium, denoted by the official nomenclature as Mg-Y-RE-Zr. It is based on the WE43 system described below (see 1.4.2). The inventor company (Syntellix AG, Hannover) offers the alloy branded Magnezix® CS as cannulated screws in a range of lengths from

10 to 40 mm and diameter 2.0 to 4.8 mm (79,90,91). Several animal studies confirmed biocompatibility (92,93). The degradation causes gas formation that is highest in the first month after implantation and decreased thereafter (94). The implant volume decreased by around 25% after 6 months when implanted in rabbit tibiae (94).

Some authors around the company (Syntellix AG) and Hannover Medical School suggest that degrading magnesium-based implants might induce bone formation in animal studies (92,95) and that the release of magnesium ions could lead to bone cell activation (95). Thus far, concrete evidence for bone regeneration in humans is lacking. However, there have been procedural successes with Mg-Y-RE-Zr in humans in fracture and osteotomy fixation. The data on the successful clinical application of Mg-Y-RE-Zr, or human use, paints the following picture:

- In 2013, the group from Hannover Medical School (Germany) published a randomized controlled pilot study in 26 patients undergoing hallux valgus surgery comparing the Mg-Y-RE-Zr screw to conventional titanium screw for osteotomy fixation (96). The outcomes in terms of procedural success and pain / function were comparable, giving the new screw credit to be used for this indication.
- In 2016, the Hannover group conducted a prospective study involving 45 Chevron osteotomies for hallux valgus correction, utilizing Mg-Y-RE-Zr screws. Among the participants, seven patients experienced metatarsal head displacement, leading to one requiring revision surgery (97).
- In 2018, Gigante et al. (Italy) reported use of Mg-Y-RE-Zr screw in juvenile / young adult in three cases for tibial spine avulsion fracture (98). They showed successful healing and functional recovery with a follow-up of 1 year.
- In 2020, Acar et al. (Turkey) published a study involving 22 patients with osteochondral lesions of the talus undergoing medial malleolar osteotomy and screw fixation (99). The study compared outcomes between patients receiving Mg-Y-RE-Zr screws and those receiving titanium screws, with a minimum follow-up period of one year. Remarkably, both groups exhibited comparable outcomes, with no reported complications.
- In 2021, Lam et al. (Hong Kong) reported three successful cases of intraarticular elbow fracture involving either the capitellum or radial head. These fractures were

treated with Mg-Y-RE-Zr screws, resulting in good functional outcomes at the 1-year follow-up (100).

- In 2024, Gazit et al. (Israel) showed data from a prospective case series involving 60 patients undergoing hallux valgus surgery, comparing Mg-Y-RE-Zr screws to titanium screws over a 1-year follow-up period (101). The study found a higher rate of hardware failure in the magnesium screw group (5/26) compared to the titanium group (0/34), although six hardware removals were required in the titanium group. Patient-reported outcome measures (PROMs) showed no discernible differences between the two groups.

However, several clinical reports paint a different picture, issuing warnings about the failures of Mg-Y-RE-Zr screws.

- In 2016, Wichelhaus et al. (Germany) reported a case study illustrating catastrophic outcomes subsequent to the fusion of three carpal bones (STT fusion) using two Mg-Y-RE-Zr screws (102). The patient exhibited symptoms of pain, severe swelling, and screw loosening, necessitating revision. A CT scan performed 6 weeks post-surgery revealed osteolysis and construct failure, accompanied by gas formations. During the revision surgery, large voids around the inserted screws, with the tissue surrounding the screws displaying a blackish discoloration were identified.
- In 2023, Haslhofer et al. (Austria) published a case series involving 18 consecutive trauma patients who underwent implantation of Mg-Y-RE-Zr screws, primarily in the shoulder region. Their findings revealed material failure in four patients, equating to a rate of 22.2% (103).

1.4.2 Alloy WE43

This is related to the above mentioned commercially used alloy (93). WE43 is composed of Mg-Y4-RE3, in wt%, and includes RE such as neodymium. The alloy was tested for skin sensitizing potential and was confirmed to bear no such potential in guinea pigs (104). The degradation rate of this alloy is comparably slow (105,106), with around one-third being degraded after one year in a rat tibia (107). Castellani et al. (2011) used immature rats and implanted transcortical pins made of a WE43-based alloy into their femoral bones. The nature of the alloy is such that it also degrades slowly, and after 6 months,

some surface corrosion became evident (108). Interestingly, the push-out force of the pins at that time point was more than 3 times higher compared to titanium pins. Based on this observation, the authors concluded an 'osteointegrative effect' (108). The histological workup did not reveal signs of inflammation or fibrosis (108). However, others reported a few inflammatory cells around WE43 in a dog tibia osteotomy (109).

1.4.3 Alloy W4

The alloy contains Mg–Y4, in wt%, and additional <0.25 wt% RE elements. In the high-quality study by Thormann et al. (2015), sheep were implanted with screws sized 8 x 23 mm into the femoral condyle and monitored for one year (105). These implants partially degraded, resulting in significant gas formation. After one year, the W4 screws were surrounded by corrosion products, connective tissue, and macrophages, indicating a lack of integration into the host bone. All W4 screws exhibited significant gas formation in the vicinity of the biomaterial. None of the screws displayed any osseous integration in the surrounding tissue, leading to a mechanically unstable condition. This study is particularly interesting as it provides macroscopic tissue sections of bone (embedded gross sections of sheep femoral condyles) with the partially degrading W4 screws after 12 weeks and 1 year, where the voids in the trabecular bone of the femoral condyle are clearly visible (105). This aspect is somewhat lost in microscopic images.

1.4.4 Alloy ZX50

This alloy consists of Mg–Zn5–Ca0.25–Mn0.15, in wt%. In vitro studies showed biocompatibility with human chondrocytes and osteoblasts (110). In immature rats, ZX50 was used experimentally as femoral pins (1.6mm diameter and 8 mm length). While considerable callus formation occurred during fast degradation of the implants, the bone function was not permanently harmed, and the bone recovered quickly after pin degradation (within 4 to 6 months) (83). The study by Kraus et al. (2011) added weight to the argument that the implants allow full bone recovery after their resorption (83). However, the degradation rate of ZX50 was deemed too rapid, and mechanical stabilization of a fracture might be endangered, as shown by Celarek et al. (2012), who observed full resorption of femoral pins after 3 months in immature rat femurs. In most samples, volcano-shaped bone growth with a hole around the pin was visible at the cortical bone (111). Fischerauer et al. (2013) explored the idea of surface-treating fast-

degrading ZX50 implants with micro-arc oxidation (MAO) to alter their initial degradation rate (84). This process generates an increased oxide layer on the surface without the addition of any new coating material. However, despite displaying minimal corrosion in the first week after implantation in rat femora, these MAO-treated pins exhibited an accelerated degradation rate after the third week, surpassing even that of the untreated ZX50 implants (84). Additionally, the attempt to decrease impurities and use ultrahigh-purity magnesium, zinc, and calcium (99.999%) instead of conventional pure materials (99.95%) as alloying partners for ZX50 did not result in significant differences and did not enhance applicability (112).

1.4.5 Alloy WZ21

This alloy consists of Mg-Y2-Zn1-Ca0.25-Mn0.15, in wt%. It was used experimentally in growing rats, were it degrades slower when compared with ZX50 (83,85). During degradation of alloy WZ21 large amounts of yttrium were measured not only at the pin boundary, but also farer away in cortical bone and in newly formed bone inside the medullary space. The locally high Y concentrations suggest migration of both yttrium and yttrium-containing intermetallic particles. After full degradation of the implant yttrium-enrichment in bone tissues disappeared almost completely (85).

1.4.6 Alloys ZX20 and ZX10

ZX20 consists of Mg-Zn1.5-Ca0.25, in wt%, while ZX10 consists of Mg-Zn1.0-Ca0.3, in wt%. That means they have significantly reduced zinc content compared to ZX50. The decrease in zinc content allows for further modulation of biocorrosion, as zinc received special attention as the most electropositive element. Even a small increase of 0.5 wt.% zinc accelerated the biodegradation rate in both simulated body conditions and in vivo (89). The higher degradation rate of ZX20 compared to ZX10 was observed upon implantation in the femurs of rats, allowing to conclude that zinc content serves as a lever to adjust the degradation rate for desired applications (89).

1.4.7 Alloy ZX00

This alloy has the least amount of Zn added, it consists of Mg–Zn0.45–Ca0.45, in wt%. It was designed without the use of RE elements and is instead exclusively composed of minerals naturally found in the human body. The corrosion rate in vitro testing was slower when compared to alloys with higher Zn concentration (e.g. ZX50, ZX20, WZ21, and

ZX10) (87,113). It has an average tensile strength of 283.6 ± 5.0 MPa, and the average elongation at fracture was determined to be 18.2 ± 2.1% (56). The implant volume reduction of 3.5 mm ZX00 screws amounted to 10% after 3 months in sheep (87). Subsequently, after 13 months, the reduction ranged from 41% to 57%, and after 25 months, it reached 61% to 72% in the same animal model (114). In a growing rat model, implant volume decrease was 19% after 6 months, mathematically projecting full resorption beyond 2 years (115). In 2018/2019, ZX00 screws were utilized in the treatment of medial malleolar fractures in 20 patients (note: the current work is a follow-up of these patients), demonstrating excellent clinical outcomes at the 3-month (56), 1-year (116), and 2½-year follow-up assessments (114).

2 METHODS

2.1 Study Design

The follow-up study uses long-term imaging data from a pilot study (n=20) in which patients were treated with ZX00 magnesium-based screws for medial malleolar fractures (56,114,116). Most cases (n=17) included additional conventional implants (screws and plates), many of which were removed in a second surgery. Final radiographs were obtained approximately 2½ years post-surgery, while CT scans, including high-resolution CT (HR-CT), were performed around 3½ years.

This thesis presents longitudinal data from 18 patients, all of whom have complete radiographs, and 15 have follow-up CT scans, including six high-resolution CTs (HR-CT). For the first time, the long-term behavior of ZX00 screws is described using both two- and three-dimensional imaging techniques. Additionally, the different post-hardware removal scenarios (short vs. long implant residence) allow for the exploration of microarchitectural changes. Clinical assessments of pain and function at the 2½-year mark further support the imaging data.

2.2 Ethical Approval

The study was registered with the local Ethics committee under 28 to 071 ex 15/16. We adhered to the principles of good clinical practice (GCP) and the Declaration of Helsinki (117).

2.3 Patients

The follow-up data was retrieved from the hospital's patient registry and PACS (picture archiving and communication system). The initial prospective cohort of 20 patients (11 males, 9 females) had a mean age of 40.1 ± 14.5 years at the time of surgery (56). All were treated with either one or two ZX00 screws at the medial malleolus between July 2018 and October 2019. All patients were otherwise healthy and between 18 and 65 years of age with ankle injuries including medial malleolar fractures. The type of injuries were

three isolated medial malleolar fractures, two bimalleolar fractures, ten trimalleolar fractures and five Maisonneuve fractures.

2.4 Implant (ZX00)

The material designated as ZX00, in accordance with ASTM standards, comprises ultra-high purity magnesium (99.99%), alloyed with zinc and calcium (0.45 wt% each) at 750°C. This alloying process was conducted jointly by ETH Zürich and de Cavis AG (both based in Switzerland). Subsequently, the material was extruded into 6 mm rods and machined into non-cannulated, distally threaded screws using CNC machining. The screws, 40 mm long and 3.5 mm in diameter, had an original volume of 243.3 mm^3, and were later sterilized and packaged (56,87). The alloy exhibits an ultimate tensile strength of 285.7 ± 3.1 MPa, an elongation at fracture of 18.2 ± 2.1% (87).

2.5 Surgery

The surgical steps followed the established procedure, including open reduction of the medial malleolar fracture, placement of two parallel temporary guide wires, cannulated drilling (2.7 mm), and final fixation with one or two ZX00 screws. All implanted ZX00 screws were 3.5 mm in diameter, 40 mm in length, and used according to the lag screw principle, with the distal threads engaging the trabecular bone. This created a stable construct with compression at the medial malleolar fracture, resulting in a typical screw placement: an 'anterior screw' positioned forward and a 'posterior screw' positioned further back. Accompanying fractures at the lateral and/or the posterior malleolus were stabilized by conventional titanium implants. The ankle was immobilized in an under-knee plaster cast for up to 6 weeks after surgery. In cases of syndesmotic instability, one or two conventional fully-threaded 3.5 mm screws were used as fibulo-tibial positioning screws, which were subsequently removed after approximately 6 to 8 weeks. Further conventional hardware removal (plates/screws) around the ankle was performed due to hardware irritation or at the patient's request, and always after a minimum of 1 year post-surgery.

2.6 Follow-up

2.6.1 2½ years: Clinical Follow-up

The clinical assessment was conducted at an average of 2½ years, with individual timeframes ranging from 1 year 6 months to 3 years 7 months. This variation was primarily due to challenges in scheduling follow-up appointments, particularly during the COVID-19 pandemic restrictions in 2020/2021. One patient (5%) was lost to follow-up after 3 months due to lack of contact, and another patient (5%) was excluded after undergoing surgery for an osteochondral lesion of the talus 17 months following ZX00 implantation (118). Consequently, comprehensive assessments were completed for 18 of the initial 20 patients. The clinical evaluation focused on identifying various complications such as skin or scar issues, infections, hypersensitivity reactions, complex regional pain syndrome (CRPS), malalignment, and the need for revision surgery. The range of motion (ROM) of the ankle was measured using a standard goniometer to assess dorsal and plantar flexion. PROMs included pain at rest, assessed using the Visual Analog Scale (VAS) (range 0 to 100), where higher scores indicate greater pain levels, and the American Orthopaedic Foot and Ankle Society (AOFAS) hindfoot score, which measures pain and function, with higher scores (maximum 100) reflecting lower pain levels and improved function.

2.6.2 2½ years: Radiographic Follow-up

Simultaneously with the clinical assessment, radiographs were performed for the 18 patients, with final radiographs taken around the 2½-year mark (range: 1 year 6 months to 3 years 7 months) after ZX00 screw implantation. Additionally, earlier radiographs obtained at 2 weeks, 6 weeks, 12 weeks, and 1 year were used to establish a baseline and monitor the radiographic dynamics of ZX00 screw resorption. Standardized anteroposterior ankle radiographs were evaluated for screw degradation (e.g., screw visibility, gas formation) and bone texture (radiographic homogeneity at the ZX00 screw implantation site). Assessment criteria utilized a semi-quantitative approach: screw visibility and gas formation were categorized as 'clearly visible', 'partially visible', or 'not visible', and the radiographic appearance of bone texture at the implantation site was graded as 'inhomogeneous', 'slightly inhomogeneous', or 'homogeneous'.

2.6.3 3½ years: CT Follow-up

Follow-up CT imaging, including both clinical CT and HR-CT, was performed on 15 of the 18 available patients, with an average follow-up period of 3½ years (range: 2 years 3 months to 4 years 6 months). These CT scans were used to identify trabecular changes (voids) at the ZX00 screw implantation sites, as well as screw holes after the removal of conventional hardware.

The HR-CT subgroup, consisting of six patients, enabled precise measurement of structural changes. HR-CT scans were performed between 2 and 3 years post-ZX00 implantation (range: 2 years 3 months to 2 years 11 months). This timeframe was particularly relevant as radiographs indicated potential screw resorption during this period (114). Patient selection for HR-CT was based on their willingness to undergo this supplementary examination. The HR-CT scans were performed using an XtremeCT II scanner (SCANCO Medical AG, Switzerland). Patients were positioned in a leg measurement cast, and the scanning area was precisely selected to cover the ZX00 implantation site from the most distal part of the tibia. During evaluation, bone outlines were manually contoured, and zones with trabecular voids (absent bone) at the implantation sites were delineated and treated as separate entities. Trabecular voids were quantified in cubic millimeters, and a three-dimensional representation of these voids was generated.

3 RESULTS

3.1 Synopsis

Table A. Implants, hardware removal, and follow-up CT scans

Implant type	Specification	Cases	Surgical removal	%	Cases with CT Follow-up	Remark
Conventional	Fibulo-tibial positioning screw(s)	9 patients	9	100%	6	see Fig. 1d, 4d-5d, 16d, and 19-20d
Conventional	Metal plate(s)	14 patients	8*	57%	6	see Fig. 5d, 8-10d, 12d, and 17d
Bioresorbable	ZX00 screw(s)	20 patients	1**	5%*	15	see Fig. 1c-5c, 8c-10c, 12c, 14c-17c, and 19c-20c
* Metal plates were removed after a median of 1½ years (range: 1.2 to 3 years)						
** Pat. 6 underwent talus OCL surgery after 17 months. During medial malleolar osteotomy, the resorbing ZX00 screws were exposed and extracted (see Fig. 6c).						

Table B. Clinical Outcomes

Subject of interest	Assessment method	Time interval	Cases	Observation	Result	Remark
Complications	Clinical	2½ years	18 patients	Without complication	100%	Definition: Skin/scar issues, infections, hypersensitivity reactions, CRPS, malalignment, need for revision surgery.
				With complication	0%	
Pain	Clinical	2½ years	18 patients	VAS (range 0-100)	1 ± 0	Lower values mean less pain.
Function	Clinical	2½ years	18 patients	AOFAS (range 0-100)	94 ± 5	Higher values mean better funcion.
				Ankle dorsal flexion, °	22 ± 6	
				Ankle plantar flexion, °	47 ± 5	

Table C. Imaging findings (radiographs, CT and HR-CT scans)

Subject of interest	Assessment method	Time interval	Cases	Observation	n	%	Remark
Subcutaneous Gas Formation	Radiographs	first 6 weeks	20 patients	Visible	8	40%	see Fig. 1c, 9c-10c, 13c-14c, 16c-17c, and 19c
				Not visible	12	60%	
ZX00 Screw Visibility	Radiographs	2½ years	18 patients	Not visible	17	94%	see Fig. 1c-5c, 7c-8c, 9c, and 12c-20c
				Partially visible	1	6%	see Fig. 10c. This final radiograph is at 1 year 9 months.
Bone Texture at ZX00 Implantation Site	Radiographs	2½ years	18 patients	Homogeneous	15	83%	see Fig. 1c-5c, 7c-9c, 12c, 14c-15c, and 17c-20c
				Slightly inhomogeneous	3	17%	see Fig. 10c, 13c, and 16c
Arthritic Changes (post-traumatic)	Radiographs	2½ years	18 patients	Mild changes	5	28%	see Fig. 7c, 12c-13c, 16c, and 17c
				Moderate changes	2	11%	see Fig. 9c, and 19c
Degree of ZX00 resorption	HR-CT	2 to 3 years	6 patients	Traces of ZX00	5	83%	see Fig. 1d-2d, 4d, 10d, and 14d
				No traces of ZX00	1	17%	see Fig. 8d
Bone Microarchitecture after Hardware Removal	CT	3½ years	11 patients (12 sites)	Screw holes in trabecular bone	12	100%	see Fig. 1d, 4d, 5d(2x), 8d-10d, 12d, 16d-17d, and 19d-20d
				Restitutio ad integrum	-	0%	
Bone Microarchitecture at ZX00 Implantation Site	CT	3½ years	15 patients	Voids in trabecular bone	15	100%	see Fig. 1c-5c, 8c-10c, 12c, 14c-17c, and 19c-20c
				Restitutio ad integrum	-	0%	

Table D: Volumetric measurement of post-ZX00-resorption voids.

Void volume (mm^3) Anterior screw	**Void volume** (mm^3) Posterior screw	**Remark**
696.5	367.2	see Fig. 1d
1030.9	1109.1	see Fig. 2d
287.0	-	see Fig. 4d. Note that Patient 4 received a single ZX00 screw.
720.0	447.6	see Fig. 8d
377.3	239.2	see Fig. 10d
708.4	574.0	see Fig. 14d
Average void volume: 596.2 ± 275.7 mm^3; initial ZX00 screw volume: 243.3 mm^3; all HR-CT scans were performed 2-3 years after ZX00 implantation.		

3.2 Individual Patient Analysis

The following section shows detailed imaging follow-up information for each patient who underwent ZX00 screw fracture fixation at the medial malleolus as part of the pilot study (3.2.1 to 3.2.20). All 20 cases presented. It is worth noting that Patient 6 was excluded after 17 months, and Patient 11 was lost to follow-up after 3 months. Therefore, a complete radiographic follow-up spanning around 2½ years is provided for 18 cases, with CT (and HR-CT) follow-up around 3½ years conducted in 15 cases.

3.2.1 Patient 1

Figure 1a. The injured ankle

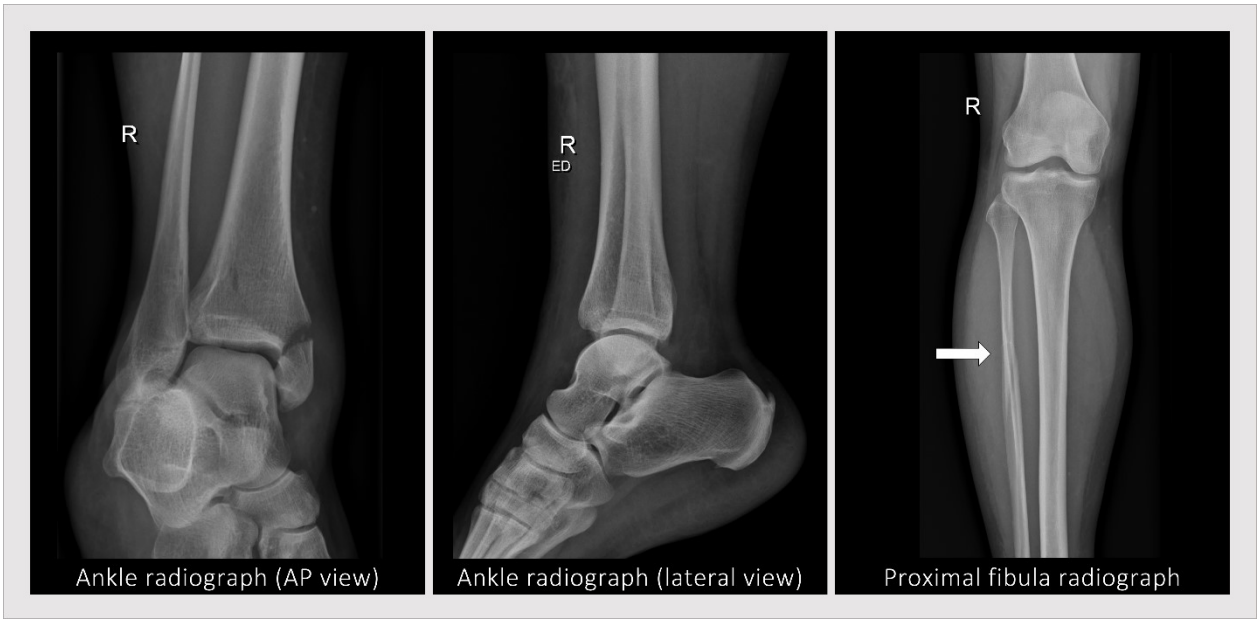

A 47-year-old female patient with a right Maisonneuve injury. Adapted from (56).

Figure 1b. Timeline

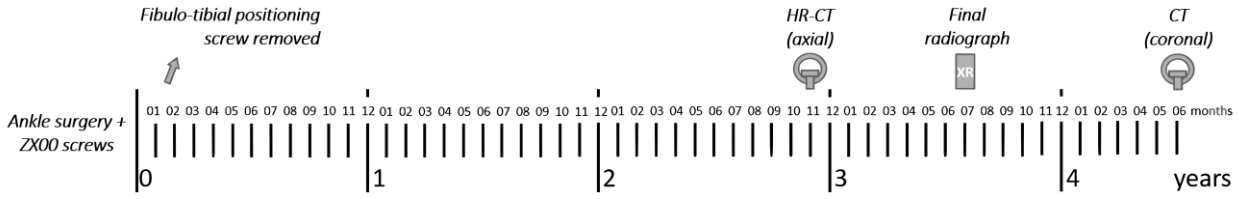

Patient 1 underwent treatment with two ZX00 screws for medial malleolar fracture and a fibulo-tibial positioning screw for syndesmotic injury. The fibulo-tibial positioning screw was removed 50 days after surgery, and no further metal removal was performed.

Table 1. Comprehensive analysis of imaging follow-up of Patient 1

Imaging Method	Technique	Timepoint	ZX00 Screw Visibility	Bone Texture at ZX00 Implantation Site	Bone Microarchitecture at ZX00 Implantation Site	Interpretation
				as it appears on radiographs	*as observed on CT*	
Radiographs	AP view	6 weeks	Clearly visible	Inhomogeneous	N/A	Resorption in progress.
	AP view	1 year	Partially visible	Inhomogeneous	N/A	Resorption and bone remodeling in progress.
	AP view	2 years (final)	Not visible	Homogeneous	N/A	Adjacent bone remodeling increased radiopacity, masking the voids in the trabecular bone.
CT	Axial HR-CT	2 years 3 months	Not visible (only traces)	N/A	Voids in trabecular bone	Resorption left voids in trabecular bone.
	Coronal CT	3 years 4 months	Not visible	N/A	Voids in trabecular bone	Resorption left voids in trabecular bone.

For comparison, see Fig. 1c-d.

Figure 1c. Radiological follow-up (AP)

The radiograph at 2 weeks illustrates the postoperative situation. At that time-point, subcutaneous gas from ZX00 degradation can be seen. The final radiograph was performed at 3 years 7 months, and the coronal CT at 4 years 6 months. Adapted from (56), and (114) with permission from Wolters Kluwer Health Inc.

Figure 1d. HR-CT (axial) and 3D reconstruction

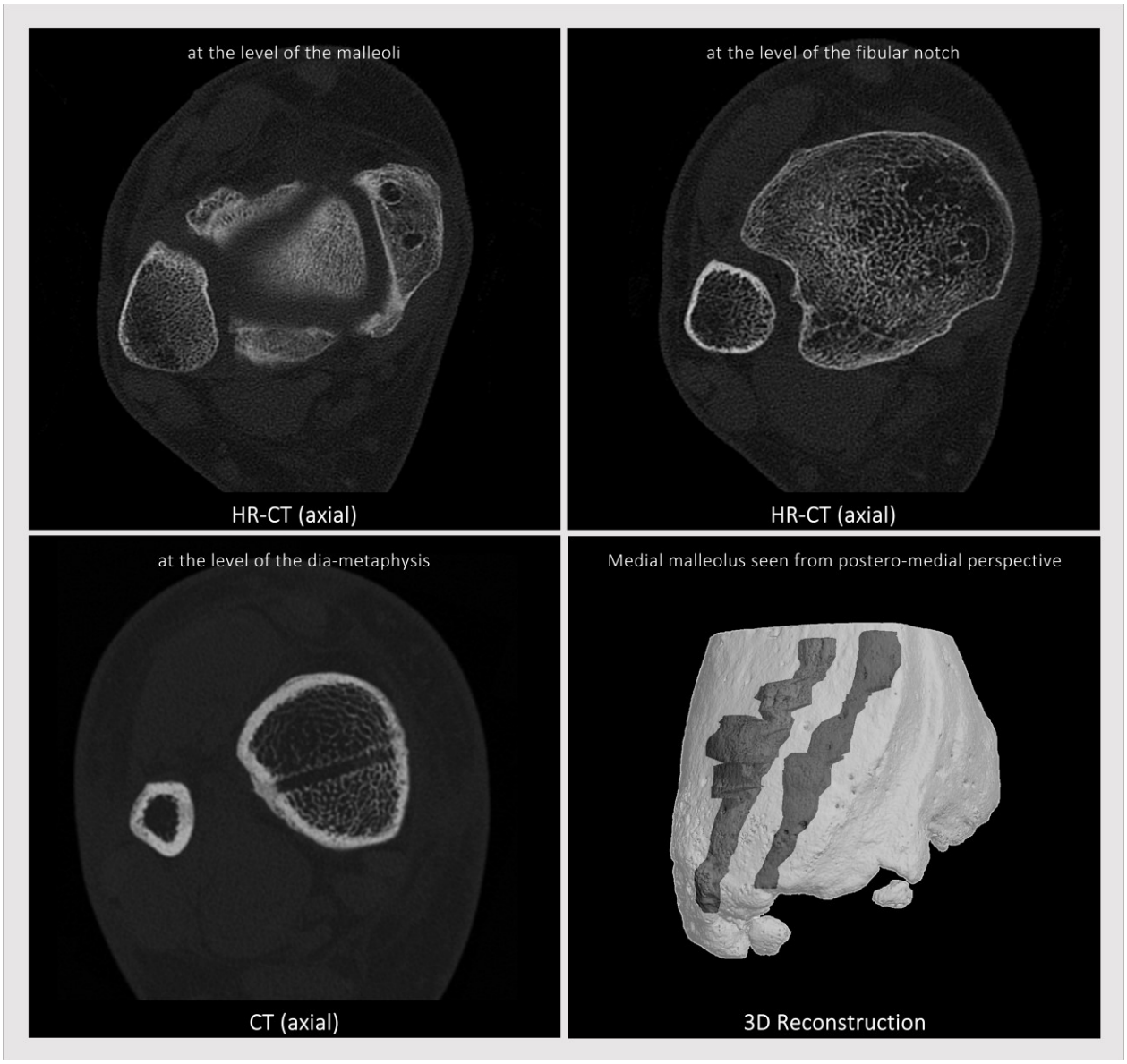

The axial plane HR-CT was performed at 2 years and 11 months. Traces of ZX00 are detectable within a sharply defined trabecular void (upper left). Moreover, the screw hole within the trabecular bone following removal of the fibulo-tibial positioning screw persists (lower left), while the cortical bone has completely healed in that region. The 3D reconstruction illustrates the extent of the trabecular voids after ZX00 resorption (anterior void: 696.5 mm^3, posterior void: 367.2 mm^3).

3.2.2 Patient 2

Figure 2a. The injured ankle

A 55-year-old female patient with a right trimalleolar injury.

Figure 2b. Timeline

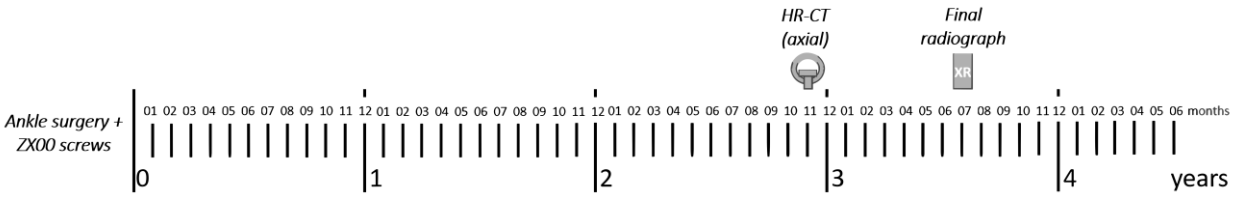

The medial malleolar fracture was treated with two ZX00 screws and the lateral malleolar fracture was treated with two lag screws and a one-third tubular plate. Hardware removal was not done.

Table 2. Comprehensive analysis of imaging follow-up of Patient 2

Imaging Method	Technique	Timepoint	ZX00 Screw Visibility	Bone Texture at ZX00 Implantation Site	Bone Microarchitecture at ZX00 Implantation Site	Interpretation
				as it appears on radiographs	*as observed on CT*	
Radiographs	AP view	6 weeks	Clearly visible	Inhomogeneous	N/A	Resorption in progress.
	AP view	1 year	Partially visible	Inhomogeneous	N/A	Resorption and bone remodeling in progress.
	AP view	3 years 7 months (final)	Not visible	Homogeneous	N/A	Adjacent bone remodeling increased radiopacity, masking the voids in the trabecular bone.
CT	Axial HR-CT	2 years 11 months	Not visible (only traces)	N/A	Voids in trabecular bone	Resorption left voids in trabecular bone.

For comparison, see Fig. 2c-d.

Figure 2c. Radiological follow-up (AP)

The radiograph at 2 weeks illustrates the postoperative situation with the ankle in a plaster cast. The final radiograph was performed at 3 years 7 months, but no coronal plane CT was available. Adapted from (56).

Figure 2d. HR-CT (axial) and 3D reconstruction

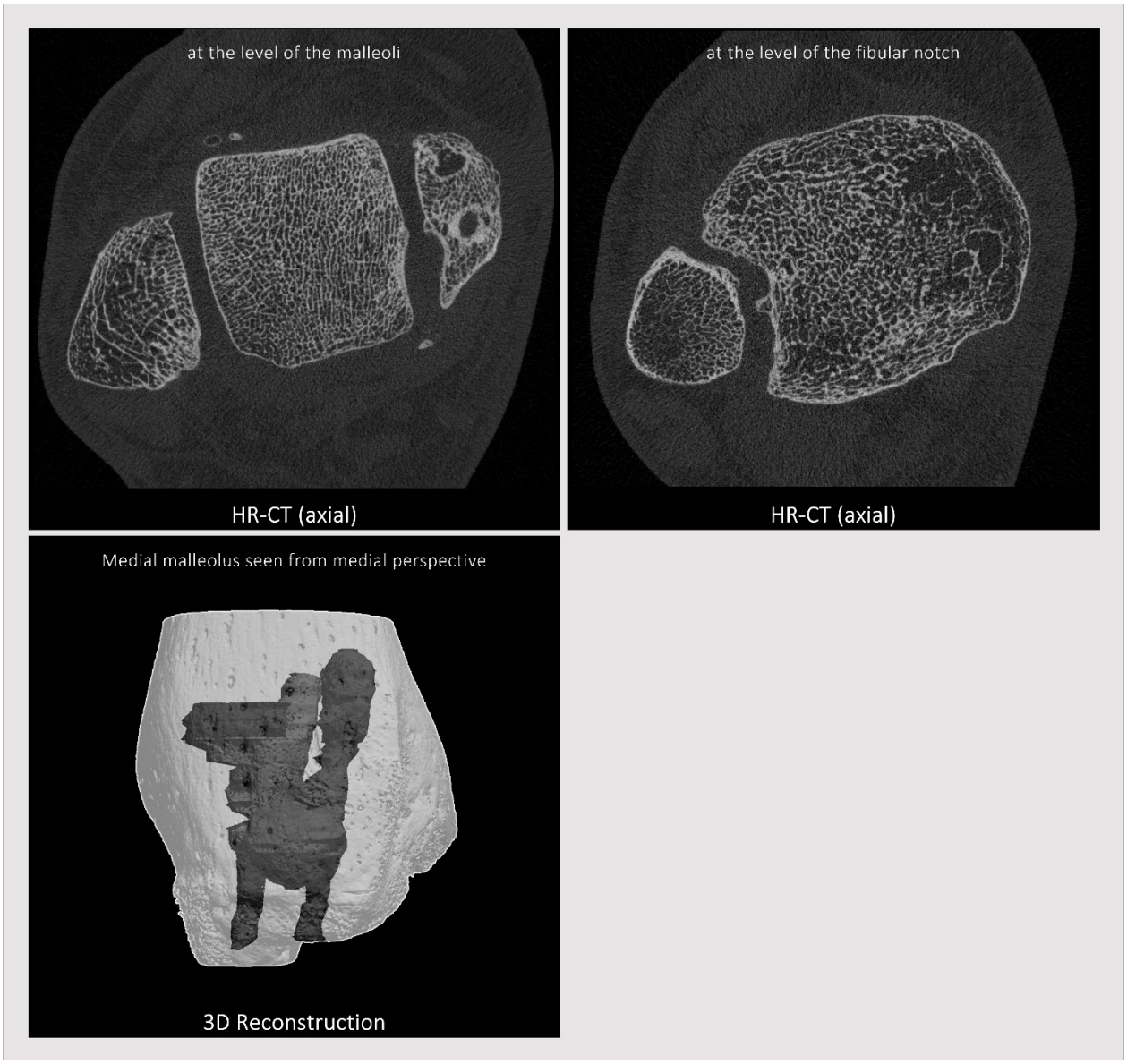

The axial plane HR-CT was performed at 2 years and 11 months. Traces of ZX00 are discernible within a well-circumscribed trabecular void (upper left).The 3D reconstruction shows the extent of trabecular voids (anterior void: 1030.9 mm^3, posterior void: 1109.1 mm^3).

3.2.3 Patient 3

Figure 3a. The injured ankle

A 57-year-old female patient with a right trimalleolar injury.

Figure 3b. Timeline

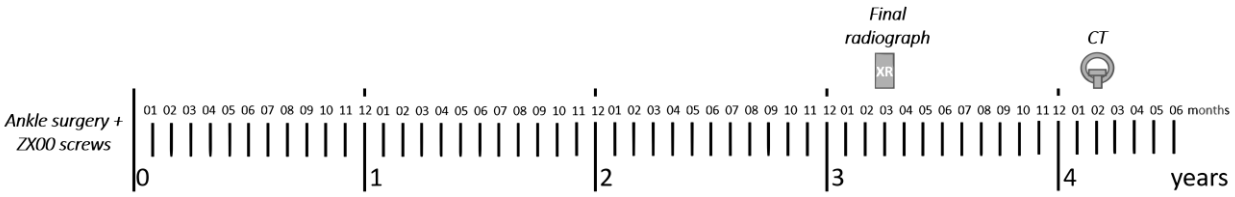

Two ZX00 screws were inserted at the medial malleolus and a lag screw and one-third tubular plate were implanted at the lateral malleolus. Hardware was not removed.

Table 3. Comprehensive analysis of imaging follow-up of Patient 3

Imaging Method	Technique	Timepoint	ZX00 Screw Visibility	Bone Texture at ZX00 Implantation Site	Bone Microarchitecture at ZX00 Implantation Site	Interpretation
				as it appears on radiographs	*as observed on CT*	
Radiographs	AP view	6 weeks	Clearly visible	Inhomogeneous	N/A	Resorption in progress.
	AP view	1 year	Partially visible	Inhomogeneous	N/A	Resorption and bone remodeling in progress.
	AP view	3 years 3 months (final)	Not visible	Homogeneous	N/A	Adjacent bone remodeling increased radiopacity, masking the voids in the trabecular bone.
CT	Coronal CT	4 years 2 months	Not visible (only traces)	N/A	Voids in trabecular bone	Resorption left voids in trabecular bone.

For comparison, see Fig. 3c-d.

Figure 3c. Radiological follow-up (AP)

The radiograph at 2 weeks illustrates the postoperative situation with the ankle in a splint. The final radiograph was performed at 3 years 3 months, and the CT at 4 years 2 months. Adapted from (114) with permission from Wolters Kluwer Health Inc.

Figure 3d. CT (axial)

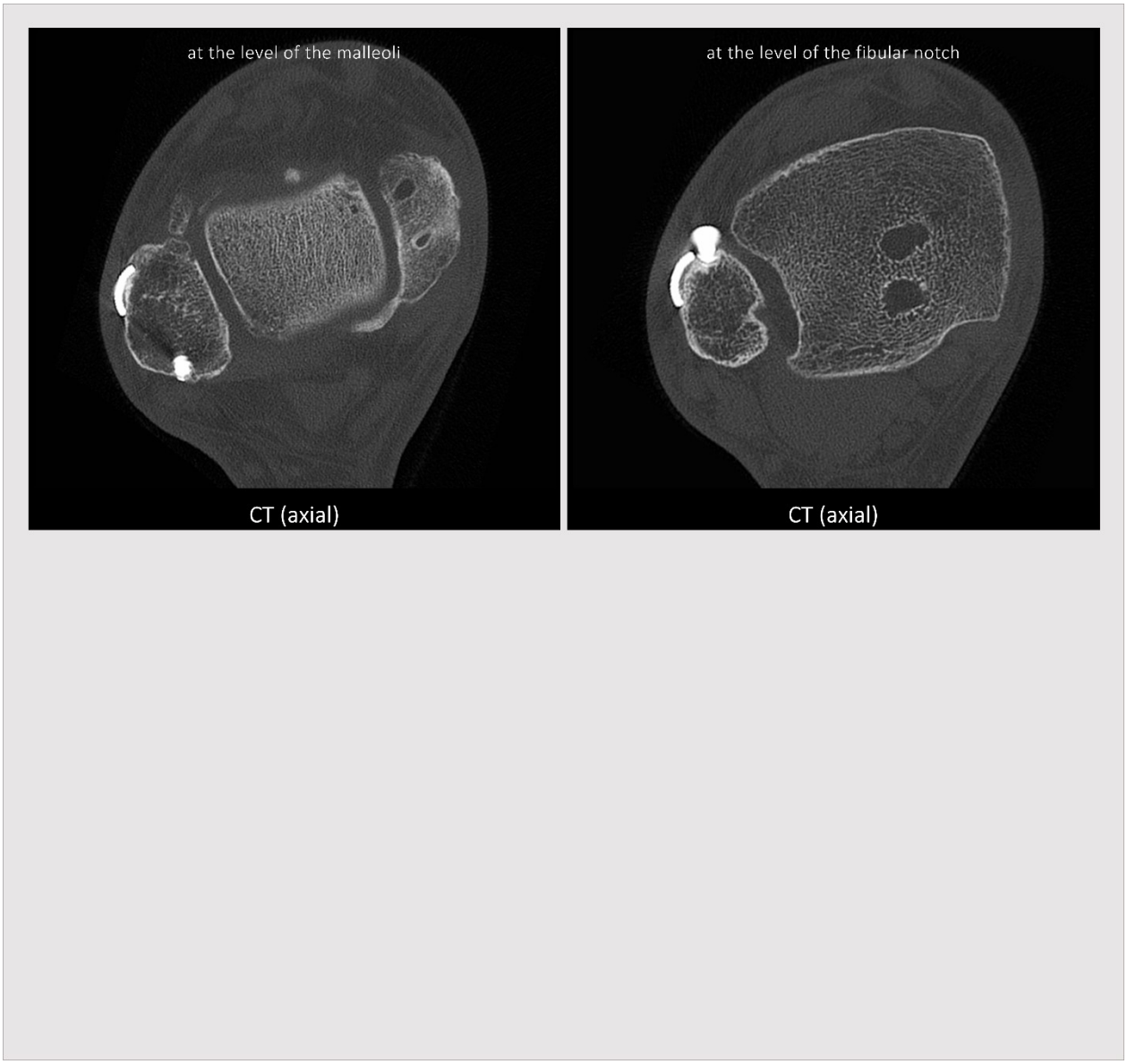

These axial CT scans, performed at 4 years 2 months, reveal two well-defined trabecular voids following ZX00 resorption.

3.2.4 Patient 4

Figure 4a. The injured ankle

A 30-year-old male patient with a right trimalleolar injury.

Figure 4b. Timeline

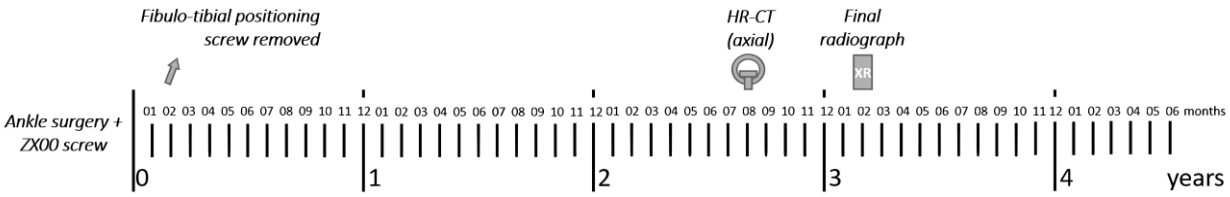

A single ZX00 screw was implanted at the medial malleolus, while a lag screw and a one-third tubular plate were used at the lateral malleolus with a fibulo-tibial positioning screw to stabilize the syndesmotic injury. The fibulo-tibial positioning screw was removed 52 days after surgery, and no further metal removal was performed.

Table 4. Comprehensive analysis of imaging follow-up of Patient 4

Imaging Method	Technique	Timepoint	ZX00 Screw Visibility	Bone Texture at ZX00 Implantation Site	Bone Microarchitecture at ZX00 Implantation Site	Bone Microarchitecture after Hardware Removal	Interpretation
				as it appears on radiographs	*as observed on CT*	*as observed on CT*	
Radiographs	AP view	6 weeks	Clearly visible	Inhomogeneous	N/A	N/A	Resorption in progress.
	AP view	1 year	Partially visible	Inhomogeneous	N/A	N/A	Resorption and bone remodeling in progress.
	AP view	3 years 2 months (final)	Not visible	Homogeneous	N/A	N/A	Adjacent bone remodeling increased radiopacity, masking the voids in the trabecular bone.
CT	Axial HR-CT	2 years 8 months	Not visible (only traces)	N/A	Voids in trabecular bone	Screw holes in trabecular bone	Resorption left voids in trabecular bone. Fibulo-tibial positioning screw removal left a hole in trabecular bone.

For comparison, see Fig. 4c-d.

Figure 4c. Radiological follow-up (AP)

The radiograph at 2 weeks illustrates the postoperative situation with the ankle in a plaster cast. The final radiograph was performed at 3 years 2 months, but no coronal plane CT was available. Adapted from (116).

Figure 4d. HR-CT (axial) and 3D reconstruction

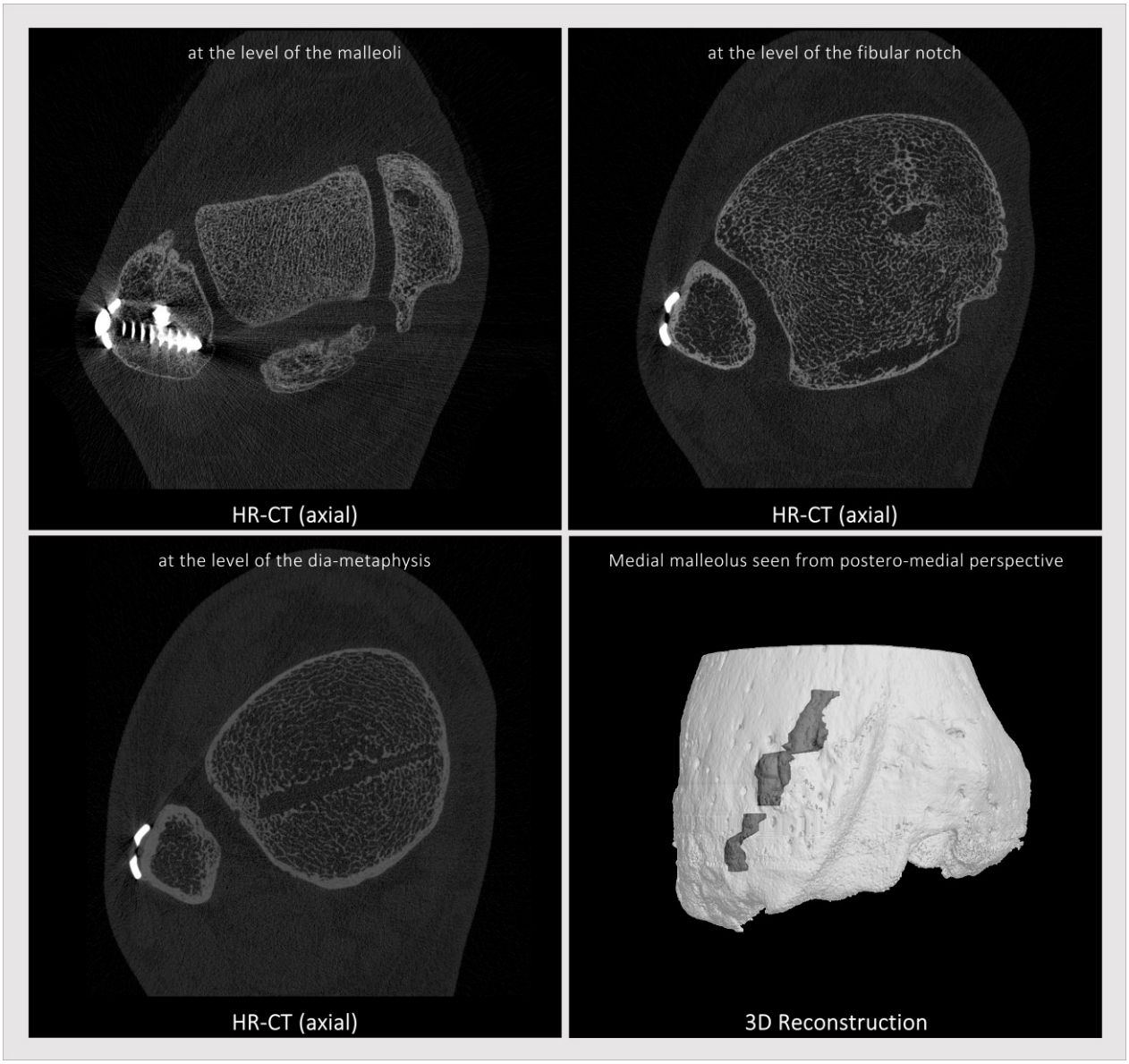

The axial plane HR-CT was performed at 2 years 8 months. Traces of ZX00 are found within a trabecular void (upper left). Interestingly, there is also an absence of trabeculae at the site of the healed fracture in the posterior malleolus (upper right) and after removal of the fibulo-tibial positioning screw (lower left). The cortical bone, however, has completely healed. The 3D reconstruction illustrates the extent of the trabecular void (volume: 287.0 mm^3) after resorption of a single ZX00 screw.

3.2.5 Patient 5

Figure 5a. The injured ankle

A 48-year-old male patient with a right trimalleolar injury.

Figure 5b. Timeline

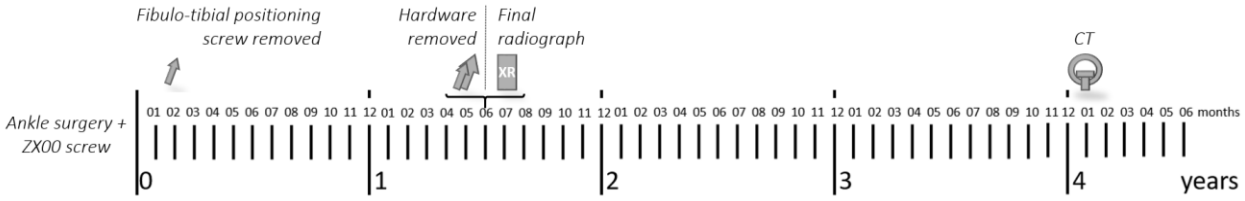

Patient 5 underwent treatment with a single ZX00 screw and a one-third tubular plate to buttress the multifragmentary fracture at the medial malleolus. A lag screw and a one-third tubular plate were used at the lateral malleolus, along with a fibulo-tibial positioning screw for syndesmotic instability. The fibulo-tibial positioning screw was removed 45 days after surgery. Plates were removed after 1 year and 6 months.

Table 5. Comprehensive analysis of imaging follow-up of Patient 5

Imaging Method	Technique	Timepoint	ZX00 Screw Visibility	Bone Texture at ZX00 Implantation Site	Bone Microarchitecture at ZX00 Implantation Site	Bone Microarchitecture after Hardware Removal	Interpretation
				as it appears on radiographs	*as observed on CT*	*as observed on CT*	
Radiographs	AP view	6 weeks	Clearly visible	Inhomogeneous	N/A	N/A	Resorption in progress.
	AP view	1 year	Partially visible	Inhomogeneous	N/A	N/A	Resorption and bone remodeling in progress.
	AP view	1 years 6 months (final)	Not visible	Homogeneous	N/A	N/A	Adjacent bone remodeling increased radiopacity, masking the voids in the trabecular bone.
CT	Axial CT	4 years 1 month	Not visible (only traces)	N/A	Voids in trabecular bone	Screw holes in trabecular bone	Resorption left voids in trabecular bone. Hardware removal left screw holes in trabecular bone.
	Coronal CT	4 years 1 month	Not visible	N/A	Voids in trabecular bone	Screw holes in trabecular bone	Resorption left voids in trabecular bone. Hardware removal left screw holes in trabecular bone.

For comparison, see Fig. 5c-d.

Figure 5c. Radiological follow-up (AP)

The radiograph at 2 weeks illustrates the postoperative situation with the ankle in a plaster cast. The final radiograph was performed at 1 year 6 months, and the coronal CT at 4 years 1 month.

Figure 5d. CT (axial)

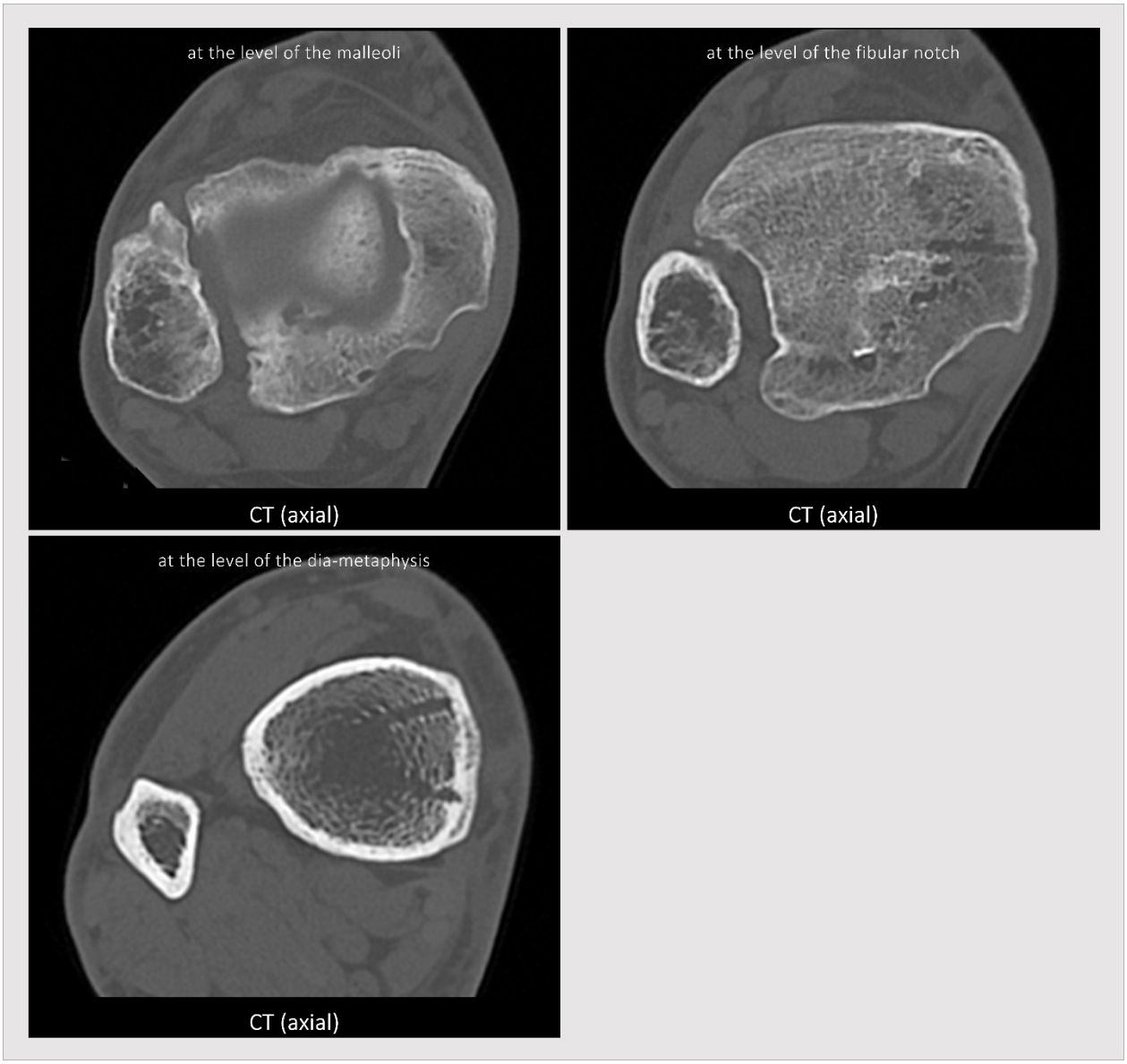

The axial CT scans performed at 4 years and 1 month show irregularities in the trabecular bone. They are linked to the resorption of the ZX00 screw at the medial malleolus (upper left), the healed fracture in the distal tibia (upper right), the removal of the fibulo-tibial positioning screw (lower left), and the plate removal (upper right, lower left).

3.2.6 Patient 6 (excluded)

Figure 6a. The injured ankle

A 45-year-old female with a medial malleolar fracture and an old osteochondral lesion of the talus. Adapted from (116) and (118).

Figure 6b. Timeline

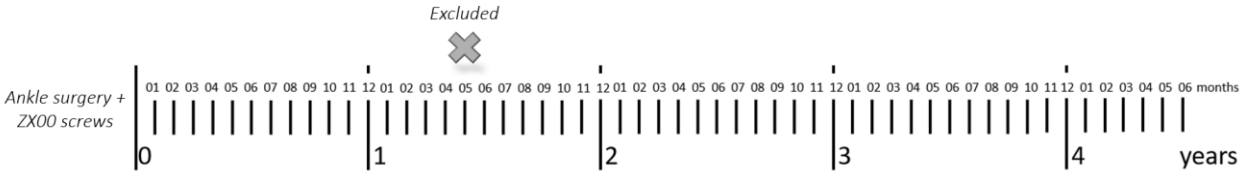

The fracture was treated with two ZX00 screws. However, after 1 year and 5 months, a second surgery became necessary to address a pre-existing, but now symptomatic, osteochondral lesion (OCL) of the talus, leading to the patient's exclusion from follow-up. During the surgery for the OCL, a medial malleolar osteotomy was required at the site of the previous ZX00 implantation, marking the first documented exposure of a resorbing ZX00 implant in a human. The complete case report is available under the provided citation (118).

Figure 6c. Radiological follow-up (AP) and second surgery

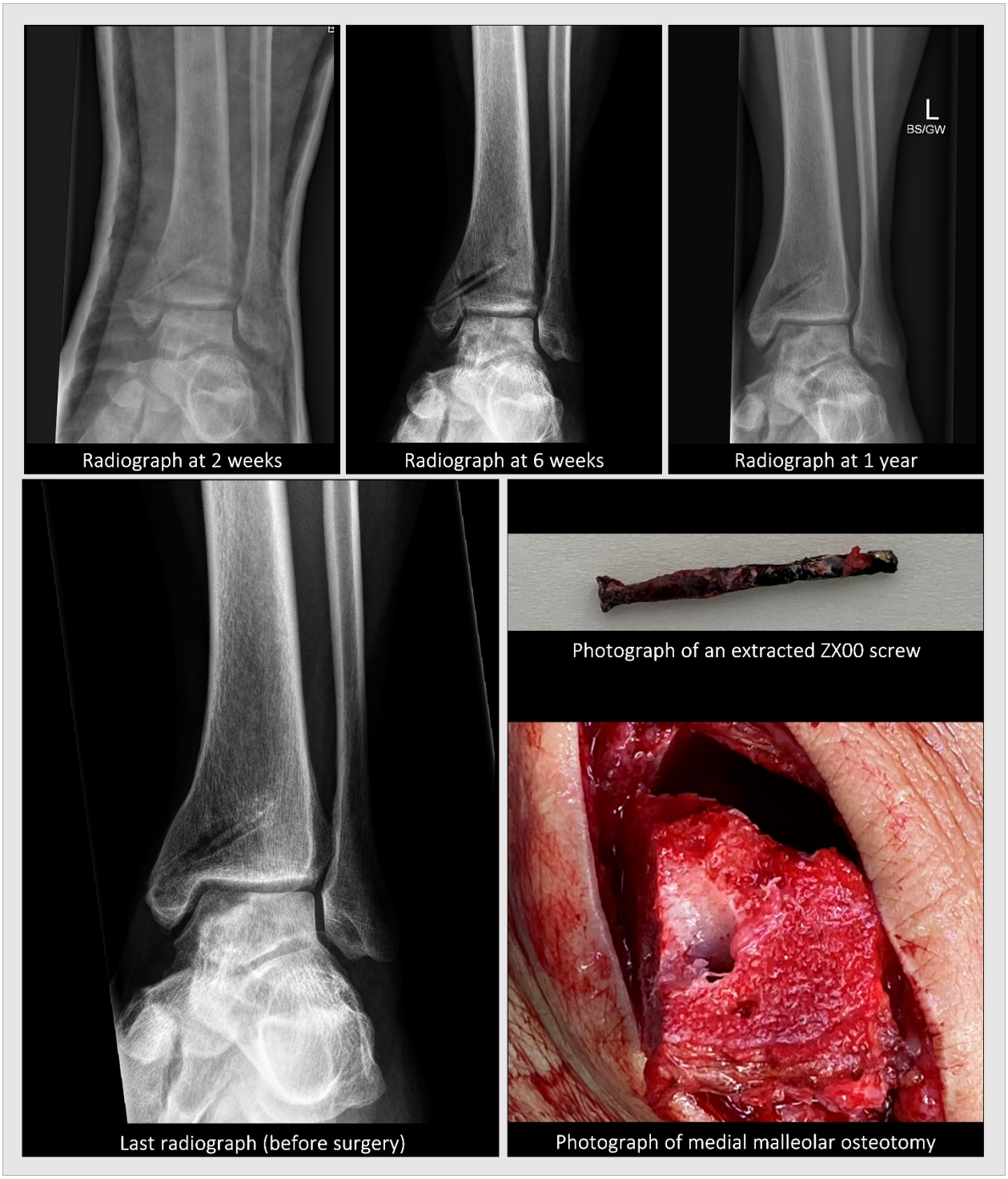

The radiograph at 2 weeks illustrates the postoperative situation with the ankle in a plaster cast. The last radiograph was performed at 1 year and 5 months, just before the second surgery. The second surgery involved a medial malleolar osteotomy for the surgical exposure of a pre-existing osteochondral lesion at the medial talus, thereby extracting the ZX00 screws after overdrilling. Adapted from (118).

This page intentionally left blank.

3.2.7 Patient 7

Figure 7a. The injured ankle

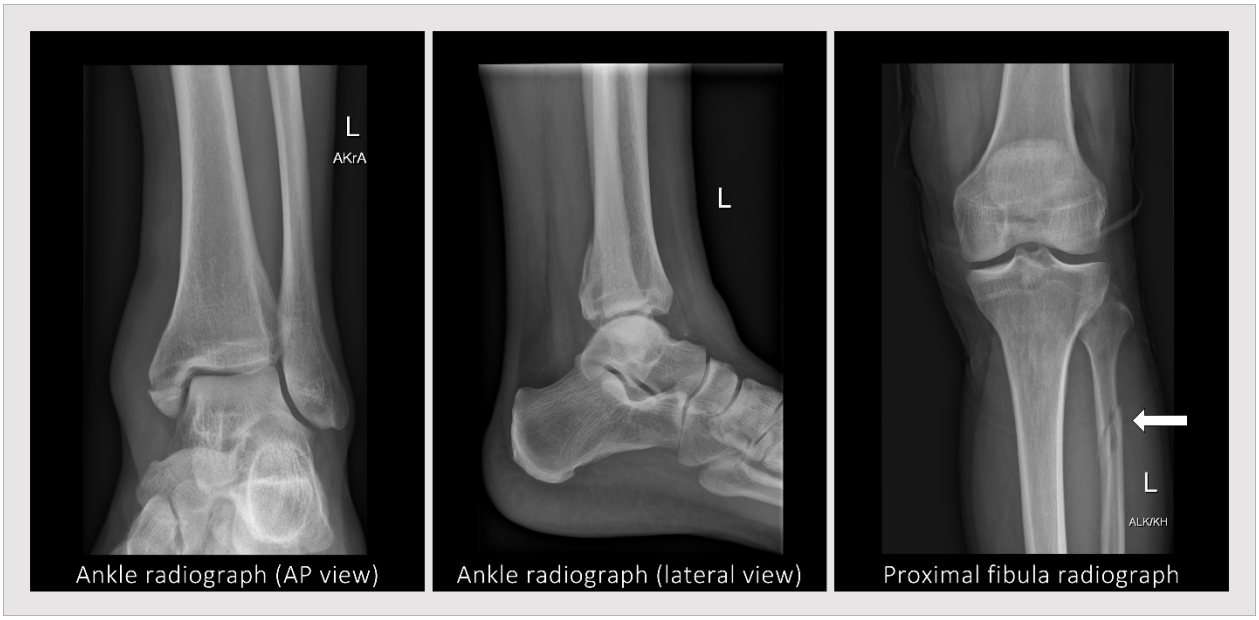

A 46-year-old male patient with a left Maisonneuve injury.

Figure 7b. Timeline

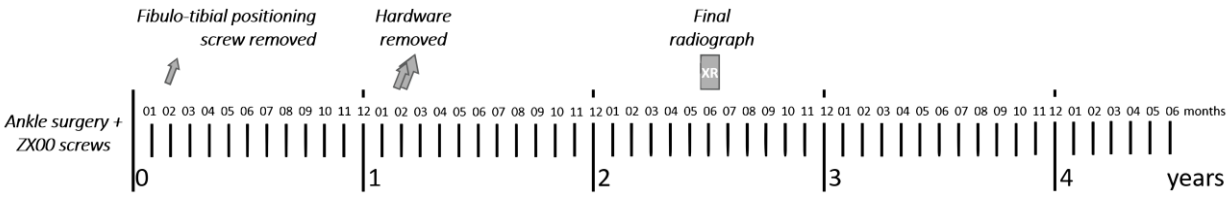

The medial malleolar fracture received two ZX00 and a one-third tubular plate for buttressing, and the syndesmotic injury was addressed with a fibulo-tibial positioning screw. The fibulo-tibial positioning screw was removed after 57 days. Further hardware removal was performed after 1 year and 2 months.

Table 7. Comprehensive analysis of imaging follow-up of Patient 7

Imaging Method	Technique	Timepoint	ZX00 Screw Visibility	Bone Texture at ZX00 Implantation Site	Interpretation
				as it appears on radiographs	
Radiographs	AP view	6 weeks	Partially visible	Inhomogeneous	Resorption in progress.
	AP view	1 year	Not visible	Homogeneous	(This radiograph is difficult to interpret.)
	AP view	2 years 6 months (final)	Not visible	Homogeneous	Adjacent bone remodeling increased radiopacity.

For comparison, see Fig. 7c.

Figure 7c. Radiological follow-up (AP)

The radiograph at 2 weeks illustrates the postoperative situation with the ankle in a plaster cast. The final radiograph was performed at 2 years 6 months, however no CT was conducted. There are mild post-traumatic arthritic changes at final follow-up.

This page intentionally left blank.

3.2.8 Patient 8

Figure 8a. The injured ankle

A 20-year-old male patient with a right trimalleolar injury.

Figure 8b. Timeline

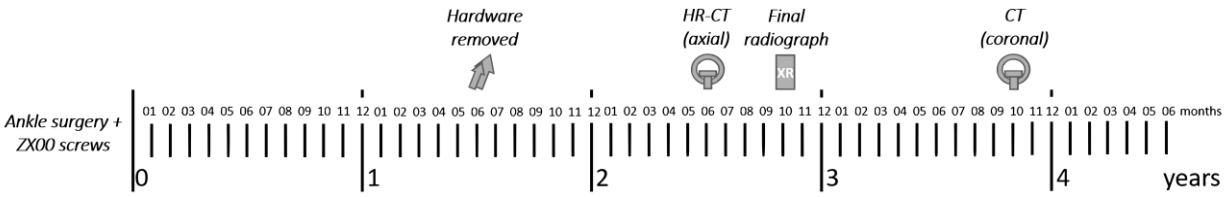

The medial malleolar fracture was treated with two ZX00 screws, lateral and posterior malleolar fractures were treated with locking compression plates (LCP). Hardware removal was performed at 1 year and 6 months.

Table 8. Comprehensive analysis of imaging follow-up of Patient 8

Imaging Method	Technique	Timepoint	ZX00 Screw Visibility	Bone Texture at ZX00 Implantation Site	Bone Microarchitecture at ZX00 Implantation Site	Bone Microarchitecture after Hardware Removal	Interpretation
				as it appears on radiographs	*as observed on CT*	*as observed on CT*	
Radiographs	AP view	6 weeks	Clearly visible	Inhomogeneous	N/A	N/A	Resorption in progress.
	AP view	1 year	Partially visible	Inhomogeneous	N/A	N/A	Resorption and bone remodeling in progress.
	AP view	2 years 10 months (final)	Not visible	Homogeneous	N/A	N/A	Adjacent bone remodeling increased radiopacity, masking the voids in the trabecular bone.
CT	Axial HR-CT	2 years 6 months	Not visible	N/A	Voids in trabecular bone	Screw holes in trabecular bone	Resorption left voids in trabecular bone. Hardware removal left screw holes / screw trajectories in trabecular bone.
	Coronal CT	3 years 10 months	Not visible	N/A	Voids in trabecular bone	Screw holes in trabecular bone	Resorption left voids in trabecular bone. Hardware removal left screw holes in trabecular bone.

For comparison, see Fig. 8c-d.

Figure 8c. Radiological follow-up (AP)

The radiograph at 2 weeks illustrates the postoperative situation with the ankle in a plaster cast. The final radiograph was performed at 2 years 10 months, and the coronal CT at 3 years 10 months. Adapted from (114) with permission from Wolters Kluwer Health Inc.

Figure 8d. HR-CT (axial) and 3D reconstruction

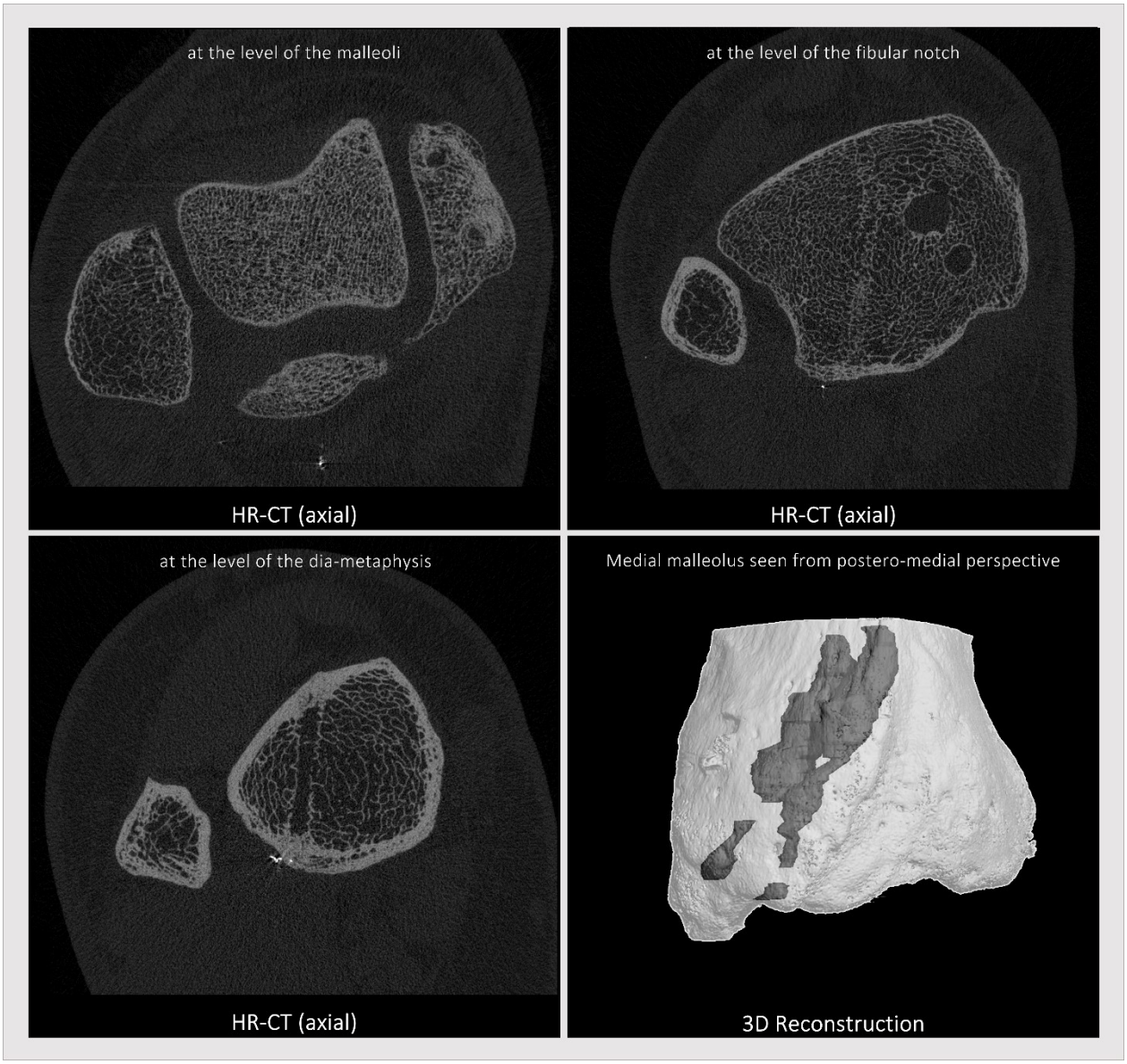

The axial plane HR-CT was performed at 2 years and 6 months, showing intra-trabecular changes for both the ZX00 following resorption at the medial malleolus and the conventional screws following removal. Obviously, a conventional screw hole after removal can either be filled with trabecular bone (upper right) and or not (lower left). The 3D reconstruction shows the extent of trabecular voids (anterior void: 720.0 mm^3, posterior void: 447.6 mm^3).

Of note, in more than 500 axial HR-CT slices of the region of interest, no remnants or traces of ZX00 were found.

3.2.9 Patient 9

Figure 9a. The injured ankle

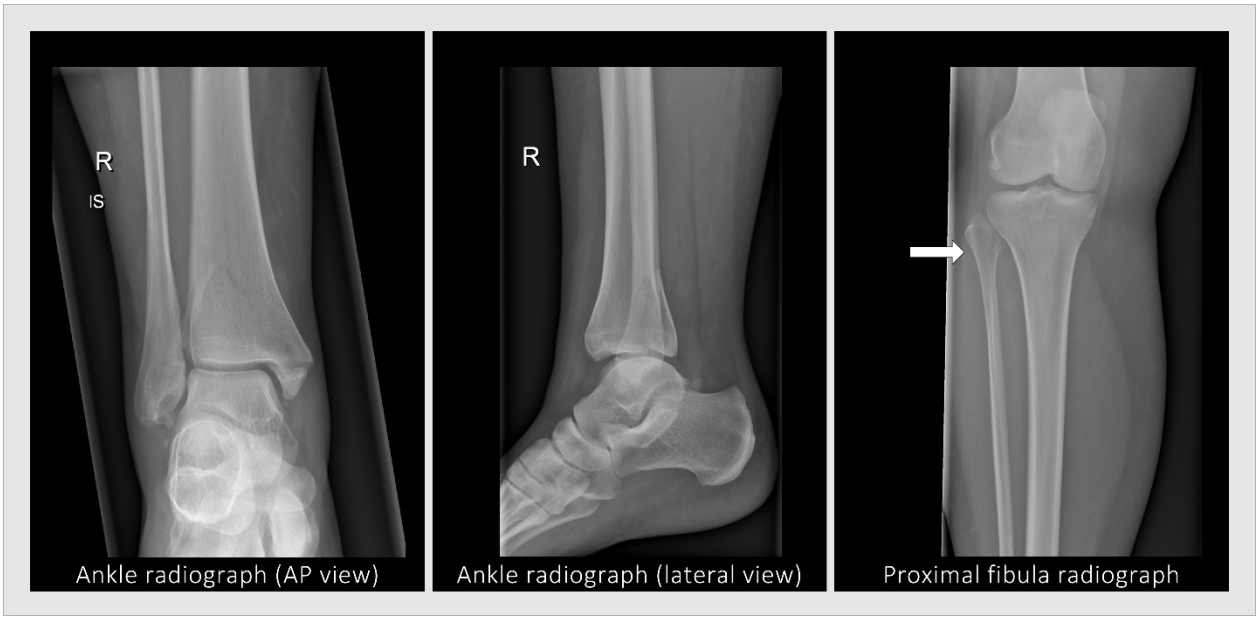

A 43-year-old female patient with a right Maisonneuve injury.

Figure 9b. Timeline

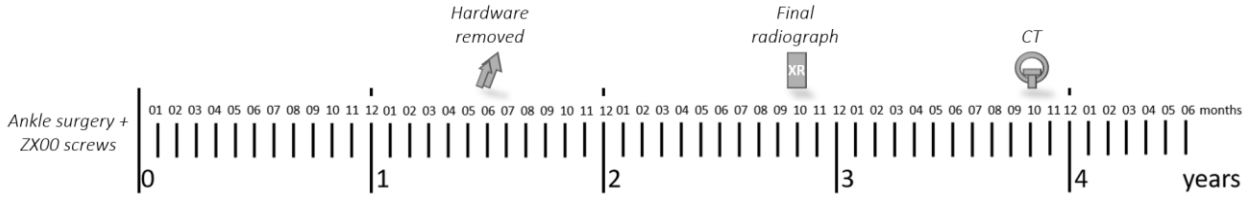

ZX00 screws were implanted at the medial malleolus and the posterior malleolar fracture was treated with a T-shaped locking compression plate (LCP). Hardware was removed after 1 year and 6 months.

Table 9. Comprehensive analysis of imaging follow-up of Patient 9

Imaging Method	Technique	Timepoint	ZX00 Screw Visibility	Bone Texture at ZX00 Implantation Site	Bone Microarchitecture at ZX00 Implantation Site	Bone Microarchitecture after Hardware Removal	Interpretation
				as it appears on radiographs	*as observed on CT*	*as observed on CT*	
Radiographs	AP view	6 weeks	Clearly visible	Inhomogeneous	N/A	N/A	Resorption in progress.
	AP view	1 year	Partially visible	Inhomogeneous	N/A	N/A	Resorption and bone remodeling in progress.
	AP view	2 years 10 months (final)	Not visible	Homogeneous	N/A	N/A	Adjacent bone remodeling increased radiopacity, masking the voids in the trabecular bone.
CT	Axial CT	3 years 10 months	Not visible	N/A	Voids in trabecular bone	Screw holes in trabecular bone	Resorption left voids in trabecular bone. Hardware removal left screw holes in trabecular bone.
	Coronal CT	3 years 10 months	Not visible	N/A	Voids in trabecular bone	Screw holes in trabecular bone	Resorption left voids in trabecular bone. Hardware removal left screw holes in trabecular bone.

For comparison, see Fig. 9c-d.

Figure 9c. Radiological follow-up (AP)

The radiograph at 2 weeks (Fig. 9c) illustrates the postoperative situation. Subcutaneous gas from ZX00 degradation is visible on radiographs up to 6 weeks. The final radiograph was performed at 2 years 10 months, and the CT at 3 years 10 months. There are moderate post-traumatic arthritic changes at final follow-up.

Figure 9d. CT (axial)

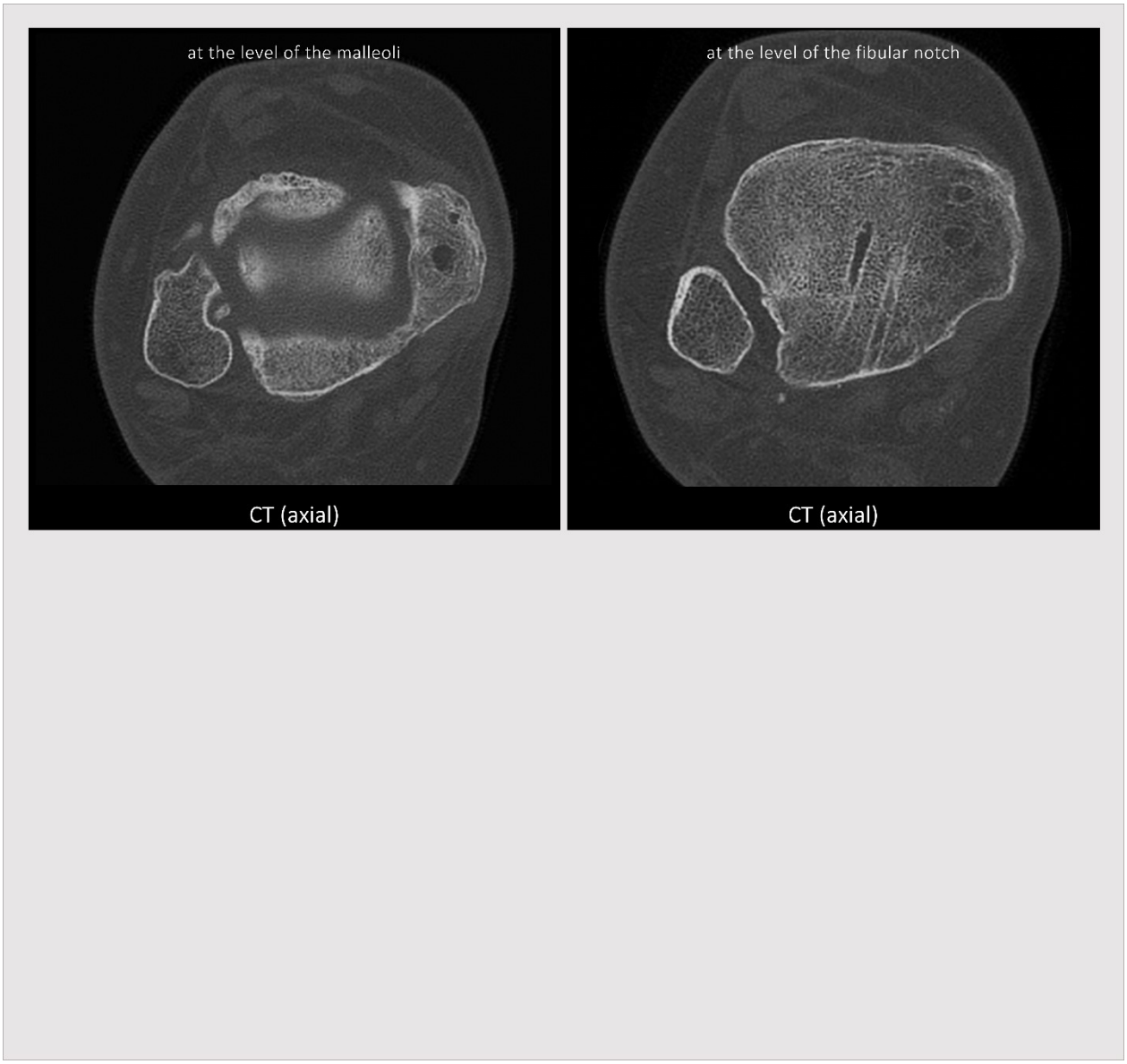

The axial CT, performed at 3 years 10 months, reveals well-defined trabecular voids after ZX00 resorption at the medial malleolus (left). Interestingly, even after more than two years following conventional hardware removal, sclerotic holes can still be observed at the sites of conventional screw placement at the posterior malleolus (right).

3.2.10 Patient 10

Figure 10a. The injured ankle

A 29-year-old male patient with a right bimalleolar injury. Adapted from (116).

Figure 10b. Timeline

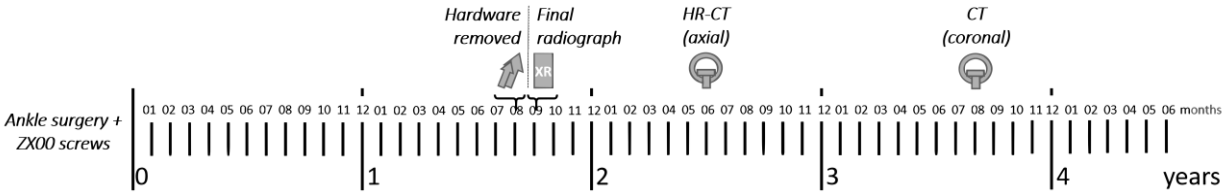

The medial malleolar fracture was treated with two ZX00 screws and the lateral malleolar fracture was treated with a lag screw and a one-third tubular plate. Hardware was removed after 1 year and 8 months.

Table 10. Comprehensive analysis of imaging follow-up of Patient 10

Imaging Method	Technique	Timepoint	ZX00 Screw Visibility	Bone Texture at ZX00 Implantation Site	Bone Microarchitecture at ZX00 Implantation Site	Bone Microarchitecture after Hardware Removal	Interpretation
				as it appears on radiographs	*as observed on CT*	*as observed on CT*	
Radiographs	AP view	6 weeks	Clearly visible	Inhomogeneous	N/A	N/A	Resorption in progress.
	AP view	1 year	Partially visible	Inhomogeneous	N/A	N/A	Resorption and bone remodeling in progress.
	AP view	1 years 9 months (final)	Partially visible	Slightly inhomogeneous	N/A	N/A	Adjacent bone remodeling in progress. The increasing radiopacity partially masks the voids in the trabecular bone.
CT	Axial HR-CT	2 years 6 months	Not visible (only traces)	N/A	Voids in trabecular bone	Screw holes in trabecular bone	Resorption left voids in trabecular bone. Hardware removal left screw holes in trabecular bone.
	Coronal CT	3 years 8 months	Not visible	N/A	Voids in trabecular bone	Screw holes in trabecular bone	Resorption left voids in trabecular bone. Hardware removal left screw holes in trabecular bone.

For comparison, see Fig. 10c-d.

Figure 10c. Radiological follow-up (AP)

The radiograph at 2 weeks illustrates the postoperative situation with the ankle in a plaster cast. Subcutaneous gas is seen at 6 weeks. The final radiograph was performed at 1 years 9 months, and the coronal CT at 3 years 8 months. Adapted from (116).

Figure 10d. HR-CT (axial) and 3D reconstruction

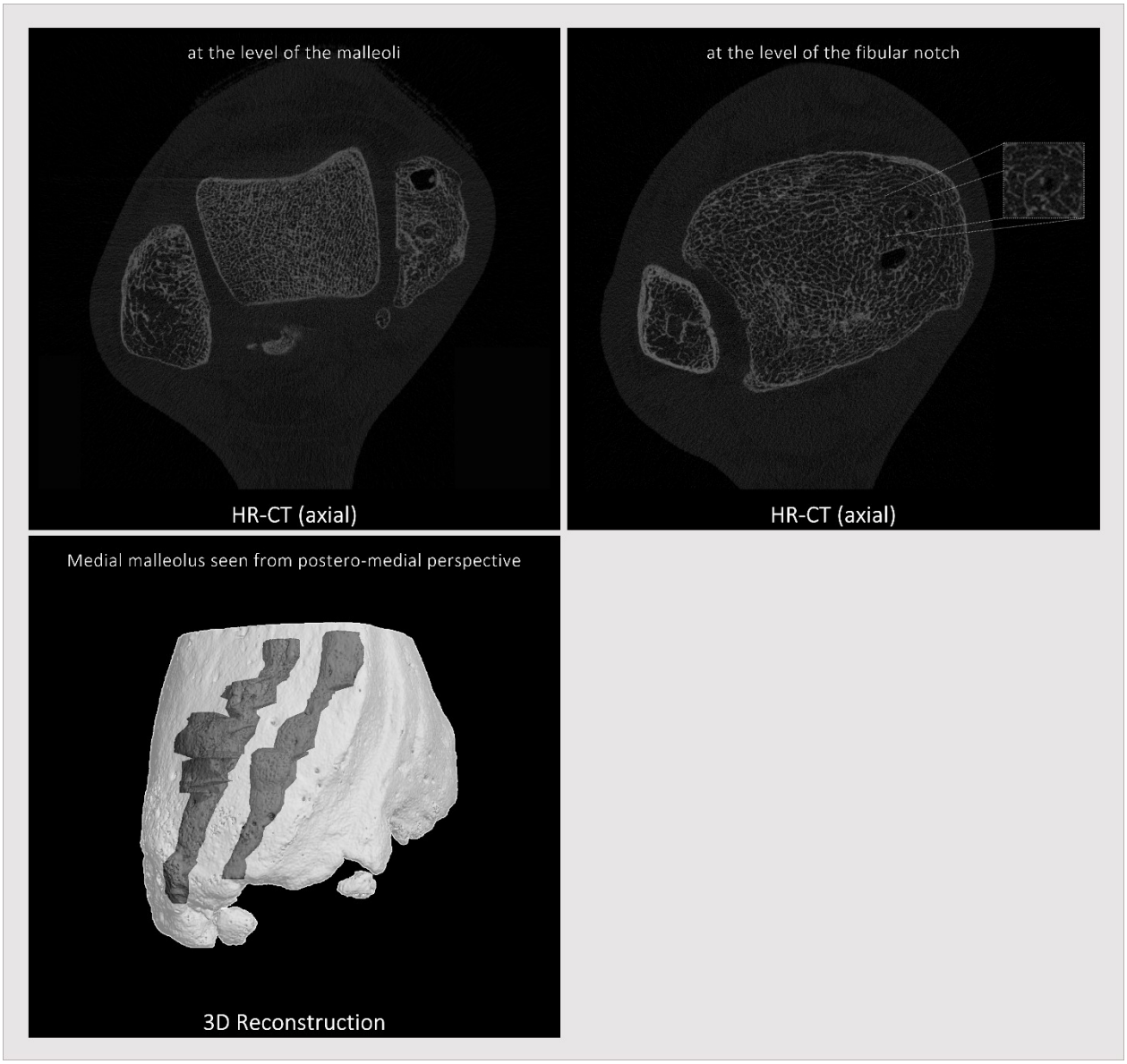

The HR-CT with axial planes was performed after 2 years 6 months. Remnants or traces of ZX00 screws within the trabecular void are visible at this time-point (upper left). The 3D reconstruction of the HR-CT illustrates the extent of absent trabeculae (anterior void: 377.3 mm^3, posterior void: 239.2 mm^3). The trabecular voids appear black (gas?) and grey (fluid?, see magnification, upper right), indicating ongoing ZX00 resorption in this case. Notably, at the lateral malleolus, where the conventional screws were placed, changes in microarchitecture are evident ten months after their removal.

3.2.11 Patient 11 (lost to follow-up)

Figure 11a. The injured ankle

An 18-year-old female patient with a left trimalleolar injury.

Figure 11b. Timeline

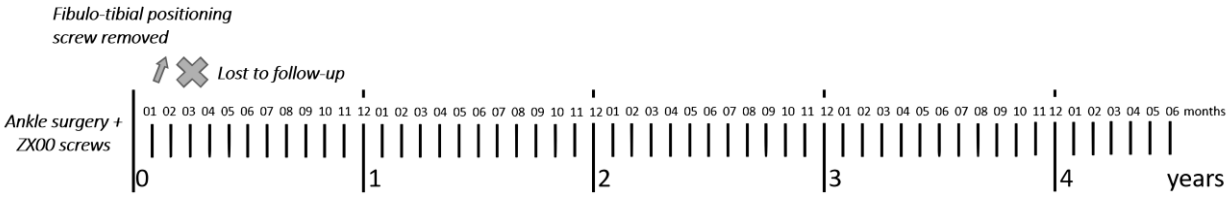

Patient 11 was treated with two ZX00 screws and a one-third tubular plate at the medial malleolus, and at the lateral malleolus, a lag screw and a one-third tubular plate were implanted, along with a fibulo-tibial positioning screw to stabilize the syndesmotic injury. The positioning screw was removed 38 days after surgery. The last radiograph was collected at 3 months, after which the patient was lost to follow-up.

Figure 11c. Radiological follow-up (AP)

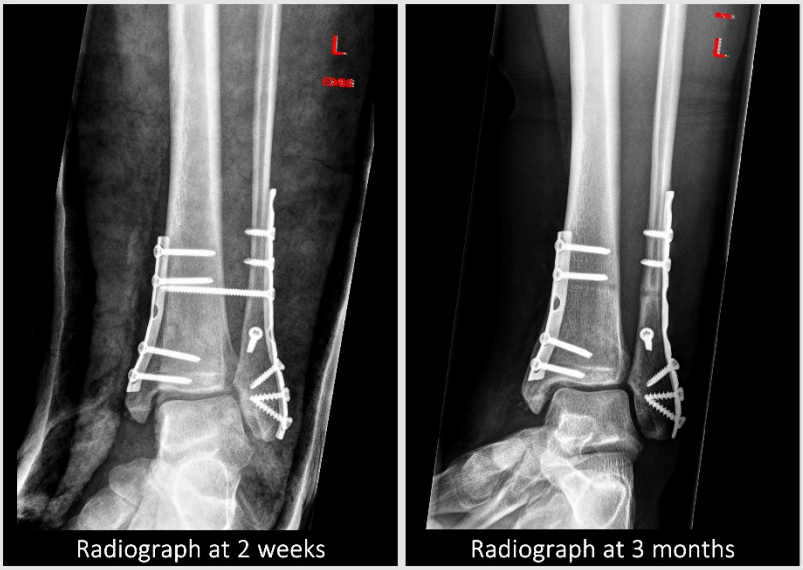

The radiograph at 2 weeks illustrates the postoperative situation with the ankle in a plaster cast. The last radiograph was performed at 3 months, then the patient was lost to follow-up.

3.2.12 Patient 12

Figure 12a. The injured ankle

A 25-year-old female patient with a left bimalleolar injury.

Figure 12b. Timeline

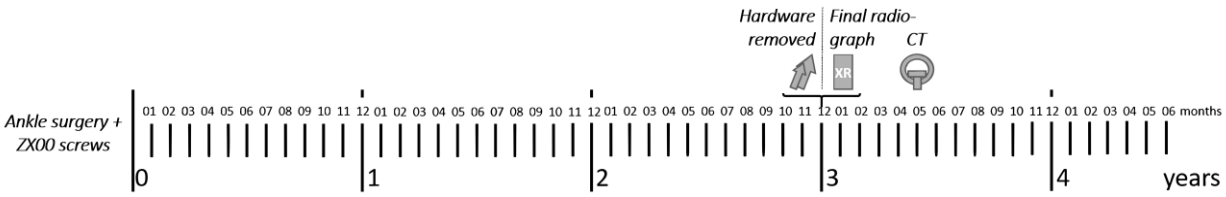

The medial malleolar fracture was treated with two ZX00 screws and the lateral malleolar fracture was treated with a lag screw and a one-third tubular plate. Hardware was removed after 3 years and 1 month.

Table 12. Comprehensive analysis of imaging follow-up of Patient 12

Imaging Method	Technique	Timepoint	ZX00 Screw Visibility	Bone Texture at ZX00 Implantation Site	Bone Microarchitecture at ZX00 Implantation Site	Bone Microarchitecture after Hardware Removal	Interpretation
				as it appears on radiographs	*as observed on CT*	*as observed on CT*	
Radiographs	AP view	6 weeks	Clearly visible	Inhomogeneous	N/A	N/A	Resorption in progress.
	AP view	1 year	Partially visible	Inhomogeneous	N/A	N/A	Resorption and bone remodeling in progress.
	AP view	3 years (final)	Not visible	Homogeneous	N/A	N/A	Adjacent bone remodeling increased radiopacity, masking the voids in the trabecular bone.
CT	Axial CT	3 years 5 months	Not visible	N/A	Voids in trabecular bone	Screw holes in trabecular bone	Resorption left voids in trabecular bone. Hardware removal left screw holes in trabecular bone.
	Coronal CT	3 years 5 months	Not visible	N/A	Voids in trabecular bone	Screw holes in trabecular bone	Resorption left voids in trabecular bone. Hardware removal left screw holes in trabecular bone.

For comparison, see Fig. 12c-d.

Figure 12c. Radiological follow-up (AP)

The radiograph at 2 weeks illustrates the postoperative situation with the ankle in a plaster cast. The final radiograph was performed at 3 years, and the CT at 3 years 5 months. There are mild post-traumatic arthritic changes at final follow-up. Adapted from (114) with permission from Wolters Kluwer Health Inc.

Figure 12d. CT (axial)

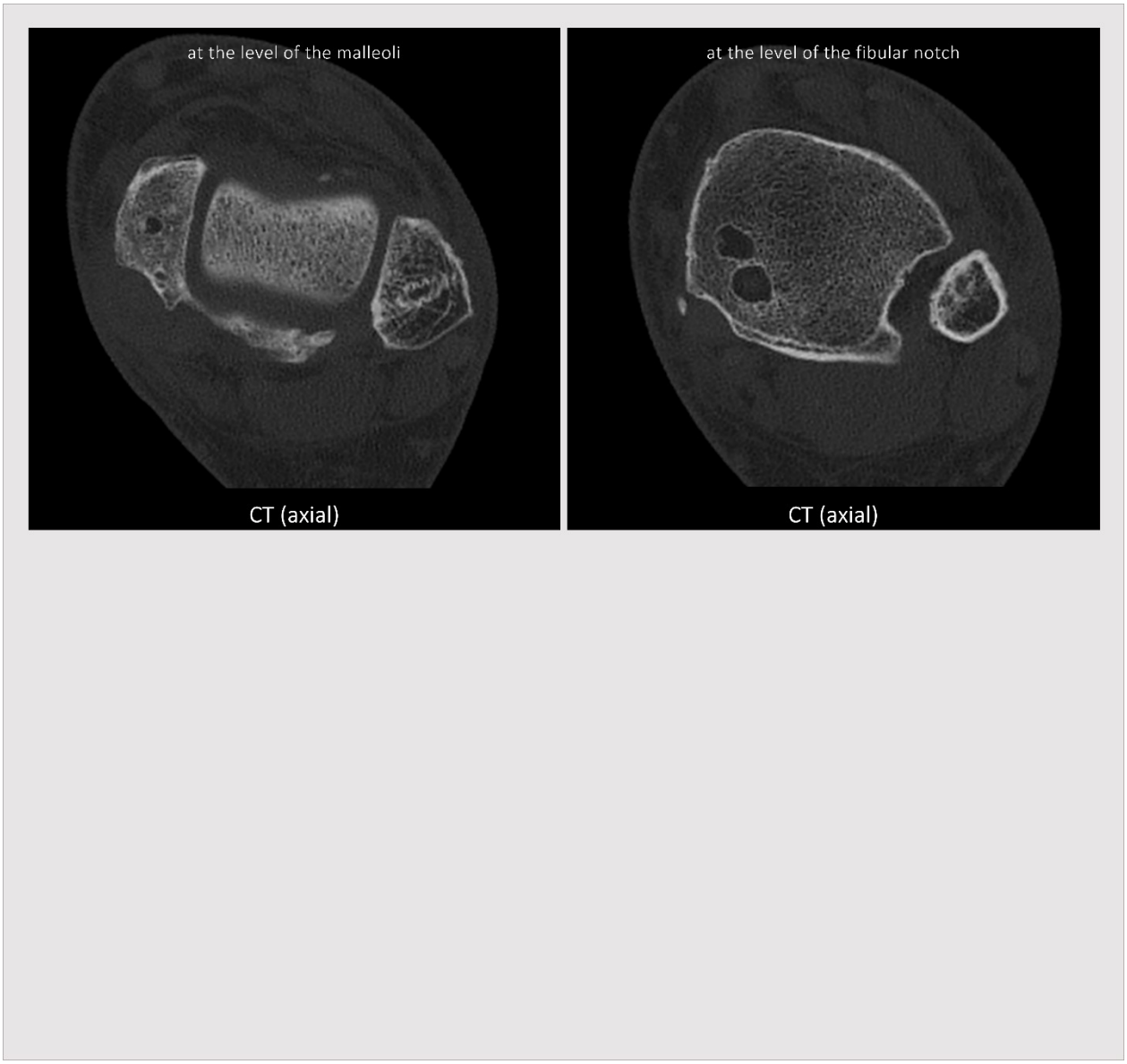

The axial plane CT, performed at 3 years 5 months, shows sharply encircled trabecular voids after ZX00 resorption at the medial malleolus. The sclerotic screw holes four months after conventional hardware removal at the lateral malleolus are also seen (left).

3.2.13 Patient 13

Figure 13a. The injured ankle

A 47-year-old male patient with a left trimalleolar injury.

Figure 13b. Timeline

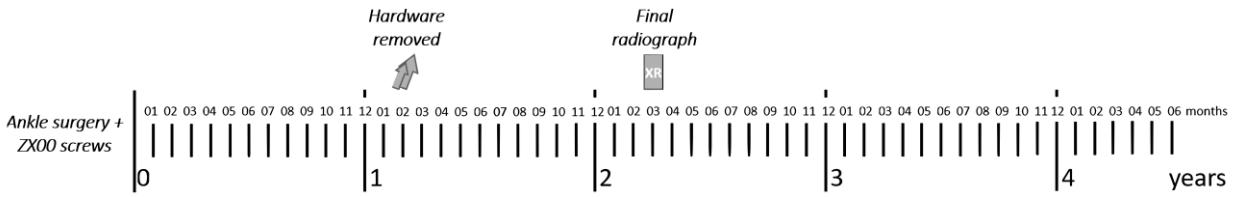

The medial malleolar fracture was treated with two ZX00 screws, the fibula fracture was treated with a one-third tubular plate for bridging and the posterior malleolar fracture was treated with a locking compression plate (LCP). Hardware was removed after 1 year and 2 months.

Table 13. Comprehensive analysis of imaging follow-up of Patient 13

Imaging Method	Technique	Timepoint	ZX00 Screw Visibility	Bone Texture at ZX00 Implantation Site	Interpretation
				as it appears on radiographs	
Radiographs	AP view	6 weeks	Clearly visible	Inhomogeneous	Resorption in progress.
	AP view	1 year	Partially visible	Inhomogeneous	Resorption and bone remodeling in progress.
	AP view	2 years 3 months (final)	Not visible	Slightly inhomogeneous	Adjacent bone remodeling increased radiopacity.

For comparison, see Fig. 13c.

Figure 13c. Radiological follow-up (AP)

The radiograph at 2 weeks illustrates the postoperative situation. At that time-point, subcutaneous gas from ZX00 degradation can be seen. The final radiograph was performed at 2 years 3 months, however no CT was conducted. There are mild post-traumatic arthritic changes at final follow-up. Adapted from (114) with permission from Wolters Kluwer Health Inc.

This page intentionally left blank.

3.2.14 Patient 14

Figure 14a. The injured ankle

A 56-year-old male patient with a left isolated medial malleolar injury.

Figure 14b. Timeline

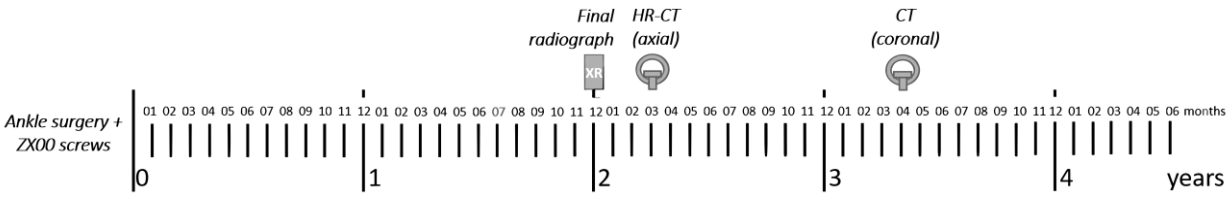

Patient 14 underwent treatment with two ZX00 screws for medial malleolar fracture.

Table 14. Comprehensive analysis of imaging follow-up of Patient 14

Imaging Method	Technique	Timepoint	ZX00 Screw Visibility	Bone Texture at ZX00 Implantation Site	Bone Microarchitecture at ZX00 Implantation Site	Interpretation
				as it appears on radiographs	*as observed on CT*	
Radiographs	AP view	6 weeks	Clearly visible	Inhomogeneous	N/A	Resorption in progress.
	AP view	1 year	Partially visible	Inhomogeneous	N/A	Resorption and bone remodeling in progress.
	AP view	2 years (final)	Not visible	Homogeneous	N/A	Adjacent bone remodeling increased radiopacity, masking the voids in the trabecular bone.
CT	Axial HR-CT	2 years 3 months	Not visible (only traces)	N/A	Voids in trabecular bone	Resorption left voids in trabecular bone.
	Coronal CT	3 years 4 months	Not visible	N/A	Voids in trabecular bone	Resorption left voids in trabecular bone.

For comparison, see Fig. 14c-d.

Figure 14c. Radiological follow-up (AP)

The radiograph at 2 weeks illustrates the postoperative situation. At that time-point, subcutaneous gas from ZX00 degradation can be seen. The final radiograph was performed at 2 years, and the coronal CT at 3 years 4 months. Adapted from (114) with permission from Wolters Kluwer Health Inc.

Figure 14d. HR-CT (axial) and 3D reconstruction

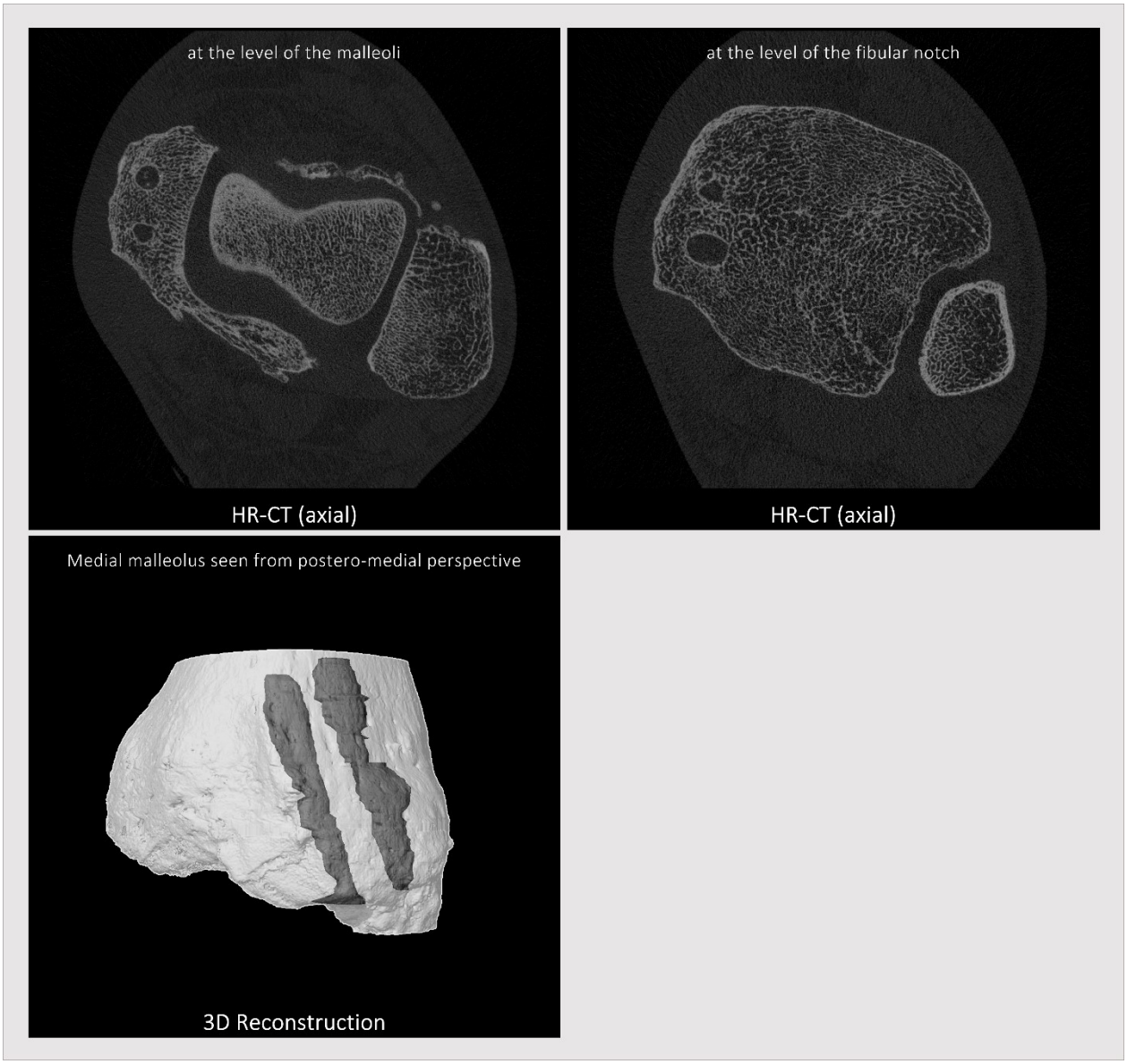

The axial plane HR-CT was performed at 2 years 3 months. Tiny traces of ZX00 are detectable within a sharply defined trabecular void (upper left) under this high resolution. The 3D reconstruction illustrates the extent of the trabecular voids (posterior void: 574.0 mm^3, anterior void: 708.4 mm^3).

3.2.15 Patient 15

Figure 15a. The injured ankle

A 44-year-old female patient with a right trimalleolar injury.

Figure 15b. Timeline

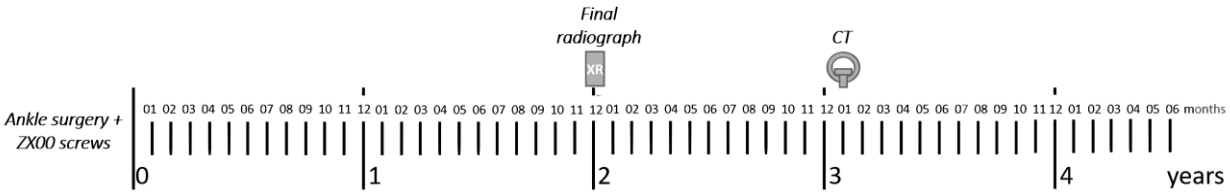

Patient 15 underwent treatment with two ZX00 screws for a medial malleolar fracture and a lag screw, along with a one-third tubular plate, for a lateral malleolar fracture. Hardware was not removed.

Table 15. Comprehensive analysis of imaging follow-up of Patient 15

Imaging Method	Technique	Timepoint	ZX00 Screw Visibility	Bone Texture at ZX00 Implantation Site	Bone Microarchitecture at ZX00 Implantation Site	Interpretation
				as it appears on radiographs	*as observed on CT*	
Radiographs	AP view	6 weeks	Clearly visible	Inhomogeneous	N/A	Resorption in progress.
	AP view	1 year	Partially visible	Inhomogeneous	N/A	Resorption and bone remodeling in progress.
	AP view	2 years (final)	Not visible	Homogeneous	N/A	Adjacent bone remodeling increased radiopacity, masking the voids in the trabecular bone.
CT	Axial CT	3 years 1 month	Not visible (only traces)	N/A	Voids in trabecular bone	Resorption left voids in trabecular bone.
	Coronal CT	3 years 1 month	Not visible	N/A	Voids in trabecular bone	Resorption left voids in trabecular bone.

For comparison, see Fig. 15c-d.

Figure 15c. Radiological follow-up (AP)

The radiograph at 2 weeks illustrates the postoperative situation with the ankle in a plaster cast. The final radiograph was performed at 2 years, and the CT at 3 years 1 months. Adapted from (116).

Figure 15d. CT (axial)

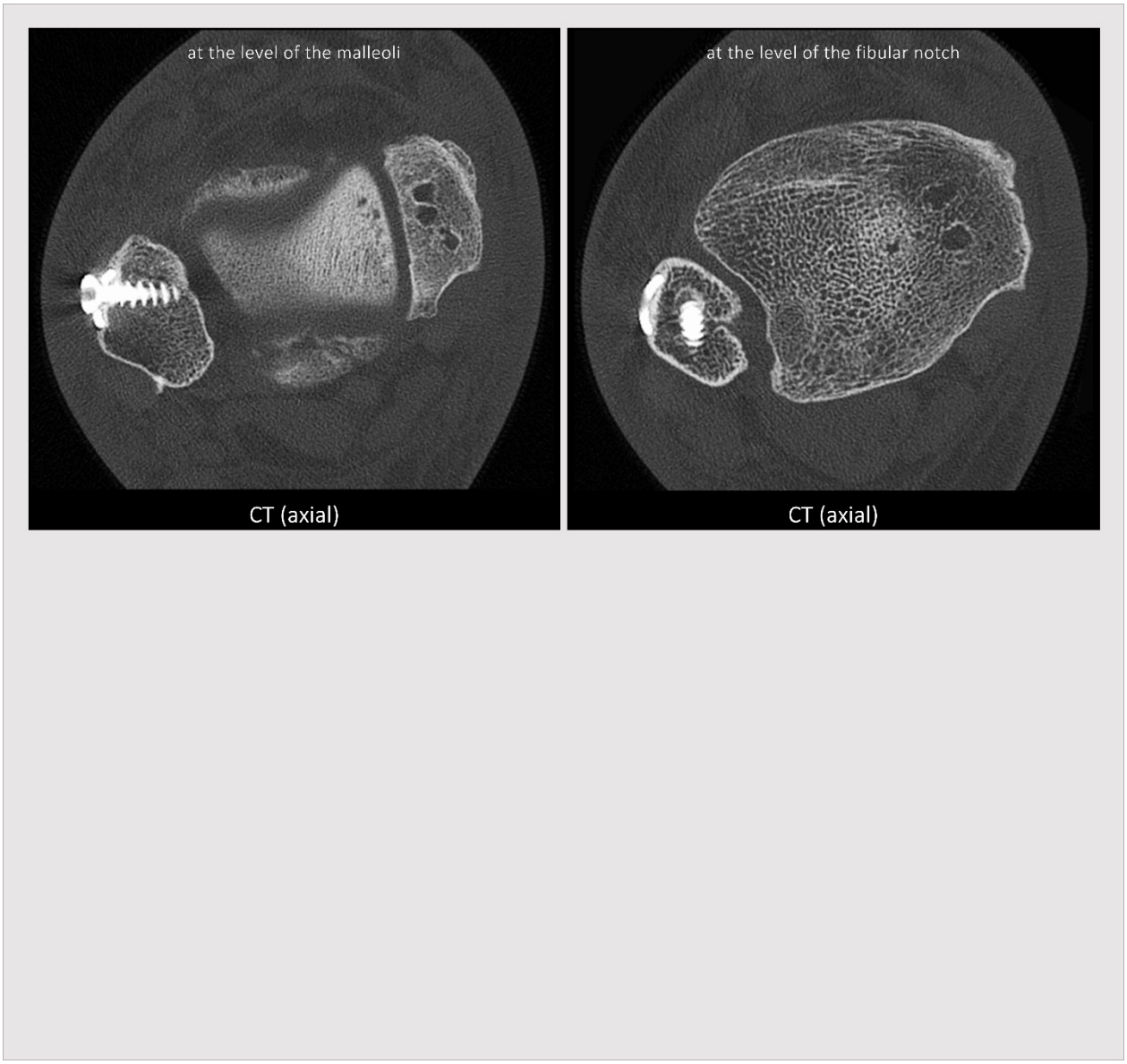

The axial CT scan conducted at 3 years 1 month reveals three voids in the trabecular bone of the medial malleolus (upper left), even though only two ZX00 screws were inserted. The resorption process results in a void around the resorbing screw and, in some cases, appears to create additional voids adjacent to it, likely due to gas formation.

3.2.16 Patient 16

Figure 16a. The injured ankle

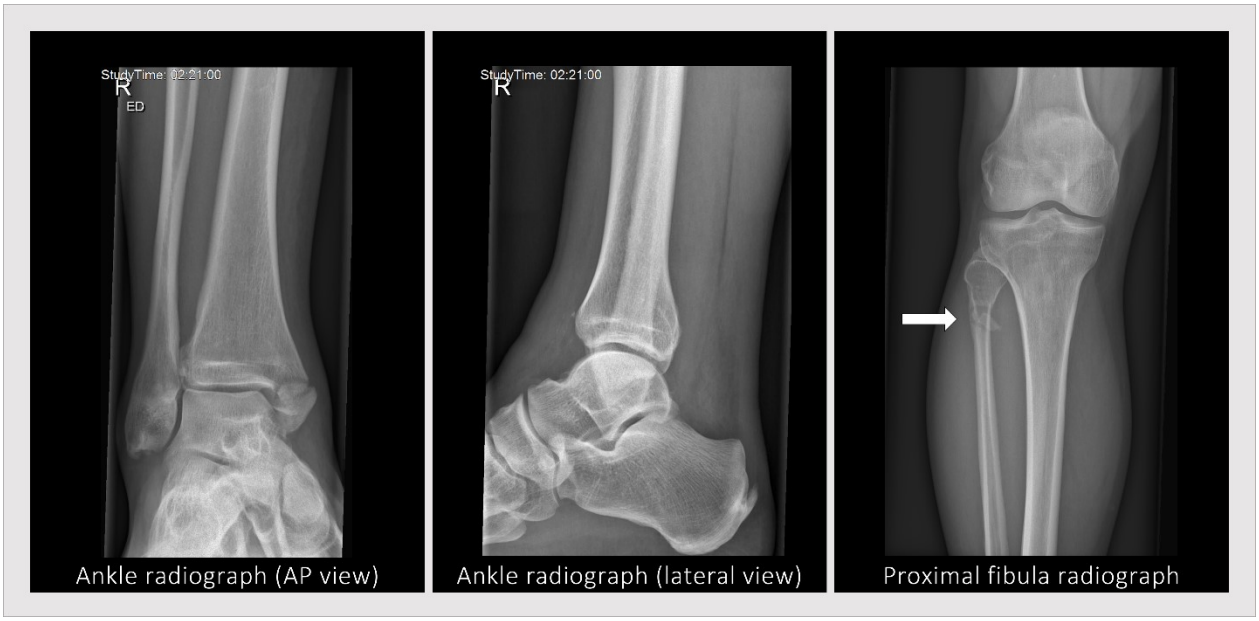

A 54-year-old male patient with a right Maisonneuve injury.

Figure 16b. Timeline

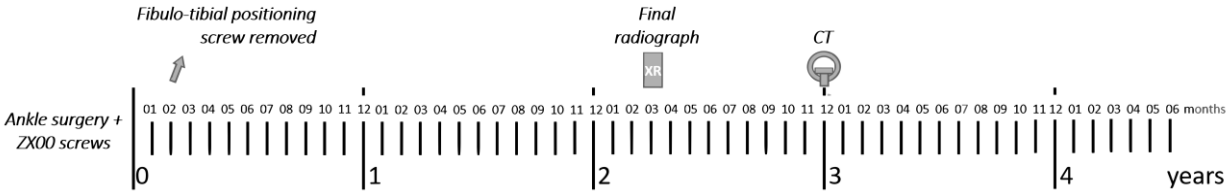

Patient 16 underwent treatment with two ZX00 screws for medial malleolar fracture and a two fibulo-tibial positioning screw for syndesmotic instability. The fibulo-tibial positioning screws were removed 63 days after fracture surgery.

Table 16. Comprehensive analysis of imaging follow-up of Patient 16

Imaging Method	Technique	Timepoint	ZX00 Screw Visibility	Bone Texture at ZX00 Implantation Site	Bone Microarchitecture at ZX00 Implantation Site	Bone Microarchitecture after Hardware Removal	Interpretation
				as it appears on radiographs	*as observed on CT*	*as observed on CT*	
Radiographs	AP view	6 weeks	Clearly visible	Inhomogeneous	N/A	N/A	Resorption in progress.
	AP view	1 year	Partially visible	Inhomogeneous	N/A	N/A	Resorption and bone remodeling in progress.
	AP view	2 years 3 months (final)	Not visible	Slightly inhomogeneous	N/A	N/A	Adjacent bone remodeling in progress. The increasing radiopacity partially masks the voids in the trabecular bone.
CT	Axial CT	3 years	Not visible	N/A	Voids in trabecular bone	Screw holes in trabecular bone	Resorption left voids in trabecular bone. Fibulo-tibial positioning screw removal left holes in trabecular bone.

For comparison, see Fig. 16c-d.

Figure 16c. Radiological follow-up (AP)

The radiograph at 2 weeks illustrates the postoperative situation with the ankle in a plaster cast. At that time-point, subcutaneous gas from ZX00 degradation can be seen. The final radiograph was performed at 2 years 3 months, and the coronal CT at 3 years. There are mild post-traumatic arthritic changes, and ossification around the syndesmosis at final follow-up.

Figure 16d. CT (axial)

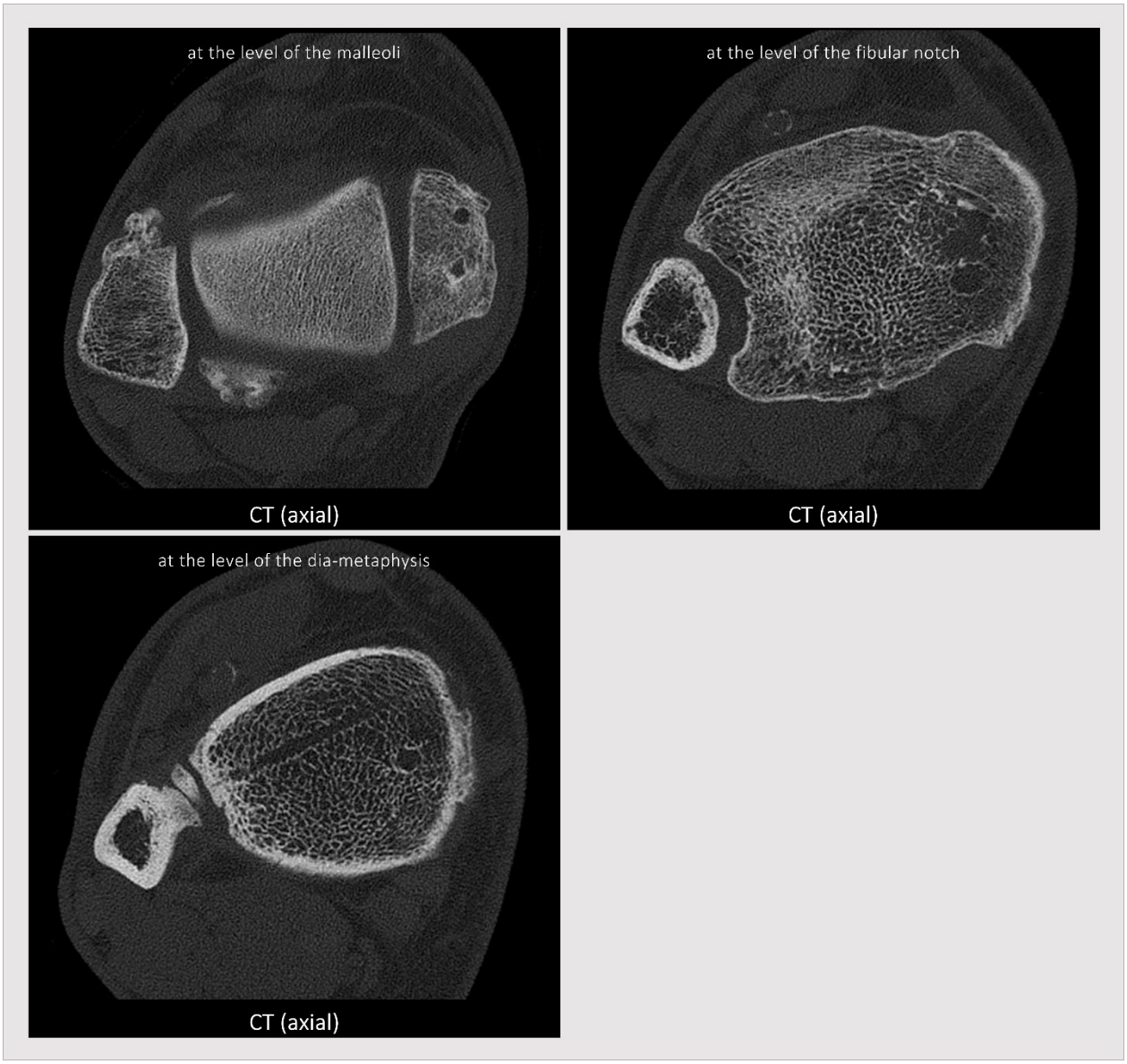

The axial CT scans (conducted at 3 years) reveal the aftermath of ZX00 resorption at the medial malleolus, showcasing trabecular voids. Furthermore, the trajectory of the fibulo-tibial positioning screw is still visible in the trabecular, but not cortical bone (lower left). This is of interest, as the conventional screw resided for only 63 days and was removed years ago. Apparently, trabecular and cortical bone follow distinct mechanisms of repair.

3.2.17 Patient 17

Figure 17a. The injured ankle

A 35-year-old female patient with a right trimalleolar injury.

Figure 17b. Timeline

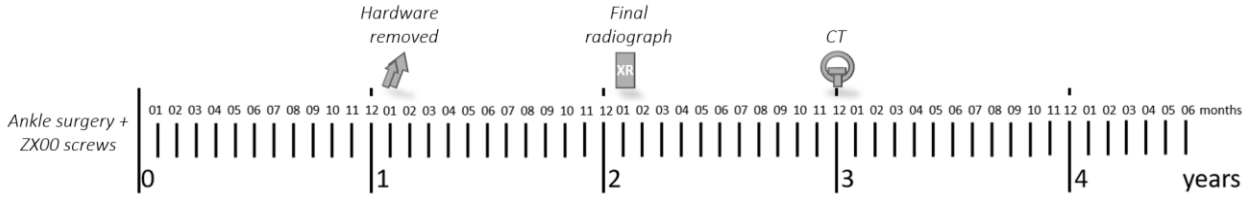

Patient 17 received treatment for a medial malleolar fracture with two ZX00 screws, a one-third tubular plate for the lateral malleolus, and a T-shaped locking compression plate (LCP) for the posterior malleolus. Hardware was removed after 1 year and 2 months.

Table 17. Comprehensive analysis of imaging follow-up of Patient 17

Imaging Method	Technique	Timepoint	ZX00 Screw Visibility	Bone Texture at ZX00 Implantation Site	Bone Microarchitecture at ZX00 Implantation Site	Bone Microarchitecture after Hardware Removal	Interpretation
				as it appears on radiographs	*as observed on CT*	*as observed on CT*	
Radiographs	AP view	6 weeks	Clearly visible	Inhomogeneous	N/A	N/A	Resorption in progress.
	AP view	1 year	Partially visible	Inhomogeneous	N/A	N/A	Resorption and bone remodeling in progress.
	AP view	2 years 1 month (final)	Not visible	Homogeneous	N/A	N/A	Adjacent bone remodeling increased radiopacity, masking the voids in the trabecular bone.
CT	Axial CT	3 years	Only traces	N/A	Voids in trabecular bone	Screw holes in trabecular bone	Resorption left voids in trabecular bone. Hardware removal left screw holes in trabecular bone.
	Coronal CT	3 years	Only traces	N/A	Voids in trabecular bone	Screw holes in trabecular bone	Resorption left voids in trabecular bone. Hardware removal left screw holes in trabecular bone.

For comparison, see Fig. 17c-d.

Figure 17c. Radiological follow-up (AP)

The radiograph at 2 weeks illustrates the postoperative situation with the ankle in a plaster cast. The radiograph at 6 weeks shows subcutaneous gas around the medial malleolus. The final radiograph was performed at 2 years 1 month, and the CT at 3 years. There are mild post-traumatic arthritic changes at final follow-up.

Figure 17d. CT (axial)

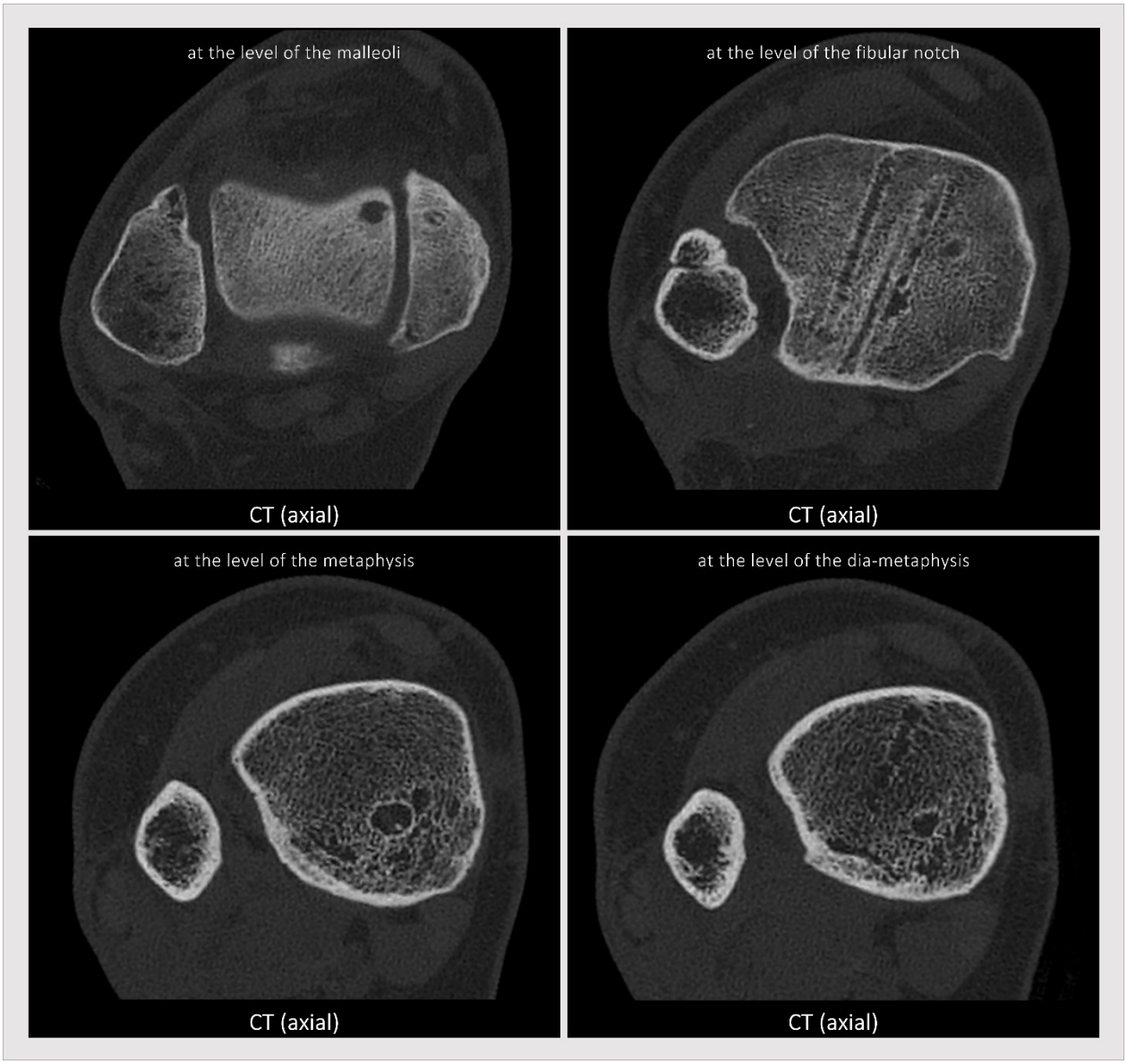

The axial CT scans at 3 years reveal both ZX00-resorption-induced trabecular voids and holes after conventional screw removal, each with sharp-edged boundaries. A degenerative ganglion cyst is noted in the talus (upper left). Sclerotic screw holes, years after conventional hardware removal, persist in the trabecular but not cortical bone (upper right). A tiny ZX00 trace remains within a larger void (lower left). Besides classical screw holes, trabecular changes around the healed fracture are evident in the posterior malleolus (lower right).

3.2.18 Patient 18

Figure 18a. The injured ankle

A 20-year-old male patient with a left isolated medial malleolar injury.

Figure 18b. Timeline

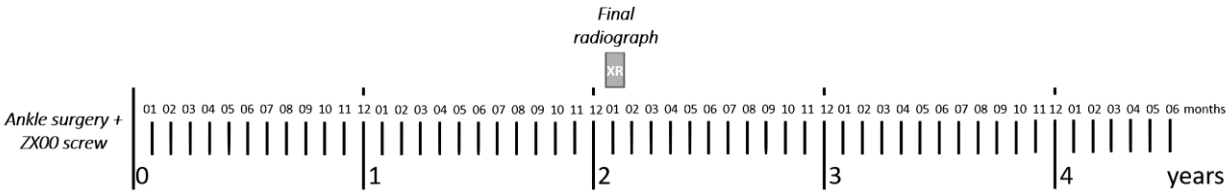

Patient 18 underwent treatment with a single ZX00 screw for medial malleolar fracture. Removal surgery was not necessary.

Table 18. Comprehensive analysis of imaging follow-up of Patient 18

Imaging Method	Technique	Timepoint	ZX00 Screw Visibility	Bone Texture at ZX00 Implantation Site	Interpretation
				as it appears on radiographs	
Radiographs	AP view	6 weeks	Clearly visible	Inhomogeneous	Resorption in progress.
	AP view	1 year	Partially visible	Inhomogeneous	Resorption and bone remodeling in progress.
	AP view	2 years 1 month (final)	Not visible	Homogeneous	Adjacent bone remodeling increased radiopacity.

For comparison, see Fig. 18c.

Figure 18c. Radiological follow-up (AP)

The radiograph at 2 weeks illustrates the postoperative situation with the ankle in a plaster cast. The final radiograph was performed at 2 years 1 months, however no CT was conducted.

This page intentionally left blank.

3.2.19 Patient 19

Figure 19a. The injured ankle

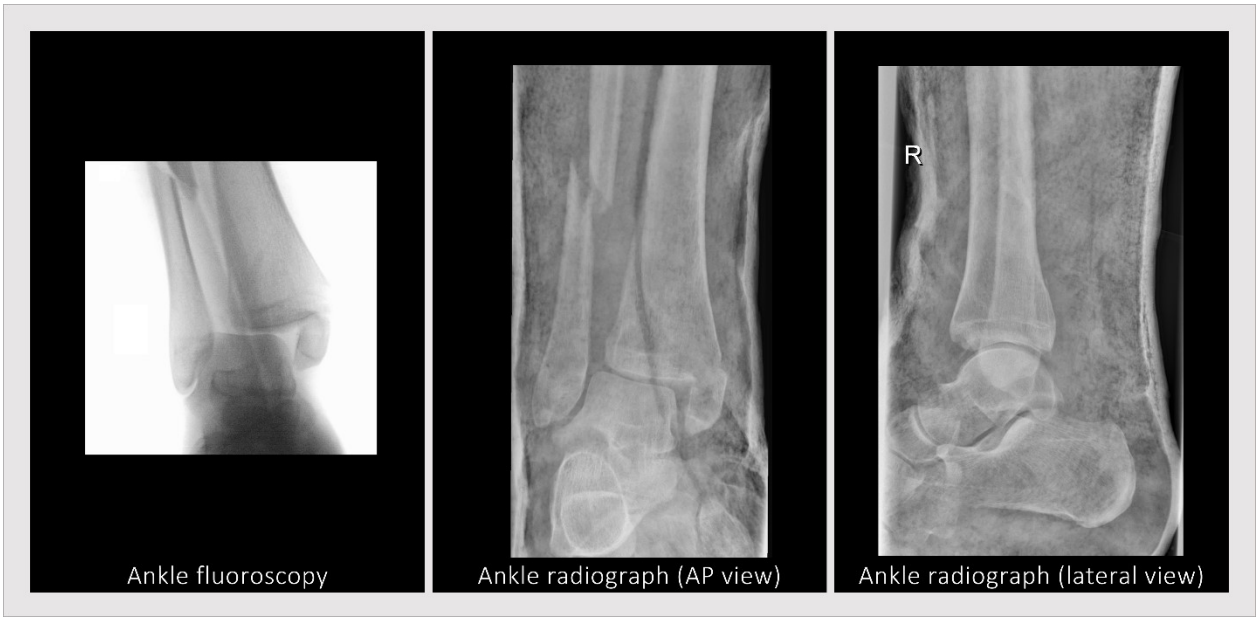

A 25-year-old female patient with a right trimalleolar injury.

Figure 19b. Timeline

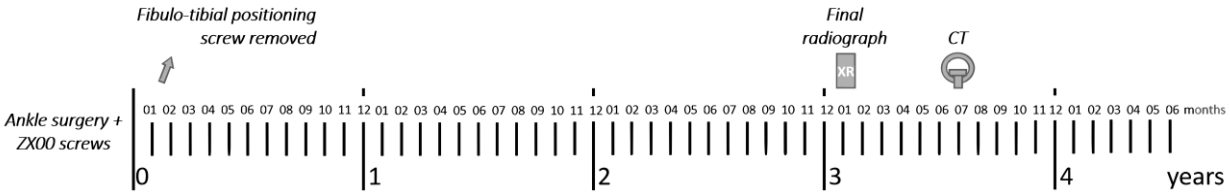

The medial malleolar fracture was treated with two ZX00 screws, while the lateral malleolar fracture was fixed with a lag screw and a one-third tubular plate. Stabilization of the posterior fragment was achieved with a single cannulated screw in the anteroposterior direction, and the syndesmotic injury was addressed with a fibulo-tibial positioning screw. The fibulo-tibial positioning screw was removed after 45 days, with no further metal removal performed.

Table 19. Comprehensive analysis of imaging follow-up of Patient 19

Imaging Method	Technique	Timepoint	ZX00 Screw Visibility	Bone Texture at ZX00 Implantation Site	Bone Microarchitecture at ZX00 Implantation Site	Bone Microarchitecture after Hardware Removal	Interpretation
				as it appears on radiographs	*as observed on CT*	*as observed on CT*	
Radiographs	AP view	6 weeks	Clearly visible	Inhomogeneous	N/A	N/A	Resorption in progress.
	AP view	1 year	Partially visible	Inhomogeneous	N/A	N/A	Resorption and bone remodeling in progress.
	AP view	3 years 1 month (final)	Not visible	Homogeneous	N/A	N/A	Adjacent bone remodeling increased radiopacity, masking the voids in the trabecular bone.
CT	Axial CT	3 years 7 months	Not visible (only traces)	N/A	Voids in trabecular bone	Screw holes in trabecular bone	Resorption left voids in trabecular bone. Fibulo-tibial positioning screw removal left a hole in trabecular bone.

For comparison, see Fig. 19c-d.

Figure 19c. Radiological follow-up (AP)

The radiograph at 2 weeks illustrates the postoperative situation, revealing subcutaneous gas from ZX00 degradation at the medial malleolus. The final radiograph was performed at 3 years 1 month, and the coronal CT at 3 years 7 months. There are moderate post-traumatic arthritic changes at final follow-up.

Figure 19d. CT (axial)

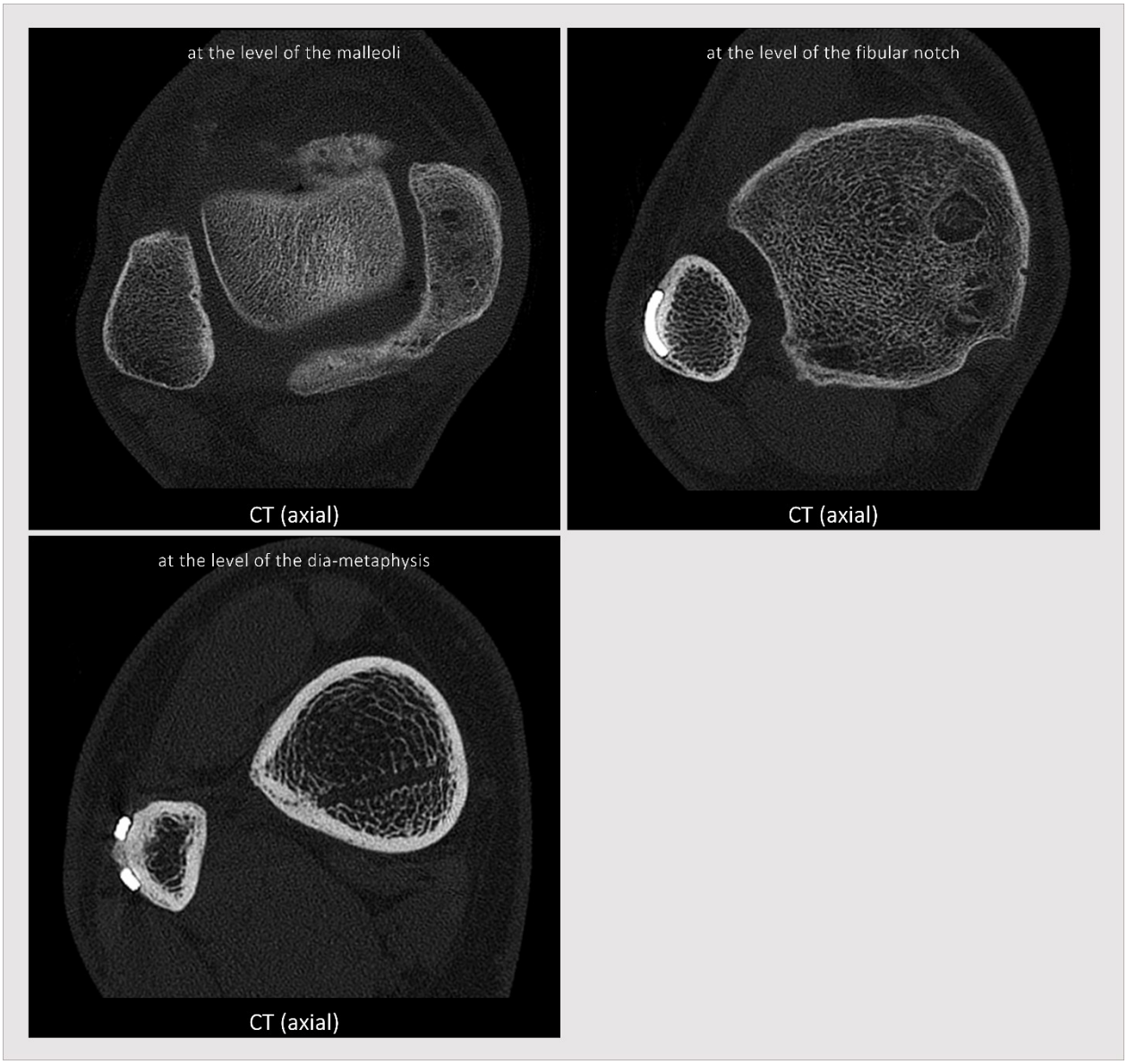

The axial CT scan, conducted at 3 years 7 months, reveals trabecular voids at the medial malleolus resulting from ZX00 resorption. Additionally, trabecular irregularities are observed at the site of the healed posterior malleolus fracture (upper right). Remarkably, the screw trajectory in the trabecular bone remains discernible even years after the removal of the conventional fibulo-tibial positioning screw (lower left). However, the cortical bone has fully healed, suggesting a differences in bone healing.

3.2.20 Patient 20

Figure 20a. The injured ankle

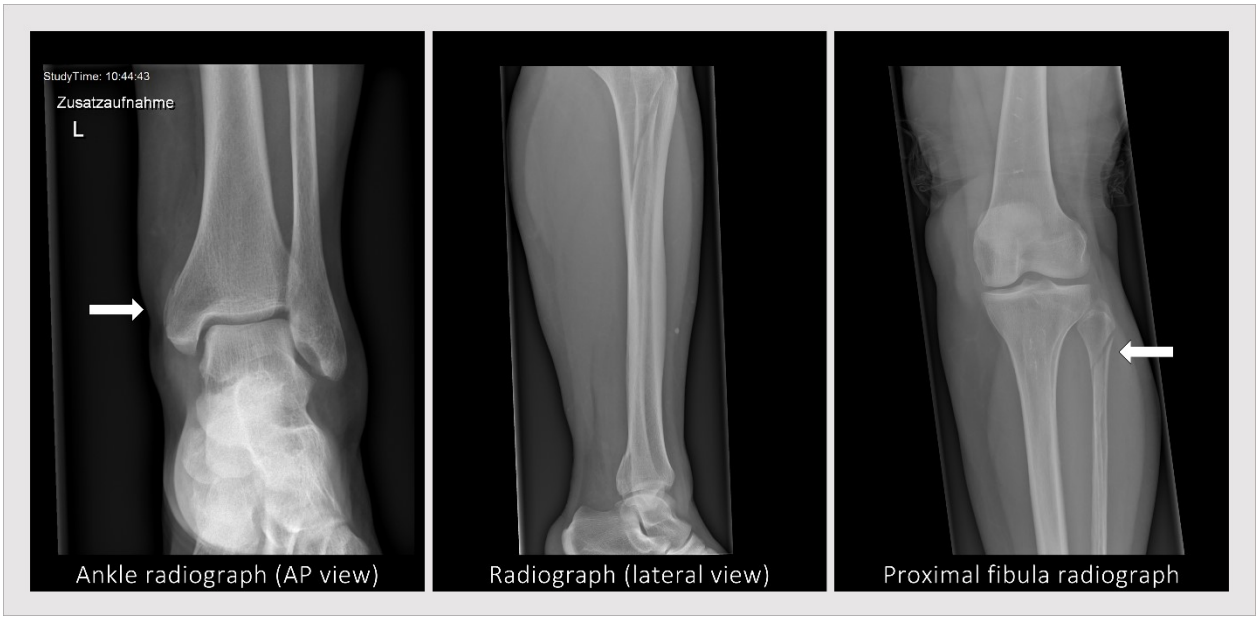

A 64-year-old male patient with a left Maisonneuve injury.

Figure 20b. Timeline

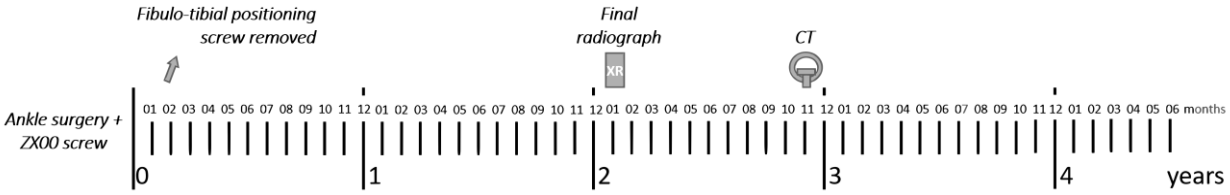

Patient 20 received treatment with a single ZX00 screw for a medial malleolar fracture and two fibulo-tibial positioning screws for syndesmotic injury. The fibulo-tibial positioning screws were removed around 6 weeks.

Table 20. Comprehensive analysis of imaging follow-up of Patient 20

Imaging Method	Technique	Timepoint	ZX00 Screw Visibility	Bone Texture at ZX00 Implantation Site	Bone Microarchitecture at ZX00 Implantation Site	Bone Microarchitecture after Hardware Removal	Interpretation
				as it appears on radiographs	*as observed on CT*	*as observed on CT*	
Radiographs	AP view	6 weeks	Clearly visible	Inhomogeneous	N/A	N/A	Resorption in progress.
	AP view	1 year	Partially visible	Inhomogeneous	N/A	N/A	Resorption and bone remodeling in progress.
	AP view	2 years 1 month (final)	Not visible	Homogeneous	N/A	N/A	Adjacent bone remodeling increased radiopacity, masking the voids in the trabecular bone.
CT	Axial CT	2 years 11 months	Not visible	N/A	Voids in trabecular bone	Screw holes in trabecular bone	Resorption left voids in trabecular bone. Fibulo-tibial positioning screw removal left holes in trabecular bone.

For comparison, see Fig. 20c-d.

Figure 20c. Radiological follow-up (AP)

The radiograph at 2 weeks illustrates the postoperative situation with the ankle in a plaster cast. The final radiograph was performed at 2 years 1 month, and the coronal CT at 2 years 11 months.

Figure 20d. CT (axial)

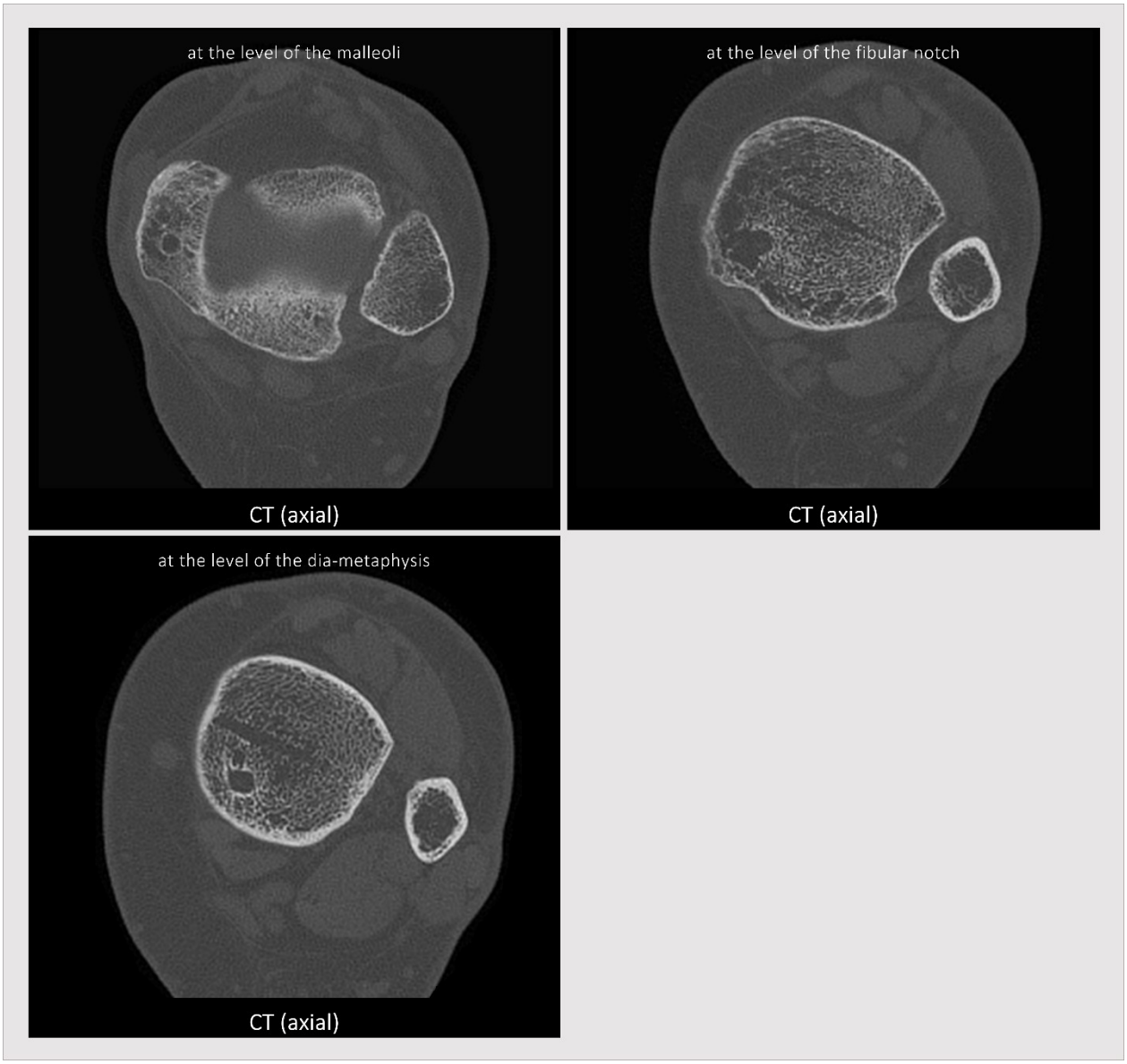

The axial CT scan, conducted at 2 years 11 months, reveals a trabecular void resulting from ZX00 screw resorption at the medial malleolus. Additionally, it displays trabecular irregularities at the healed medial and posterior malleolus fracture (upper right). Moreover, the screw trajectory within the trabecular bone following conventional removal of the fibulo-tibial positioning screw persists (upper right, lower left), while the cortical bone has completely healed in that region.

4 DISCUSSION

4.1 Scope and Framing

The present thesis aims to investigate the progression of ZX00 bone screw resorption beyond the first year. We gathered data from patients enrolled in a pilot study who underwent ZX00 screw treatment for medial malleolar fractures. A total of 20 patients received one or two ZX00 screws, with all surgeries conducted between 2018 and 2019 at the Medical University of Graz. By the **3-month follow-up**, it was evident that all fractures had healed, and all 20 patients exhibited excellent clinical and functional outcomes (56). At the **1-year follow-up**, 19 patients (one lost to follow-up) continued to fare well, with no instances of reoperation or other clinical complications (116). By 2020, the first patients attended their two-year appointments, though no follow-up protocol existed beyond one year. Radiographs taken after two years showed ongoing improvement, with increasingly homogeneous bone texture at the ZX00 screw site. These observations sparked our interest to continue follow-up. However, due to organizational constraints around COVID-19 restrictions, radiographic follow-up beyond 1 year was not conducted at fixed intervals but rather occurred between 1 year 6 months and 3 years 7 months after the initial surgery. In the end, it comprised 18 patients, as one case was excluded due to unrelated second ankle surgery for a pre-existing osteochondral lesion of the talus (118).

On average, this amounted to a **2½-year follow-up**, including final radiographs and clinical assessments. Clinical scores remained excellent for the 18 patients from the initial cohort of 20. Radiographs showed a homogeneous bone texture, with the ZX00 screws no longer visible (114).

This current work, for the first time, presents comprehensive long-term CT images, with scans available for 15 out of the remaining 18 cases. The CT examinations were conducted as a reaction to provide clarity regarding the astonishingly good findings in the final radiographs (114). Patients were specifically called in to the hospital for CT scans. Among the 15 scanned patients, 6 underwent high-resolution CT scans allowing quantification of the structural changes. On average, CT examinations of these 15 patients were conducted as a **3½-year follow-up** (range: 2 years 3 months to 4 years 6 months).

The central idea of this thesis is to draw conclusions from the findings in final radiographs taken, on average, after 2½ years, and CT images performed thereafter, on average, after 3½ years. Additionally, the study presents clinical outcomes, including pain and function. It examines changes of bone following ZX00 screw resorption and conventional hardware removal. Finally, it discusses cost-effectiveness and offers ideas on potential future applications for ZX00 screws.

4.2 Clinical Outcomes

At the 2½-year follow-up, there were no complications (0%) such as skin or scar issues, infections, hypersensitivity reactions, CRPS, malalignment, or the need for revision surgery (see 3.1, Table B). Similarly, pain levels were minimal, as reflected by a VAS score of 1 out of 100. Functional outcomes were generally high, with patients achieving an average AOFAS score of 94 out of 100 points (114). Considering that restricted function is often indicated by reduced dorsiflexion following an ankle fracture (119), our patients performed well, with an average dorsiflexion of 22° (see 3.1, Table B). There was no case of symptomatic post-traumatic ankle arthritis. Given the nature of the ankle injuries, with ¾ of our patients experiencing higher-order fractures such as trimalleolar and Maisonneuve injuries, the procedural success of the surgical interventions can be deemed excellent. As specified above, this is supported by consistently low pain levels and high functional outcomes at both the 1-year and 2½-year follow-up periods (56,114). However, other studies have reported that every second patient with trimalleolar fractures may exhibit residual deficits at the 1-year mark (120). When looking at long-term functional outcomes following surgical fixation of unstable ankle fractures (among them 75% Weber B and 19% Weber C fractures), a follow-up study involving 141 patients revealed encouraging results. After a mean follow-up period of 11.6 years, the majority of patients demonstrated improved long-term functional scores compared to those assessed at 1 year (31). Notably, radiographic analysis revealed arthritic changes in 63% of cases, including 31% with mild, 22% with moderate, and 10% with severe changes (31). Hence, the radiographic finding of mild and moderate post-traumatic changes in 39% of our patients perfectly aligns with the literature (31,120,121).

4.3 Imaging

4.3.1 Different Findings on Radiographs and CTs

The radiographs at around 2½ years post-implantation consistently show no visible signs of the ZX00 screws. This finding suggest the disappearance of ZX00 screws, alongside a recovery of the bony aspect at the site of previous fractures and ZX00 screw implantations. By this stage, the radiographic bone texture exhibits a predominantly homogeneous appearance in most cases (83%), or at least shows a trend towards increasing homogeneity (17%) (see 3.1, Table C). While these observations might suggest full screw resorption and comprehensive bone tissue regeneration (*restitutio ad integrum*), a significant revelation emerges from our CT images. The CT images at around 3½ years post-implantation reveal noteworthy alterations in bone microarchitecture characterized by trabecular voids across all ZX00 implantation sites (see 3.1, Table C). This discovery is of fundamental importance, as it impacts how post-fracture bone healing is assessed and whether bone regeneration (*restitutio ad integrum*) can be achieved in the context of magnesium-based implants. The limited availability of follow-up CT scans for commercially available Mg-Y-RE-Zr alloy (Magnezix®) implants might suggest some underlying considerations that warrant further investigation (57,90,96–101,122–125). This raises the following questions for this thesis: Why do radiographs and CT scans produce such different results, and what conclusions can be drawn from our cohort, with final radiographs taken at 2½ years and CT scans at 3½ years?

Additionally, changes in bone microarchitecture following the removal of conventional hardware will be examined and compared to those observed after the resorption of bioresorbable implants.

Figure 21. Different Findings on Radiographs and CTs

Postoperative radiographs were obtained at (A) 6 weeks, (B) 1 year, and (C) 3 years and 7 months after ankle surgery for our Patient 1. The case was successfully treated with two ZX00 screws for a medial malleolus fracture and a conventional fibulo-tibial positioning screw for syndesmotic instability, which was removed after 6 weeks (white arrow indicating the metal screw's position). Axial CT slices at four different levels (D) reveal a lack of trabecular structure following both the removal of the conventional screw (white arrow) and ZX00 resorption. Reproduced from (114) with permission of Wolters Kluwer Health Inc.

4.3.2 An Explanatory Model

Radiographs are produced when X-rays pass through the body and are absorbed at different rates by different tissues. Dense materials like bone absorb more X-rays, appearing bright on the image, while less dense materials like soft tissue allow more X-rays to pass through, appearing dark. Immediately after implantation, magnesium-based ZX00 screws appear as a rather bright structure on radiographs similar to bone (122). As the screws resorb over time, they become less dense and thus less visible on subsequent radiographs until they are eventually not visible on radiographs around 2½ years (114). As summation images, radiographs provide a two-dimensional representation of structures such as bones, often concealing underlying structures that are overlaid. However, when examined with three-dimensional imaging techniques (e.g. CT), residual voids or holes as a consequence of resorption of bioresorbable screws become apparent (102,114,126). Bone tissue is dynamic and undergoes continuous remodeling processes to adapt to mechanical stresses and strain (4). The remodeling extends beyond the initial fracture healing phase and continues past the first year. In our cohort, up to 2½ years post-ZX00 implantation, ongoing reinforcement of the adjacent trabecular bone around previously formed trabecular voids likely occurred. We suppose that happened in response to the demands for redistributing mechanical loads in the altered microarchitecture with sclerotic rim-sealed defects. This compensation by adjacent bone tissue gives a homogeneous bone appearance after ZX00 screw resorption on radiographs, despite the presence of trabecular voids in reality. The phenomenon is explained by the summation effect in radiographs. It is essentially the same as after the removal of conventional screws, where the radiographic impression appears homogeneous, even though screw holes persist. This is well known in clinical practice after removal surgery and also demonstrated by our results from the 11 patients for whom CT scans were available after hardware removal (see 3.1, Table C). In all cases, the remaining screw holes are visible on CT years after removal, while the corresponding radiographs appear homogeneous (due to the summation effect). Recognizing the constraints of radiographs in assessing bone healing emphasizes the necessity of additional imaging techniques, especially CT scans, for thorough evaluation and ongoing monitoring of bioresorbable implants (127).

4.3.3 Advanced Imaging of Polymers

Much can be learned from the long-term imaging of polymer implants. This knowledge can be partially transferred and compared to the imaging of magnesium-based implants. A Swedish research group (127) conducted an 18-year radiographic study examining patients who underwent arthroscopic Bankart repair with bioresorbable anchors composed of either PGA (polyglycolic acid) or PLLA (poly-L-lactic acid) in a randomized prospective trial. The findings showcased cystic bone holes in the glenoid, evident on both radiographs and CT scans. Remarkably, radiographs showed a considerable discrepancy, with 73% of drill holes appearing healed in the PGA group compared to 35% in the PLLA group. However, the use of CT imaging unveiled a different picture. It demonstrated that a large number of drill holes remained unhealed in a majority of cases in both groups. This underscores the limitations of assessments of holes with radiographs. (127). A follow-up report from Barber et al. (USA) (124) indicated that PLLA and PGA suture anchors, following arthroscopic rotator cuff repair, completely degraded after 3 years. However, distinguishable bony changes persisted on CT scans in all cases (128). Barber and Dockery in 2006 (129) shed light on the fate of PLLA interference screws after anterior cruciate ligament repair using patellar tendon autograft. They reported that the screws were completely degraded after approximately 8 years. In some cases, the resorbed PLLA screw left a 'ghost sign' within the tunnels, all of which exhibited a sclerotic rim. Importantly, the PLLA material was not replaced by bone, causing the anterior cruciate ligament graft tunnels to be filled with non-ossified material (129). Arama et al. (Australia) (130) published a study in 2015 on the 5-year follow-up after anterior cruciate ligament repair. They observed progressive resorption of PLLA screws but incomplete ossification of the tunnel (130). Sundaraj et al. (Australia) (131) reported a 13-year follow-up study on anterior cruciate ligament repair with PLLA interference screws in 2020. They observed complete or nearly complete resorption of the screws over time, however, with minimal changes in tunnel volumes and negligible ossification (131). These studies across different body regions (shoulder, knee) demonstrate radiological changes that do not suggest bone regeneration (*restitutio ad integrum*) after resorption of polymer implants (127–131). Even if the clinical outcomes are favorable, and thus the primary success of the surgical intervention is undisputed, bone regeneration cannot be inferred from 'good-looking' X-rays after treatment with polymer implants.

4.3.4 Advanced Imaging of Mg-Y-RE-Zr

While the body of literature is full of material studies and laboratory testing around magnesium-based implants, there is still little clinical evidence and even less long-term imaging in humans. Naturally, among these limited clinical reports, the majority pertain to Mg-Y-RE-Zr, marketed as Magnezix®, the first commercially available magnesium-based implant in the European market (79).

Several authors investigated the use of magnetic resonance imaging (MRI) as modality for follow-up assessments. One argument in favor of this approach is that magnesium-based implants produce fewer artifacts on MRI scans, which could be considered a beneficial side effect compared to titanium implants (132). In a case series of Mg-Y-RE-Zr fixated Chevron osteotomies in hallux valgus surgery, MRI was used for postoperative follow-up (123). The MRI scans revealed bone marrow edema surrounding the degrading implant, which diminished over time, although residual signals persisted even after three years (123). Furthermore, subchondral cysts were detected with MRI. While the authors interpreted these as osteoarthritic changes, it is plausible that they are instead a consequence of implant degradation and previous gas release (124). These changes are probably in accordance with findings in animal studies that reported the presence of a corrosion layer, connective tissue (56,92), frequently accompanied by adipocytes, numerous macrophages, and occasionally foreign-body cells (=fused macrophages) adjacent to degrading magnesium-based implants (93). Others speak of 'new bone formation' based on MRI studies 1 year after Mg-Y-RE-Zr screw fixation but do not provide CT scans to endorse this finding (98). Overall, CT follow-up data on magnesium-based implants in humans are scarce in the limited literature available. This lack of data suggests a reluctance to report longitudinal data on bone microarchitecture changes following Mg-Y-RE-Zr implantation. Therefore, it is valuable to examine the rare clinical follow-up CT images provided by other researchers. The following reports focus on Mg-Y-RE-Zr screws, the first and, for a long time, the only magnesium-based screws available for clinical use:

Polat et al. (Turkey) (133) showed the case of a 19-year-old male treated with an Mg-Y-RE-Zr screw for scaphoid fracture with a 4-year follow-up CT. The screw was definitely visible on the CT after 4 years (133). Meier et al. (Germany) (132) in 2017 described a

series of five scaphoid fractures and Mg-Y-RE-Zr screw treatment, with three patients experiencing osteolysis and cystic changes around the implant. A CT three months after implantation was presented illustrating the cystic changes around the clearly visible screw (132). Of note, all fractures were healed by one year (132). Kose et al. (Turkey) (54) presented a 2-year CT scan following medial malleolar fracture fixation with Mg-Y-RE-Zr screws, revealing complete fracture healing, however the screws remained clearly visible (54). May et al. (Turkey) (55) published a 1-year CT image of a 21-year-old male patient who had M-Y-RE-Zr screws implanted at the medial malleolus. The scan showed the screws clearly visible without significant signs of resorption (55). Leonhardt et al. (Germany) (126) presented CT images 1 year after Mg-Y-RE-Zr screw fixation of mandibular condyle fractures with clear screw visibility and radiolucent regions (126).

4.3.5 Advanced Imaging of ZX00

Radiographs show subcutaneous gas formations released by ZX00 degradation in 40% (8/20) of our cases for up to six weeks (see 3.1, Table C) without causing clinical complications or wound issues, addressing initial concerns about potential complications (56). Other authors have reported the presence of subcutaneous gas in the soft tissue with Mg-Y-RE-Zr screws, also without associated complications (55,79,97,99,101,134).

As previously published (118), our Patient 6 underwent surgical exposure of ZX00 screws around 1½ years after implantation at the medial malleolus. A 1-year CT scan revealed trabecular voids surrounding the degrading screws (118). An unplanned medial malleolar osteotomy exposed the screws at their implantation site (Fig. 6c). This case provides key insights into degradation after 1½ years, with macroscopic examination showing partially degraded screws surrounded by a sclerotic layer, indicating the bone's attempt to shield against degradation. The need to overdrill the partially resorbed screws for extraction suggests some degree of bone-implant contact (118).

Our CT images at approximately 3½ years showed 100% voids in the trabecular bone of the medial malleolus (see 3.1, Table C). These voids appear to result from the resorption of the ZX00 implants, creating well-circumscribed and bordered areas of resorption. Furthermore, these voids persist in CT studies at later time points (4 years and beyond; see Fig. 1c, and 3c-d), suggesting biological inertia after resorption is complete.

In a subgroup of six patients, HR-CT measurements of ZX00 implantation sites, taken between 2 and 3 years post-implantation, revealed a mean void volume of 596.2 mm³ (see 3.1, Table D). During this period, HR-CT scans showed only traces of ZX00 screws within the voids (Fig. 1d-2d, 4d, 8d, and 14d), with one case showing no evidence of screw remnants (Fig. 10d). These findings confirm that the ZX00 screws largely disintegrated within 2 to 3 years after implantation.

4.3.6 Advanced Imaging after Hardware Removal

We confirm a 100% of cases with persistence of screw holes in trabecular bone after conventional hardware removal with long-term CT follow-up (see 3.1, Table C). This applies to both fibulo-tibial positioning screws (Fig. 1d, 4d-5d, 16d, 19-20d) and screws/plates around the ankle (Fig. 5d, 8d-10d, 12d, 17d).

In our cohort, nine cases involved conventional fibulo-tibial screws used to transfix the injured syndesmosis, which remained in place for six to eight weeks (see Methods). All available CT scans (Fig. 1d, 4d-5d, 16d, 19-20d) revealed persistent screw holes in the trabecular bone, while the cortical bone appeared fully reconstituted. This observation raises questions about bone healing mechanisms. One possibility is that the distance between the screw hole edges (>2 mm) hinders trabecular bone healing (25). Alternatively, healing might occur primarily at the cortical level, with the trabecular bone recovering by reinforcing the trabecular structures around the sclerotic screw hole (68).

In our cohort, 14 cases were treated with additional plates and screws, of which eight (57%) had the hardware removed within 1½ years after fracture surgery (see 3.1, Table A). CT follow-ups approximately 3½ years later revealed persistent sclerotic screw holes in all six cases we could assess (Fig. 5d, 8–10d, 12d, 17d). One single screw position seemed to be refilled with trabecular bone, with only the trajectory remaining visible (Fig. 8d). This could be due to stimulation from the screw removal process, possibly enhanced by the patient’s young age (20 years). Overall, persistent screw holes were evident in all other cases.

4.4 Bone Response

What do we know from animal studies? In contrast to the findings in our human model, animal studies have reported osteointegration of immature (juvenile) bone with the slow-degrading magnesium-based implants WE43 (108) and ZX00 (115). Various hypotheses emerged, suggesting a mechanism through which magnesium might stimulate bone formation (108,135,136). It has been observed that the corrosion process releases gas bubbles and degradation products, and a bone growth response occurs in the developing animal (83,85). Additionally, bone regeneration subsequent to the resorption of various magnesium-based alloys has been reported in juvenile rats (83,85). These discoveries were specifically conducted on the shaft (cortical bone) of the femur. Mesenchymal stem cells are found in the periosteum, endosteum, and bone marrow of long bones, where they can be mobilized for tissue healing (137). However, the factors contributing to bone regeneration in these juvenile animals remain unclear. It is theorized that implant corrosion may aid bone healing by releasing beneficial ions (92,95). Alternatively, the implant's complete dissolution and resorption may enable cortical bone healing in immature animal. However, this phenomenon has not been observed in the bone of mature (old) animals (86). In ovariectomy-induced rats, which serve as an osteoporotic, aged animal model, implantation of ZX00 pins in the tibia showed no osteointegration (86). Instead, giant voids surrounded by sclerotic rims were observed at the implantation site, specifically in the trabecular bone of the proximal tibia (86). While these effects were less pronounced, they were still evident in healthy, aged rats. (86). In juvenile rats, a layer of bone apposition was observed at the corroding ZX00 implant. The new bone was separated from the surrounding bone by soft tissue and corrosion layer and connected to it via small bridges (86,115). Similar findings were reported for sheep (138). In contrast, the present study on ZX00 in humans, CT scans showed trabecular voids with dense walls. While histological confirmation was not possible, the case with surgical exposure revealed a sclerotic cavity (Fig. 6c). This finding indicates an expired local inflammatory reaction that led to shielding of the decomposing ZX00 implant (139,140). The macroscopic finding, however, did not indicate a foreign body granuloma or extensive fibrotic tissue, as seen with polymer implants (141–144). The reaction triggered by ZX00, which caused sclerotic encapsulation of voids twice the initial screw volume (596.2 ± 275.7 mm^3), requires further histological investigation in future studies.

4.5 Cost-Effectiveness and Practical Considerations

All 20 patients received medial malleolar ZX00 implants, with 14 requiring additional hardware (plates or screws) for fracture stabilization around the ankle. Of these, eight (57%) had the conventional hardware removed, on average, 1½ years post-surgery (see 3.1, Table A). Notably, no additional incisions were required for the medial malleolus, as the ZX00 screws resorbed without complications. This resulted in a 100% reduction in the need for medial malleolar incisions during hardware removal surgery in our cohort. Furthermore, nine patients needed fibulo-tibial positioning screws for syndesmotic instability, which were removed after six to eight weeks. Despite being a minor procedure, it incurs additional costs of around EUR 1,000 in the European Union (32). If bioresorbable ZX00 screws were used as positioning screws, priced at approximately EUR 500 each, the total expense for two screws would be comparable to the removal costs of conventional screws. However, the use of ZX00 screws would eliminate the need for a second surgery, providing a cost-effective alternative by reducing patient discomfort, surgical risks, and indirect costs such as sick leave, while easing the burden on operating room capacity.

Speaking from our experience, the ZX00 material is notably softer in handling compared to materials traditionally familiar to surgeons (such as surgical steel or titanium). Careful consideration is required during screw insertion to prevent stripping of the screw head. Instructional courses for surgeons before first time clinical application are recommended. Additionally, it is worth noting that some surgeons have encountered challenges with insertion and handling of Mg-Y-RE-Zr screws, citing increased friction resistance and decreased stability during insertion compared to titanium screws (132).

It is of clinical interest to note that skin crepitation due to subcutaneous gas from the degrading implants has been reported (125), a clinical finding that we have also observed in our patients with ZX00 screws. Patients should be informed that this is a harmless issue and not a serious condition. Both patients and medical personnel unfamiliar with this phenomenon might mistakenly interpret it as cellulitis or gas gangrene.

4.6 Limitations

A major limitation of this study is the variability in follow-up time points beyond the first year, preventing definitive statements about ZX00 resorption timing. Although HR-CT detected traces of ZX00 in five out of six cases, these traces were not quantified. Osteoporosis screening was not performed before ZX00 implantation, so potential interactions between screw resorption and osteoporosis could not be assessed, despite evidence suggesting this alloy may not be suitable for osteoporotic bone (86). While there is strong evidence indicating different reactions of cortical and trabecular bone to ZX00 resorption (88), our study could not definitively assess cortical bone due to anatomical limitations at the medial malleolus. Two cases (10%) were lost: one due to loss of contact after 3 months and one due to a second surgery after 17 months. The small sample size precludes assessment of gender effects, and the pilot study design introduces potential selection bias, as patients were recruited based on their willingness to participate and the surgeons' judgment of their suitability for the intervention.

4.7 General Outlook and Future Perspective

This study provides insights into the evolution of ZX00 screws within human bone, featuring radiographs taken approximately 2½ years post-implantation and further details revealed through subsequent CT scans conducted about a year later, around 3½ years post-implantation. It confirms that ZX00 screws effectively stabilize fractures until union and demonstrate bioresorbability. All six HR-CT scans from the 2 to 3-year interval show near-complete to complete resorption of ZX00 screws, with only some traces, if any, remaining. The ZX00 implant meets biocompatibility standards, with no clinical complications, including among them infections or hypersensitivity reactions. While some patients had subcutaneous gas formation in the first weeks after implantation, these were incidental and not clinically significant. Radiographs at 2½ years showed homogeneous bone texture, but CT scans a year later revealed trabecular voids at all ZX00 implantation sites (100%). Our observations do not indicate an osteogenic effect from the magnesium-based alloy in our adult cohort (95,139). Radiographs alone may not fully assess the extent of healing or determine if bone regeneration (*restitutio ad integrum*) has occurred. The persistence of trabecular voids raises questions; however, conventional screws also leave sclerotic holes long after removal, a phenomenon recognized since the early days of bone implants (68,66). Biomechanically, ZX00 screw resorption occurs in a controlled manner, maintaining stability for primary bone healing according to AO/ASIF principles (14), with no re-fractures or complications in our cohort. Future applications for ZX00 screws may include fixation of medial malleolus fractures, as demonstrated in this study, as well as their use as fibulo-tibial positioning screws in syndesmotic instability and as K-wires for tension band osteosynthesis in simple olecranon fractures. When combined with a bioresorbable wire or tape, it is possible to create a fully bioresorbable construct (145). The feasibility of using ZX00 screws for fractures involving the growth plates (epiphyseal plates) in children and adolescents remains a topic of future development and research (146). Overall, this study demonstrates that ZX00 screws are a safe option for fracture fixation in adults and are genuinely bioresorbable without clinical complications in the long term. Furthermore, this study lays the groundwork for ZX00 imaging beyond the first year.

5 REFERENCES

1. McKibbin B. The biology of fracture healing in long bones. J Bone Joint Surg Br. 1978 May;60-B(2):150–62.

2. Einhorn TA. The cell and molecular biology of fracture healing. Clin Orthop. 1998 Oct;(355 Suppl):S7-21.

3. Duan Z wei, Lu H. Effect of Mechanical Strain on Cells Involved in Fracture Healing. Orthop Surg. 2021 Apr;13(2):369.

4. Perren SM. Physical and biological aspects of fracture healing with special reference to internal fixation. Clin Orthop. 1979;(138):175–96.

5. Elliott DS, Newman KJH, Forward DP, Hahn DM, Ollivere B, Kojima K, et al. A unified theory of bone healing and nonunion: BHN theory. Bone Jt J. 2016 Jul 1;98-B(7):884–91.

6. Chen JC, Jacobs CR. Mechanically induced osteogenic lineage commitment of stem cells. Stem Cell Res Ther. 2013;4(5):107.

7. ElHawary H, Baradaran A, Abi-Rafeh J, Vorstenbosch J, Xu L, Efanov JI. Bone Healing and Inflammation: Principles of Fracture and Repair. Semin Plast Surg. 2021 Aug;35(3):198–203.

8. Breeland G, Sinkler MA, Menezes RG. Embryology, Bone Ossification. In: StatPearls [Internet]. Treasure Island (FL): StatPearls Publishing; 2023 [cited 2023 Oct 22]. Available from: http://www.ncbi.nlm.nih.gov/books/NBK539718/

9. Wagner DO, Aspenberg P. Where did bone come from? Acta Orthop. 2011 Aug;82(4):393–8.

10. Hirasawa T, Kuratani S. Evolution of the vertebrate skeleton: morphology, embryology, and development. Zool Lett. 2015 Jan 13;1:2.

11. Tani S, Chung U il, Ohba S, Hojo H. Understanding paraxial mesoderm development and sclerotome specification for skeletal repair. Exp Mol Med. 2020 Aug;52(8):1166–77.

12. Marsell R, Einhorn TA. THE BIOLOGY OF FRACTURE HEALING. Injury. 2011 Jun;42(6):551–5.

13. Shapiro F. Bone development and its relation to fracture repair. The role of mesenchymal osteoblasts and surface osteoblasts. Eur Cell Mater. 2008 Apr 1;15:53–76.

14. Perren SM. EVOLUTION OF THE INTERNAL FIXATION OF LONG BONE FRACTURES: THE SCIENTIFIC BASIS OF BIOLOGICAL INTERNAL FIXATION:

CHOOSING A NEW BALANCE BETWEEN STABILITY AND BIOLOGY. J Bone Joint Surg Br. 2002 Nov 1;84-B(8):1093–110.

15. Lewallen DG, Chao EY, Kasman RA, Kelly PJ. Comparison of the effects of compression plates and external fixators on early bone-healing. J Bone Joint Surg Am. 1984 Sep;66(7):1084–91.

16. Leunig M, Hertel R, Siebenrock KA, Ballmer FT, Mast JW, Ganz R. The evolution of indirect reduction techniques for the treatment of fractures. Clin Orthop. 2000 Jun;(375):7–14.

17. Egol KA, Kubiak EN, Fulkerson E, Kummer FJ, Koval KJ. Biomechanics of locked plates and screws. J Orthop Trauma. 2004 Sep;18(8):488–93.

18. Reikerås O. Healing of osteotomies under different degrees of stability in rats. J Orthop Trauma. 1990;4(2):175–8.

19. Wu JJ, Shyr HS, Chao EY, Kelly PJ. Comparison of osteotomy healing under external fixation devices with different stiffness characteristics. J Bone Joint Surg Am. 1984 Oct;66(8):1258–64.

20. Aro HT, Kelly PJ, Lewallen DG, Chao EYS. The Effects of Physiologic Dynamic Compression on Bone Healing Under External Fixation. Clin Orthop Relat Res. 1990 Jul;256:260.

21. Uusitalo H, Rantakokko J, Ahonen M, Jämsä T, Tuukkanen J, KäHäri V, et al. A metaphyseal defect model of the femur for studies of murine bone healing. Bone. 2001 Apr;28(4):423–9.

22. Bernhardsson M, Sandberg O, Aspenberg P. Experimental models for cancellous bone healing in the rat. Acta Orthop. 2015 Nov 2;745–50.

23. Siclari VA, Zhu J, Akiyama K, Liu F, Zhang X, Chandra A, et al. Mesenchymal Progenitors Residing Close to the Bone Surface Are Functionally Distinct from Those in the Central Bone Marrow. Bone. 2013 Apr;53(2):575–86.

24. Bernhardsson M. Healing Processes in Cancellous Bone [Internet]. Linköping: Linköping University Electronic Press; 2018 [cited 2023 Oct 22]. (Linköping University Medical Dissertations; vol. 1652). Available from: http://urn.kb.se/resolve?urn=urn:nbn:se:liu:diva-152349

25. Sandberg OH, Aspenberg P. Inter-trabecular bone formation: a specific mechanism for healing of cancellous bone. Acta Orthop. 2016 Oct;87(5):459–65.

26. Charnley J, Baker SL. COMPRESSION ARTHRODESIS OF THE KNEE : A Clinical and Histological Study. J Bone Joint Surg Br. 1952 May 1;34-B(2):187–99.

27. Aspenberg P, Sandberg O. Distal radial fractures heal by direct woven bone formation. Acta Orthop. 2013 Jun;84(3):297–300.

28. Bernhardsson M. Healing Processes in Cancellous Bone. 2018 [cited 2023 Oct 22]; Available from: https://urn.kb.se/resolve?urn=urn:nbn:se:liu:diva-152349

29. Weber BG. Die Verletzungen des oberen Sprunggelenkes. 2., überarb. und erg. Aufl. Bern: Huber; 1972. 241 p. (Aktuelle Probleme in der Chirurgie).

30. Willett K, Keene DJ, Mistry D, Nam J, Tutton E, Handley R, et al. Close Contact Casting vs Surgery for Initial Treatment of Unstable Ankle Fractures in Older Adults: A Randomized Clinical Trial. JAMA. 2016 Oct 11;316(14):1455–63.

31. Regan DK, Gould S, Manoli A, Egol KA. Outcomes Over a Decade After Surgery for Unstable Ankle Fracture: Functional Recovery Seen 1 Year Postoperatively Does Not Decay With Time. J Orthop Trauma. 2016 Jul;30(7):e236-241.

32. Fenelon C, Murphy EP, Galbraith JG, Kearns SR. The burden of hardware removal in ankle fractures: How common is it, why do we do it and what is the cost? A ten-year review. Foot Ankle Surg. 2019 Aug 1;25(4):546–9.

33. Harper MC. Ankle fracture classification systems: a case for integration of the Lauge-Hansen and AO-Danis-Weber schemes. Foot Ankle. 1992 Sep;13(7):404–7.

34. Lampridis V, Gougoulias N, Sakellariou A. Stability in ankle fractures: Diagnosis and treatment. EFORT Open Rev. 2018 May;3(5):294–303.

35. Farr JN, Melton III LJ, Achenbach SJ, Atkinson EJ, Khosla S, Amin S. Fracture Incidence and Characteristics in Young Adults Aged 18 to 49 Years: A Population-Based Study. J Bone Miner Res. 2017;32(12):2347–54.

36. Court-Brown CM, Caesar B. Epidemiology of adult fractures: A review. Injury. 2006 Aug;37(8):691–7.

37. Bergh C, Wennergren D, Möller M, Brisby H. Fracture incidence in adults in relation to age and gender: A study of 27,169 fractures in the Swedish Fracture Register in a well-defined catchment area. PLOS ONE. 2020 Dec 21;15(12):e0244291.

38. Jensen SL, Andresen BK, Mencke S, Nielsen PT. Epidemiology of ankle fractures. A prospective population-based study of 212 cases in Aalborg, Denmark. Acta Orthop Scand. 1998 Feb;69(1):48–50.

39. Vanderkarr MF, Ruppenkamp JW, Vanderkarr M, Parikh A, Holy CE, Putnam M. Incidence, costs and post-operative complications following ankle fracture – A US claims database analysis. BMC Musculoskelet Disord. 2022 Dec 26;23(1):1129.

40. SooHoo NF, Krenek L, Eagan MJ, Gurbani B, Ko CY, Zingmond DS. Complication rates following open reduction and internal fixation of ankle fractures. J Bone Joint Surg Am. 2009 May;91(5):1042–9.

41. Hodgson S. AO Principles of Fracture Management. Ann R Coll Surg Engl. 2009 Jul;91(5):448–9.

42. Park YH, Choi WS, Choi GW, Kim HJ. Ideal angle of syndesmotic screw fixation: A CT-based cross-sectional image analysis study. Injury. 2017 Nov;48(11):2602–5.

43. Bell DP, Wong MK. Syndesmotic screw fixation in Weber C ankle injuries--should the screw be removed before weight bearing? Injury. 2006 Sep;37(9):891–8.

44. Wang Z, Tang X, Li S, Wang X, Gong L, Zhong T, et al. Treatment and outcome prognosis of patients with high-energy transsyndesmotic ankle fracture dislocation-the “Logsplitter” injury. J Orthop Surg. 2017 Jan 10;12(1):3.

45. Heier K, Collinge CA. Chapter 21 - Fractures and Dislocations of the Ankle. In: Sanders R, editor. Core Knowledge in Orthopaedics: Trauma [Internet]. Philadelphia: Mosby; 2008. p. 351–79. Available from: https://www.sciencedirect.com/science/article/pii/B978032303424110021X

46. Toolan BC, Koval KJ, Kummer FJ, Sanders R, Zuckerman JD. Vertical Shear Fractures of the Medial Malleolus: A Biomechanical Study of Five Internal Fixation Techniques. Foot Ankle Int. 1994 Sep 1;15(9):483–9.

47. Böstman O, Hirvensalo E, Vainionpää S, Mäkelä A, Vihtonen K, Törmälä P, et al. Ankle fractures treated using biodegradable internal fixation. Clin Orthop. 1989 Jan;(238):195–203.

48. Cicchinelli LD, González San Juan M, Aycart Testa J. Current concepts of absorbable fixation in first ray surgery. Clin Podiatr Med Surg. 1996 Jul;13(3):533–47.

49. Frøkjaer J, Møller BN. Biodegradable fixation of ankle fractures. Complications in a prospective study of 25 cases. Acta Orthop Scand. 1992 Aug;63(4):434–6.

50. Dijkema AR, van der Elst M, Breederveld RS, Verspui G, Patka P, Haarman HJ. Surgical treatment of fracture-dislocations of the ankle joint with biodegradable implants: a prospective randomized study. J Trauma. 1993 Jan;34(1):82–4.

51. Bucholz RW, Henry S, Henley MB. Fixation with bioabsorbable screws for the treatment of fractures of the ankle. J Bone Joint Surg Am. 1994 Mar;76(3):319–24.

52. Springer MA, van Binsbergen EA, Patka P, Bakker FC, Haarman HJ. [Resorbable rods and screws for fixation of ankle fractures. A randomized clinical prospective study]. Unfallchirurg. 1998 May;101(5):377–81.

53. Jin T, Jin-feng H, Wei-chun G, Ling Y, Sheng-hao Z. Research and application of absorbable screw in orthopedics: a clinical review comparing PDLLA screw with metal screw in patients with simple medial malleolus fracture. Chin J Traumatol. 2013 Feb 1;16(1):27–30.

54. Kose O, Turan A, Unal M, Acar B, Guler F. Fixation of medial malleolar fractures with magnesium bioabsorbable headless compression screws: short-term clinical and radiological outcomes in eleven patients. Arch Orthop Trauma Surg. 2018 Aug;138(8):1069–75.

55. May H, Alper Kati Y, Gumussuyu G, Yunus Emre T, Unal M, Kose O. Bioabsorbable magnesium screw versus conventional titanium screw fixation for medial malleolar fractures. J Orthop Traumatol Off J Ital Soc Orthop Traumatol. 2020 Dec;21:9.

56. Holweg P, Herber V, Ornig M, Hohenberger G, Donohue N, Puchwein P, et al. A lean bioabsorbable magnesium-zinc-calcium alloy ZX00 used for operative treatment of medial malleolus fractures. Bone Jt Res. 2020 Aug 19;9(8):477–83.

57. Xie K, Wang L, Guo Y, Zhao S, Yang Y, Dong D, et al. Effectiveness and safety of biodegradable Mg-Nd-Zn-Zr alloy screws for the treatment of medial malleolar fractures. J Orthop Transl. 2021 Mar 1;27:96–100.

58. Williams BR, McCreary DL, Chau M, Cunningham BP, Pena F, Swiontkowski MF. Functional Outcomes of Symptomatic Implant Removal Following Ankle Fracture Open Reduction and Internal Fixation. Foot Ankle Int. 2018 Jun;39(6):674–80.

59. Minkowitz RB, Bhadsavle S, Walsh M, Egol KA. Removal of painful orthopaedic implants after fracture union. J Bone Joint Surg Am. 2007 Sep;89(9):1906–12.

60. Kasai T, Matsumoto T, Iga T, Tanaka S. Complications of implant removal in ankle fractures. J Orthop. 2019 Feb 28;16(3):191–4.

61. Tsai SW, Ma HH, Hsu FW, Chou TFA, Chen KH, Chiang CC, et al. Risk factors for refracture after plate removal for midshaft clavicle fracture after bone union. J Orthop Surg. 2019 Dec 21;14(1):457.

62. Siu JW, Chan C, Swarup I, Sabatini CS. Rate of Refracture After Removal of Hardware in Pediatric Femur Fractures. J Pediatr Orthop. 2023 Sep 1;43(8):e674–9.

63. Zhu Y, Hu J, Zhan T, Zhu K, Zhang C. Refracture after plate removal of midshaft clavicle fractures after bone union-incidence, risk factors, management and outcomes. BMC Musculoskelet Disord. 2023 Apr 19;24(1):308.

64. Knudsen CS, Arthurs GI, Hayes GM, Langley-Hobbs SJ. Long bone fracture as a complication following external skeletal fixation: 11 cases. J Small Anim Pract. 2012 Dec;53(12):687–92.

65. Brooks DB, Burstein AH, Frankel VH. The biomechanics of torsional fractures. The stress concentration effect of a drill hole. J Bone Joint Surg Am. 1970 Apr;52(3):507–14.

66. Rosson J, Murphy W, Tonge C, Shearer J. Healing of residual screw holes after plate removal. Injury. 1991 Sep;22(5):383–4.

67. Johnson CaptBA, Fallat LM. The effect of screw holes on bone strength. J Foot Ankle Surg. 1997 Nov 1;36(6):446–51.

68. Burstein AH, Currey J, Frankel VH, Heiple KG, Lunseth P, Vessely JC. Bone strength. The effect of screw holes. J Bone Joint Surg Am. 1972 Sep;54(6):1143–56.

69. Alizade C, Jafarov A, Berchenko G, Bicer OS, Alizada F. Investigation of the process intergrowth of bone tissue into the hole in titanium implants (Experimental research). Injury. 2022 Aug;53(8):2741–8.

70. Tarallo L, Mugnai R, Zambianchi F, Adani R, Catani F. Volar plate fixation for the treatment of distal radius fractures: analysis of adverse events. J Orthop Trauma. 2013 Mar 19;

71. Aspenberg P. Black holes in bone – irresistible attractors of foreign materials? Acta Orthop. 2009 Feb 26;80(1):2–3.

72. Hirn M, de Silva U, Sidharthan S, Grimer RJ, Abudu A, Tillman RM, et al. Bone defects following curettage do not necessarily need augmentation. Acta Orthop. 2009 Feb;80(1):4–8.

73. Yanagawa T, Watanabe H, Shinozaki T, Takagishi K. Curettage of benign bone tumors without grafts gives sufficient bone strength. Acta Orthop. 2009 Feb 26;80(1):9–13.

74. Partio N, Huttunen TT, Mäenpää HM, Mattila VM. Reduced incidence and economic cost of hardware removal after ankle fracture surgery: a 20-year nationwide registry study. Acta Orthop. 91(3):331–5.

75. Böstman O, Pihlajamäki H. Routine implant removal after fracture surgery: a potentially reducible consumer of hospital resources in trauma units. J Trauma. 1996 Nov;41(5):846–9.

76. Naumann MG, Sigurdsen U, Utvåg SE, Stavem K. Incidence and risk factors for removal of an internal fixation following surgery for ankle fracture: A retrospective cohort study of 997 patients. Injury. 2016 Aug;47(8):1783–8.

77. Reith G, Schmitz-Greven V, Hensel KO, Schneider MM, Tinschmann T, Bouillon B, et al. Metal implant removal: benefits and drawbacks--a patient survey. BMC Surg. 2015 Aug 7;15:96.

78. Syntellix AG. Quality management – Syntellix AG, Hannover [Internet]. [cited 2024 Mar 9]. Available from: https://www.syntellix.de/en/company/made-in-germany/quality-management.html

79. Seitz JM, Lucas A, Kirschner M. Magnesium-Based Compression Screws: A Novelty in the Clinical Use of Implants. JOM - J Miner Met Mater Soc. 2016 Apr 1;68:1177–82.

80. Device Classification Under Section 513(f)(2)(De Novo); Absorbable Metallic Bone Fixation Fastener (RemeOs Screw, Bioretec Ltd.) [Internet]. [cited 2024 Mar 9]. Available from: https://www.accessdata.fda.gov/scripts/cdrh/cfdocs/cfpmn/denovo.cfm?id=DEN220030

81. RemeOs™ Screw - Magnesium screw implants - Bioretec Ltd. [Internet]. [cited 2024 Mar 9]. Available from: https://bioretec.com/products/6/remeos-screw-magnesium-screw-implants

82. Zhang B, Hou Y, Wang X, Wang Y, Geng L. Mechanical properties, degradation performance and cytotoxicity of Mg–Zn–Ca biomedical alloys with different compositions. Mater Sci Eng C. 2011 Dec 1;31(8):1667–73.

83. Kraus T, Fischerauer SF, Hänzi AC, Uggowitzer PJ, Löffler JF, Weinberg AM. Magnesium alloys for temporary implants in osteosynthesis: in vivo studies of their degradation and interaction with bone. Acta Biomater. 2012 Mar;8(3):1230–8.

84. Fischerauer SF, Kraus T, Wu X, Tangl S, Sorantin E, Hänzi AC, et al. In vivo degradation performance of micro-arc-oxidized magnesium implants: a micro-CT study in rats. Acta Biomater. 2013;9(2):5411–20.

85. Amerstorfer F, Fischerauer SF, Fischer L, Eichler J, Draxler J, Zitek A, et al. Long-term in vivo degradation behavior and near-implant distribution of resorbed elements for magnesium alloys WZ21 and ZX50. Acta Biomater. 2016 Sep 15;42:440–50.

86. Sommer NG, Hirzberger D, Paar L, Berger L, Ćwieka H, Schwarze UY, et al. Implant degradation of low-alloyed Mg–Zn–Ca in osteoporotic, old and juvenile rats. Acta Biomater. 2022 Jul 15;147:427–38.

87. Holweg P, Berger L, Cihova M, Donohue N, Clement B, Schwarze U, et al. A lean magnesium-zinc-calcium alloy ZX00 used for bone fracture stabilization in a large growing-animal model. Acta Biomater. 2020 Sep 1;113:646–59.

88. Marek R, Ćwieka H, Donohue N, Holweg P, Moosmann J, Beckmann F, et al. Degradation behavior and osseointegration of Mg-Zn-Ca screws in different bone regions of growing sheep: a pilot study. Regen Biomater. 2023;10:rbac077.

89. Cihova M, Martinelli E, Schmutz P, Myrissa A, Schäublin R, Weinberg AM, et al. The role of zinc in the biocorrosion behavior of resorbable Mg–Zn–Ca alloys. Acta Biomater. 2019 Dec;100:398–414.

90. Biber R, Pauser J, Geßlein M, Bail HJ. Magnesium-Based Absorbable Metal Screws for Intra-Articular Fracture Fixation. Case Rep Orthop. 2016;2016:1–4.

91. Leonhardt H, Franke A, McLeod NMH, Lauer G, Nowak A. Fixation of fractures of the condylar head of the mandible with a new magnesium-alloy biodegradable cannulated headless bone screw. Br J Oral Maxillofac Surg. 2017 Jul;55(6):623–5.

92. Waizy H, Diekmann J, Weizbauer A, Reifenrath J, Bartsch I, Neubert V, et al. In vivo study of a biodegradable orthopedic screw (MgYREZr-alloy) in a rabbit model for up to 12 months. J Biomater Appl. 2014 Jan;28(5):667–75.

93. Naujokat H, Seitz JM, Açil Y, Damm T, Möller I, Gülses A, et al. Osteosynthesis of a cranio-osteoplasty with a biodegradable magnesium plate system in miniature pigs. Acta Biomater. 2017 Oct 15;62:434–45.

94. Diekmann J, Bauer S, Weizbauer A, Willbold E, Windhagen H, Helmecke P, et al. Examination of a biodegradable magnesium screw for the reconstruction of the anterior cruciate ligament: A pilot in vivo study in rabbits. Mater Sci Eng C Mater Biol Appl. 2016 Feb;59:1100–9.

95. Witte F, Kaese V, Haferkamp H, Switzer E, Meyer-Lindenberg A, Wirth CJ, et al. In vivo corrosion of four magnesium alloys and the associated bone response. Biomaterials. 2005 Jun 1;26(17):3557–63.

96. Windhagen H, Radtke K, Weizbauer A, Diekmann J, Noll Y, Kreimeyer U, et al. Biodegradable magnesium-based screw clinically equivalent to titanium screw in hallux valgus surgery: short term results of the first prospective, randomized, controlled clinical pilot study. Biomed Eng OnLine. 2013 Jul 3;12:62.

97. Plaass C, Ettinger S, Sonnow L, Koenneker S, Noll Y, Weizbauer A, et al. Early results using a biodegradable magnesium screw for modified chevron osteotomies. J Orthop Res. 2016 Dec 1;34(12):2207–14.

98. Gigante A, Setaro N, Rotini M, Finzi SS, Marinelli M. Intercondylar eminence fracture treated by resorbable magnesium screws osteosynthesis: A case series. Injury. 2018 Nov;49 Suppl 3:S48–53.

99. Acar B, Kose O, Unal M, Turan A, Kati YA, Guler F. Comparison of magnesium versus titanium screw fixation for biplane chevron medial malleolar osteotomy in the treatment of osteochondral lesions of the talus. Eur J Orthop Surg Traumatol Orthop Traumatol. 2020 Jan;30(1):163–73.

100. Lam WH, Tso CY, Tang N, Cheung WH, Qin L, Wong RMY. Biodegradable magnesium screws in elbow fracture fixation: Clinical case series. J Orthop Trauma Rehabil. 2021 Jan 12;2210491720986983.

101. Gazit T, Robinson D, Khawalde K, Eisa M, Qassem K, Heller E, et al. Foot Surgery Using Resorbable Magnesium Screws. J Foot Ankle Surg. 2024 Jan 1;63(1):79–84.

102. Wichelhaus A, Emmerich J, Mittlmeier T. A Case of Implant Failure in Partial Wrist Fusion Applying Magnesium-Based Headless Bone Screws. Case Rep Orthop. 2016;2016:7049130.

103. Haslhofer DJ, Gotterbarm T, Klasan A. High Complication Rate and High Percentage of Regressing Radiolucency in Magnesium Screw Fixation in 18 Consecutive Patients. J Pers Med. 2023 Feb 17;13(2):357.

104. Witte F, Abeln I, Switzer E, Kaese V, Meyer-Lindenberg A, Windhagen H. Evaluation of the skin sensitizing potential of biodegradable magnesium alloys. J Biomed Mater Res A. 2008;86A(4):1041–7.

105. Thormann U, Alt V, Heimann L, Gasquere C, Heiss C, Szalay G, et al. The biocompatibility of degradable magnesium interference screws: An experimental study with sheep. BioMed Res Int. 2015;2015.

106. Lindtner RA, Castellani C, Tangl S, Zanoni G, Hausbrandt P, Tschegg EK, et al. Comparative biomechanical and radiological characterization of osseointegration of a biodegradable magnesium alloy pin and a copolymeric control for osteosynthesis. J Mech Behav Biomed Mater. 2013 Dec;28:232–43.

107. Oshibe N, Marukawa E, Yoda T, Harada H. Degradation and interaction with bone of magnesium alloy WE43 implants: A long-term follow-up in vivo rat tibia study. J Biomater Appl. 2019 Apr;33(9):1157–67.

108. Castellani C, Lindtner RA, Hausbrandt P, Tschegg E, Stanzl-Tschegg SE, Zanoni G, et al. Bone-implant interface strength and osseointegration: Biodegradable magnesium alloy versus standard titanium control. Acta Biomater. 2011 Jan;7(1):432–40.

109. Marukawa E, Tamai M, Takahashi Y, Hatakeyama I, Sato M, Higuchi Y, et al. Comparison of magnesium alloys and poly-l-lactide screws as degradable implants in a canine fracture model. J Biomed Mater Res B Appl Biomater. 2016;104(7):1282–9.

110. Pichler K, Kraus T, Martinelli E, Sadoghi P, Musumeci G, Uggowitzer PJ, et al. Cellular reactions to biodegradable magnesium alloys on human growth plate chondrocytes and osteoblasts. Int Orthop. 2014 Apr 21;38(4):881–9.

111. Celarek A, Kraus T, Tschegg EK, Fischerauer SF, Stanzl-Tschegg S, Uggowitzer PJ, et al. PHB, crystalline and amorphous magnesium alloys: promising candidates for bioresorbable osteosynthesis implants? Mater Sci Eng C Mater Biol Appl. 2012 Aug 1;32(6):1503–10.

112. Hofstetter J, Martinelli E, Pogatscher S, Schmutz P, Povoden-Karadeniz E, Weinberg AM, et al. Influence of trace impurities on the in vitro and in vivo degradation of biodegradable Mg-5Zn-0.3Ca alloys. Acta Biomater. 2015 Sep;23:347–53.

113. Martinez DC, Dobkowska A, Marek R, Ćwieka H, Jaroszewicz J, Płociński T, et al. *In vitro and in vivo* degradation behavior of Mg-0.45Zn-0.45Ca (ZX00) screws for orthopedic applications. Bioact Mater. 2023 Oct 1;28:132–54.

114. Labmayr V, Suljevic O, Sommer NG, Schwarze UY, Marek RL, Brcic I, et al. Mg-Zn-Ca Alloy (ZX00) Screws Are Resorbed at a Mean of 2.5 Years After Medial Malleolar Fracture Fixation: Follow-up of a First-in-humans Application and Insights From a Sheep Model. Clin Orthop. 2023 Aug 21;

115. Grün NG, Holweg P, Tangl S, Eichler J, Berger L, van den Beucken JJJP, et al. Comparison of a resorbable magnesium implant in small and large growing-animal models. Acta Biomater. 2018 Sep 15;78:378–86.

116. Herber V, Labmayr V, Sommer NG, Marek R, Wittig U, Leithner A, et al. Can Hardware Removal be Avoided Using Bioresorbable Mg-Zn-Ca Screws After Medial Malleolar Fracture Fixation? Mid-Term Results of a First-In-Human Study. Injury. 2022 Mar;53(3):1283–8.

117. World Medical Association. World Medical Association Declaration of Helsinki: Ethical Principles for Medical Research Involving Human Subjects. JAMA. 2013 Nov 27;310(20):2191–4.

118. Holweg P, Labmayr V, Schwarze U, Sommer NG, Ornig M, Leithner A. Osteotomy after medial malleolus fracture fixed with magnesium screws ZX00 - A case report. Trauma Case Rep. 2022 Oct 4;42:100706.

119. Valderrabano V, Horisberger M, Russell I, Dougall H, Hintermann B. Etiology of ankle osteoarthritis. Clin Orthop. 2009 Jul;467(7):1800–6.

120. Hong CC, Nashi N, Prosad Roy S, Tan KJ. Impact of trimalleolar ankle fractures: how do patients fare post-operatively? Foot Ankle Surg Off J Eur Soc Foot Ankle Surg. 2014 Mar;20(1):48–51.

121. Donken CCMA, Verhofstad MHJ, Edwards MJ, van Laarhoven CJHM. Twenty-one-year follow-up of supination-external rotation type II-IV (OTA type B) ankle fractures: a retrospective cohort study. J Orthop Trauma. 2012 Aug;26(8):e108-114.

122. Biber R, Pauser J, Brem M, Bail HJ. Bioabsorbable metal screws in traumatology: A promising innovation. Trauma Case Rep. 2017 Apr 1;8:11–5.

123. Modrejewski C, Plaaß C, Ettinger S, Caldarone F, Windhagen H, Stukenborg-Colsman C, et al. Degradationsverhalten bioresorbierbarer Magnesium-Implantate bei distalen Metatarsale-1-Osteotomien im MRT. Fuß Sprunggelenk. 2015 Sep 1;13(3):156–61.

124. Plaass C, von Falck C, Ettinger S, Sonnow L, Calderone F, Weizbauer A, et al. Bioabsorbable magnesium versus standard titanium compression screws for fixation of distal metatarsal osteotomies – 3 year results of a randomized clinical trial. J Orthop Sci. 2018 Mar 1;23(2):321–7.

125. Unal M, Demirayak E, Ertan MB, Kilicaslan OF, Kose O. Bioabsorbable Magnesium Screw Fixation for Tibial Tubercle Osteotomy; A Preliminary Study. Acta Bio Medica Atenei Parm. 2021;92(6):e2021263.

126. Leonhardt H, Ziegler A, Lauer G, Franke A. Osteosynthesis of the Mandibular Condyle With Magnesium-Based Biodegradable Headless Compression Screws Show Good Clinical Results During a 1-Year Follow-Up Period. J Oral Maxillofac Surg Off J Am Assoc Oral Maxillofac Surg. 2021 Mar;79(3):637–43.

127. Constantinou CC, Sernert N, Rostgård-Christensen L, Kartus J. Large Drill Holes Are Still Present in the Long Term After Arthroscopic Bankart Repair With Absorbable Tacks: An 18-Year Randomized Prospective Study. Am J Sports Med. 2020 Jul 1;48(8):1865–72.

128. Barber FA, Dockery WD, Cowden CH. The degradation outcome of biocomposite suture anchors made from poly L-lactide-co-glycolide and β-tricalcium phosphate. Arthrosc J Arthrosc Relat Surg Off Publ Arthrosc Assoc N Am Int Arthrosc Assoc. 2013 Nov;29(11):1834–9.

129. Barber FA, Dockery WD. Long-term absorption of poly-L-lactic Acid interference screws. Arthrosc J Arthrosc Relat Surg Off Publ Arthrosc Assoc N Am Int Arthrosc Assoc. 2006 Aug;22(8):820–6.

130. Arama Y, Salmon LJ, Sri-Ram K, Linklater J, Roe JP, Pinczewski LA. Bioabsorbable Versus Titanium Screws in Anterior Cruciate Ligament Reconstruction Using Hamstring Autograft: A Prospective, Blinded, Randomized Controlled Trial With 5-Year Follow-up. Am J Sports Med. 2015 Aug;43(8):1893–901.

131. Sundaraj K, Salmon LJ, Heath EL, Winalski CS, Colak C, Vasanji A, et al. Bioabsorbable Versus Titanium Screws in Anterior Cruciate Ligament Reconstruction Using Hamstring Autograft: A Prospective, Randomized Controlled Trial With 13-Year Follow-up. Am J Sports Med. 2020 May;48(6):1316–26.

132. Meier R, Panzica M. First results with a resorbable MgYREZr compression screw in unstable scaphoid fractures show extensive bone cysts [Article in German]. Handchir · Mikrochir · Plast Chir. 2017 Feb;49(1):37–41.

133. Polat O, Toy S, Kibar B. Surgical outcomes of scaphoid fracture osteosynthesis with magnesium screws. Jt Dis Relat Surg. 2021;32(3):721–8.

134. Aktan C, Ertan MB, Turan A, Kose O. Fixation of Small Osteochondral Fragments in a Comminuted Distal Humerus Fracture with Magnesium Bioabsorbable Screws: A Case Report. Cureus. 10(12):e3752.

135. Zreiqat H, Howlett CR, Zannettino A, Evans P, Schulze-Tanzil G, Knabe C, et al. Mechanisms of magnesium-stimulated adhesion of osteoblastic cells to commonly used orthopaedic implants. J Biomed Mater Res. 2002 Nov;62(2):175–84.

136. Witte F, Ulrich H, Rudert M, Willbold E. Biodegradable magnesium scaffolds: Part 1: appropriate inflammatory response. J Biomed Mater Res A. 2007 Jun;81(3):748–56.

137. Pajarinen J, Lin T, Gibon E, Kohno Y, Maruyama M, Nathan K, et al. Mesenchymal stem cell-macrophage crosstalk and bone healing. Biomaterials. 2019 Mar 1;196:80–9.

138. Martinez DC, Dobkowska A, Marek R, Ćwieka H, Jaroszewicz J, Płociński T, et al. In vitro and in vivo degradation behavior of Mg-0.45Zn-0.45Ca (ZX00) screws for orthopedic applications. Bioact Mater. 2023 Oct;28:132–54.

139. Suljevic O, Fischerauer SF, Weinberg AM, Sommer NG. Immunological reaction to magnesium-based implants for orthopedic applications. What do we know so far? A systematic review on in vivo studies. Mater Today Bio [Internet]. 2022 Jun 1 [cited 2023 Jan 29];15. Available from: https://pubmed.ncbi.nlm.nih.gov/35757033/

140. Anderson JM, Rodriguez A, Chang DT. Foreign body reaction to biomaterials. Semin Immunol. 2008 Apr;20(2):86–100.

141. Schrumpf MA, Lee AT, Weiland AJ. Foreign-Body Reaction and Osteolysis Induced by an Intraosseous Poly-L-Lactic Acid Suture Anchor in the Wrist: Case Report. J Hand Surg. 2011 Nov 1;36(11):1769–73.

142. Bergsma EJ, Rozema FR, Bos RRM, Bruijn WCD. Foreign body reactions to resorbable poly(l-lactide) bone plates and screws used for the fixation of unstable zygomatic fractures. J Oral Maxillofac Surg. 1993 Jun 1;51(6):666–70.

143. Seino D, Fukunishi S, Yoshiya S. Late foreign-body reaction to PLLA screws used for fixation of acetabular osteotomy. J Orthop Traumatol Off J Ital Soc Orthop Traumatol. 2007 Dec;8(4):188–91.

144. Böstman O, Hirvensalo E, Mäkinen J, Rokkanen P. Foreign-body reactions to fracture fixation implants of biodegradable synthetic polymers. J Bone Joint Surg Br. 1990 Jul;72(4):592–6.

145. Crozier-Shaw G, Mahon J, Bayer TC. The use of bioabsorbable compression screws & polyethylene tension band for fixation of displaced olecranon fractures. J Orthop. 2020 Aug 29;22:525–9.

146. Grün NG, Holweg PL, Donohue N, Klestil T, Weinberg AM. Resorbable implants in pediatric fracture treatment. Innov Surg Sci. 2018 May 29;3(2):119–25.